T-AM-Sy1 THE BIOPHYSICAL CYTOLOGY OF INTERCELLULAR COMMUNICATION. D.A. Goodenough, Dept. of Anatomy, Harvard Medical School, Boston, MA 02115.

Intercellular communication is mediated either by the diffusion of informational molecules through intervening extracellular spaces between cells, or by diffusion of molecules between the cytoplasms of conjoined cells through a regulatable, private pathway which avoids the extracellular space. The plasma membrane specialization which mediates the latter mode of communication is called the gap junction (nexus). This intercellular junction is composed of an assembly of cylindrical subunits (connexons), which span both the joined cells' plasma membranes and a 2-3 nm extracellular gap. Structural studies have set the maximum diameter of the axial channel in each connexon at 2nm. Fluorescent-probe microinjection studies set a 1200 dalton (≈1.4nm) upper limit for anionic molecules which can pass intercellularly through the junctional channels. Under a variety of conditions, most cells have a mechanism to close the junctional channels, switching the gap junctions from a low to a high resistance state, thereby terminating communication with neighboring cells. Coordinated x-ray diffraction and electron microscopy of isolated, high-resistance gap junctions suggest that each connexon spanning the paired lipid bilayers is composed of a dimer of polypeptide hexamers, with a two-fold symmetry plane in the center of the 2nm gap. Trypsin insensitive x-ray diffraction maxima are resolved at 0.47nm on the meridan (electron density profile), which are sampled by an 8nm interference function (separation between bilayer centers). These observations indicate significant β-conformation in the junctional polypeptides at the level of the membrane hydrophobic interiors. Ultrarapid freezing (2msec) of living tissues on copper surfaces at $4^{\circ}K$ reveal dramatic changes in the states of aggregation of the connexons in the membrane plane under different physiological conditions; these differences may be related to changes in junctional resistance.

T-AM-Sy2 COMMUNICATION AT TRIADS AND DYADS OF SKELETAL MUSCLE. Clara Franzini-Armstrong, Department of Anatomy, University of Pennsylvania, Philadelphia, Pa. 19104.

Triads and dyads are junctionsbetween elements of transverse tubular system and sarcoplasmic reticulum in muscle fibers. The junctions are not electrically communicating at resting membrane potentials. Interiors of SR and T-tubules are not in continuity and the ionic composition of the two compartments are different. Following exposure of the muscle to hypertonic solutions the T-tubules swell, thus behaving as extracellular compartments but the SR does not. Depolarization of the T-tubule's membrane above a threshold value results in a large release of calcium to the fibrils. The mechanism of transmission at this junction has not been determined. Morphological evidence indicates that the junction is asymmetric, i.e. that the internal architectures of the two membranes participating in the junction are not identical. The space separating the two membranes is approximately 10 nm wide and is occupied by loosely arranged material which forms bridges (feet) joining the two membranes. The feet are closely associated with the SR membrane and it is likely that they are composed of one or two proteins that are uniquely associated with the heavy microsomal fraction (K. Campbell). Recent results indicate that the feet may be continuous with structures occupying the interior of T-tubules' membranes and thus may provide a direct physical link between the junctional membranes. It is speculated that sites of calcium release are located in the junctional regions of the SR membrane. Supported by MDAA (H.M. Watts Center) and by NIH (HL-15835-08).

T-AM-Sy3 INITIAL STEPS IN EXOCYTOSIS AT LIMULUS AMEBOCYTES. R.L. Ornberg and T.S. Reese, Section on Functional Neuroanatomy, LNNS, NINCDS, NIH, Bethesda, Maryland 20014.

The initial steps in exocytosis at Limulus amebocytes were captured with rapid-freezing. Amebocytes were used because they degranulate precipitously when exposed to endotoxin, so secretory events can be synchronized; their environment ressembles sea water, so they freeze well; and large numbers are available since they are virtually the only cell in Limulus blood. Furthermore, amebocyte secretory granules are large, so we expected that the processes leading to exocytosis after stimulation with endotoxin might be relatively slow, which would allow us to study them with a rapid-freezing technique that freezes tissues in a few msecs. Prior to endotoxin application, secretory granules at the periphery of amebocytes are separated from the plasmalemma by a narrow region of cytoplasm criss-crossed with fibrous elements seen in both freeze-substituted and freeze-etched cells. At 1-5 secs after endotoxin, the plasmalemma overlying each granule dimples in, closing the gap that separates it from the granule. Then, a small aperture appears at one or, rarely, several points along this apposition and quickly widens to let out the contents of the secretory granule. The presence of fibrous elements where the plasmalemma dimples towards the secretory granule, exactly where exocytosis subsequently begins, suggests that a contractile process is involved in at least the "approach" step of exocytosis in these cells, and that this process may depend in some way on the fibrous connections between the granule and the plasmalemma.

T-AM-Sy4 CELL-TO-CELL COMMUNICATION AND DIFFERENTIATION. Norton B. Gilula, The Rockefeller University, New York, New York 10021

Cells in most metazoan animal organisms can communicate with each other through direct physical connections or cell junctions. The gap junction is presently regarded as a prime candidate for providing the necessary structural pathway for communication between cells. The communication pathways are characterized by a low-resistance transfer of ions, dyes, and low-molecular weight metabolites. Macromolecular substances are not transferred through these pathways. Gap junctions have been isolated and characterized as enriched subcellular fractions from rat, mouse, and bovine liver. Two prominent polypeptides are present in fractions from all three sources: 47,000 daltons and 27,000 daltons. The two polypeptides are chemically similar on the basis of mapping approaches. During cellular differentiation, gap junctional communication is a common feature both in vivo and in culture. Recent studies have indicated that patterns of uncoupling can be associated with relevant events in differentiation. In addition, a model co-culture system has been devised to demonstrate that hormonal stimulation can be transferred between communicating heterologous cell types (myocardial cells and ovarian granulosa cells).

T-AM-A1 AN EXACT THEORY FOR THE INTERACTION OF ORGANIC PHOSPHATES WITH HEMOGLOBIN. Gary K. Ackers, Johns Hopkins Univ., Baltimore, Md. 21218.

An exact theory has been derived for the dependence of hemoglobin oxygen affinity (i.e. the median oxygen concentration) upon total concentration of organic phosphate and hemoglobin, and upon the fundamental binding constants of the system. The new theory opens up the possibility of carrying out interpretable experiments in previously inaccessible regions of the experimental variables where the concentrations of hemoglobin-phosphate complexes and unbound phosphate are of comparable magnitude. Some illustrative applications to human hemoglobin will be presented, and the ranges of validity of the earlier approximate theories have been evaluated. The theory is general and could be applied to other experimental systems. Supported by grants from the USPHS and the NSF.

T-AM-A2 STRUCTURAL DEPENDENCE OF REDOX POTENTIAL OF CYTOCHROME c. Ajay Pande*, Antony F. Saturno* and Yash P. Myer, Institute of Hemoproteins, SUNYA, Albany, N.Y. 12222.

The high redox potential of HH cytochrome c, and of hemoproteins in general, has been related to heme stereochemistry, selectivity of axial coordinating ligands, the extent of hydrophobicity, and recently, inversely to the extent of heme exposure. We have correlated the alteration of redox potential of cytochrome c with increasing urea concentrations to characteristics of various intermediate forms discerned through equilibrium studies using the 695-nm absorptivity and tryptophan fluorescence, as well as stopped-flow studies of the folding process. The intermediate forms were further characterized with regard to the extent of exposure of heme through reactivity of the axial ligates toward group-specific reagent, circular dichroism spectra, and pH and temperature stability. The stereochemistry of heme, associated with coordination configuration and/or protein conformation, is determined by resonance Raman studies. The redox potential is found to be insensitive to the loosening of the heme crevice and alteration of hydrophobicity, as long as perturbation is limited to the front part of the crevice. Since no alteration of heme stereochemistry was seen upon change in the coordination configuration and/or protein conformation, the possibility of heme stereochemistry as a potential determinant is also ruled out. Since only the transition involving alterations in the region of tryptophan-heme, the deepest part of the crevice, correlates with potential alterations, 1:1, this structure of the protein thus seems to be critical for the high redox potential.

(Supported by National Science Foundation Grant #PCM 77-07441)

T-AM-A3 ORIGIN OF HYPERFINE INTERACTIONS IN HEME-BOUND WATER PROTONS. Mahendra K. Mallick*, S. K. Mun, Shantilata Mishra, Jane C. Chang, and T. P. Das, Physics Department, State University of New York, Albany, New York 12222.

Information on proton hyperfine interactions in hemoglobin derivatives are available from a variety of techniques among them proton resonance shift, ENDOR, line width of proton spectra and proton relaxation measurements. The theoretical understanding of proton hyperfine data can provide a valuable test of calculated spin distributions in these molecules. In earlier work[1] we have analysed hyperfine interactions of mesoprotons in high spin heme compounds and hemoglobin derivatives. The present work focusses on the protons in ligand water molecules, the two systems chosen for study being metmyoglobin and divalent manganese prophyrin in aqueous solution. In metmyoglobin, we find +4.7MHz and +1.1MHz respectively from dipolar and direct contact effects, adding up to a total of 5.8MHz, in reasonable agreement with the experimental magnitude of 6.02±0.08 MHz from ENDOR measurements[2]. A similar trend in relative contributions from different mechanisms is also found in the manganese compound. The significant contributions from the direct contact mechanism illustrates the delocalized nature of the spin-distribution in metmyglobin and in heme compounds in general, a feature that has been verified from earlier theoretical studies of other properties such as the ^{57}Fe, ^{14}N and mesoproton hyperfine interactions. The possible influence of exchange polarization effects will be discussed. (Grant support NIH, AL15196)

1. M.K. Mallick, S.K. Mun, S. Mishra, J.C. Chang and T.P. Das, Bull. Am. Phys. Soc. 22 336 (1977)
2. C.F. Mulks, C.P. Scholes, L.C. Dickinson and A. Lapidot, Communicated to J. Am. Chem. Soc. (1978)

T-AM-A4 THE ELECTRONIC AND MAGNETIC PROPERTIES OF THE HEME IN A MODEL SYSTEM OF CYTO CHROME C. E.K. Yang*, L.E. Vickery**, and K. Sauer, Department of Chemistry and Laboratory of Chemical Biodynamics, Lawrence Berkeley Laboratory, University of California, Berkeley, California 94720.

Detailed ligand binding effects have been examined in a model system of cytochrome c, the N-acetylated ferric heme octapeptide (N-H8PT) directly isolated from horse heart cytochrome c.[1] The room temperature absorption spectral and magnetic measurements show that complexes of the N-H8PT with various external ligands generally behave as expected from their ligand field considerations. The N-acetylated methionine complex of the N-H8PT which shares identical axial coordination as the parent molecule, however, exhibits thermal equilibrium of spins between high and low spin states while cytochrome c exists in the purely low spin state. Temperature dependence of paramagnetic susceptibility of the methionine complex yields $\Delta H^\circ = -7.6$ Kcal/mole and $\Delta S^\circ = -25.9$ e.u. for a high spin to low spin transition demonstrating a compensation effect between the two thermodynamic parameters. The low temperature EPR spectrum of the methionine complex indicates a low spin ground state with g values at 2.91, 2.31 and 1.51 which are distinct from the g values of cytochrome c. The axial (Δ) and rhombic (V) distortion parameters correspond to 1200 cm^{-1} and 780 cm^{-1}, respectively.[2] From these results, a model can be proposed to account for the uniqueness of the methionine complex: a change in Fe-S distance may play a role in regulating the redox properties of cytochrome c.

1. H. Tuppy and S.Paleus, Acta Chem. Scand., 9, 353 (1955)
2. C.P.S. Taylor: Biochem.Biophys.Acta 491, 137 (1977)

*present address-Johnson Research Foundation, University of Penna, Phila, PA 19104. **Dept. of Physiology, University of California, Irvine, California 92717

T-AM-A5 LOW TEMPERATURE PROTON NMR IN DEOXYMYOGLOBIN AND A NEW MODEL FOR THE LOW-LYING Fe^{2+} STATES. O. Lumpkin* and W. T. Dixon* (Intr. by B. Zimm), University of California, San Diego, La Jolla, Ca. 92093.

In order to study the electronic structure of the heme Fe^{2+} ion we have measured proton spin-lattice relaxation rates versus applied magnetic field and temperature in deoxymyoglobin at liquid ^4He temperatures. The results show that the electronic relaxation time τ_e satisfies $10^{-7} < \tau_e < 10^{-4}$s and that there is at least one excited electronic state within 2 cm^{-1} of the ground state. An interpretation of these findings consistent with Mossbauer magnetic susceptibility, and EPR experiments is found if the low lying electronic states derive from a nearly degenerate orbital doublet (d_{xy}, d_{yz}) mixed by an effective spin-orbit interaction ≈ 1 cm^{-1}. In particular, without the usual assumption of rapid electronic relaxation, we show that the temperature dependence of the Mossbauer spectrum may be due to motional narrowing. The reduction in spin-orbit interaction is, we believe, due primarily to a Jahn-Teller type coupling between Fe^{2+} electronic states and low frequency vibrational modes.

T-AM-A6 PROTON NUCLEAR MAGNETIC RESONANCE STUDIES OF HEMOGLOBIN M BOSTON. S. Takahashi*, A. K. -L. C. Lin*, and C. Ho, Department of Biological Sciences, University of Pittsburgh, Pittsburgh, Pa. 15260.

Proton nuclear magnetic resonance at 250 MHz using the correlation spectroscopy mode has been used to investigate Hb M Boston in both D_2O and H_2O at pH 7 and 27°C. Due to the amino acid substitution at the distal histidine residue (α58E7 His → Tyr), the iron atoms in the two α chains of this mutant Hb remain in the ferric state and do not combine with ligands. Hence, it provides an excellent opportunity (i) to make assignments of the ferrous hyperfine shifted proton resonances of the β chains in human normal adult hemoglobin and (ii) to investigate the effect of ligation of the normal β chains on the structure of the α chains by monitoring the hyperfine shifted proton resonances of the ferric α chains. In addition, the exchangeable proton resonances of this mutant hemoglobin allow us to follow the quaternary structural transition upon oxygenation. The results from Hb M Boston not only have confirmed our earlier spectral assignments but also have provided new insights into the structure-function relationship in hemoglobin. (Supported by research grants from the National Institutes of Health and the National Science Foundation.)

T-AM-A7 PROTON NUCLEAR MAGNETIC RELAXATION STUDIES OF SICKLE CELL HEMOGLOBIN. I. M. Russu and C. Ho, Department of Biological Sciences, University of Pittsburgh, Pittsburgh, Pa. 15260.

Proton nuclear magnetic relaxation techniques have been used to study the polymerization process of sickle cell hemoglobin (Hb S). Previous ^1H nuclear magnetic resonance (NMR) studies from this laboratory have shown that several C2 protons of histidyl residues are excellent probes to investigate the surface conformational differences between human normal adult hemoglobin (Hb A) and Hb S. Spin-lattice relaxation rate (T_1^{-1}) measurements of these C2 protons of histidyl residues were obtained on a Bruker WH 360/180 NMR spectrometer. The experiments were carried out as a function of Hb concentration (10 to 17%) and temperature (17 to 37°C) in 0.1M Bis-Tris buffer in D_2O at pH 6.9. We have found that the T_1^{-1} values of these C2 protons of histidyl residues are sensitive to Hb concentration and temperature. For example, at a Hb S concentration of 13.5% or less and at a temperature of 25°C or less, the T_1^{-1} values of the ten observable C2 protons of histidyl residues of deoxy Hb S are the same as the corresponding ones in deoxy Hb A except for the C2 proton of β2 histidine, whose T_1^{-1} value is larger in Hb S than in Hb A. When the temperature or Hb concentration is increased further, three additional resonances in Hb S start to have T_1^{-1} values larger than the corresponding ones in Hb A. One of them is due to β146 histidine and the other two resonances have not been assigned. The T_1^{-1} values for C2 protons of certain histidyl residues are sensitive to those factors that can affect the polymerization of Hb S. The relationship between these results and the polymerization of Hb S will be discussed. (Supported by research grants from the National Institutes of Health.)

T-AM-A8 INVESTIGATIONS ON THE ORIGIN OF OBSERVED CHANGES IN ^{14}N HYPERFINE INTERACTION IN NITROSYLHEMOGLOBIN. S. K. Mun, Jane C. Chang and T.P. Das, Department of Physics, State University of New York, Albany, NY 12222.

In an earlier report, we had described our investigations on the electronic structures of four forms of nitrosylhemoglobin, with straight and bent NO bond and protonated and deprotonated proximal imidazole ligand[1]. Our investigations showed that the energy level arrangement did not differ significantly among these four structures, the unpaired electron always occupying an orbital of d_{z^2} symmetry, indicating that these types of changes in NOHb cannot by themselves explain the transition from 9-line to 3-line pattern observed under action of IHP or changes of pH. We have now studied the influence of changes in the length of the Fe-N_ϵ bond associated with the proximal imidazole and find substantial decreases in the isotropic ^{14}N hyperfine constant for the imidazole for Fe-N_ϵ bond extensions of 0.5Å and 1.0Å but not enough to make the hyperfine pattern in the EPR signal appear as a three-line one. This indicates that substantial additional extensions beyond 1.0Å would be required to explain the 3-line pattern as suggested in the literature[2]. Results will be presented for the completely ruptured systems involving the five-liganded NO-heme system. The influence of changes in orientations of Fe-N_ϵ bond and imidazole plane have also been studied and will be discussed. Grant support, NIH, HL15196.

1. J. Peisach, Ann. N.Y. Acad. Sci. 244, 187 (1975)

2. M.F. Perutz, J.V. Kilmartin, K. Nagai, A. Szabo and S.R. Simon, Biochemistry 15 378 (1976); J.C. Maxwell, W.S. Caughey, Biochemistry, 15, 388 (1976)

T-AM-A9 RESONANCE RAMAN SPECTROSCOPY OF METMYOGLOBIN HYDROXIDE, S.A. Asher and T.M. Schuster, Division of Applied Sciences, Harvard University, Cambridge, MA 02138 and Biological Sciences Group, University of Connecticut, Storrs, Conn. 06268.

Resonance Raman spectra and excitation profiles have been obtained within the 570-630 nm absorption band of purified Sperm whale Metmyoglobin hydroxide (MetMbOH). A large enhancement occurs for a Raman peak at 492 cm^{-1} which is shown by isotopic substitution of ^{18}O for ^{16}O to be almost purely a Fe - O stretch. The Fe-O vibration in MetMbOH occurs about 5 cm^{-1} to lower energy than the corresponding vibration at 497 cm^{-1} in human Methemoglobin hydroxide (MetHBOH) (S. Asher, L. Vickery, T. Schuster and K. Sauer, Biochem. (1977) 16, 5849) reflecting differences in the conformation of the heme between MetHbOH and MetMbOH. Excitation profile measurements indicate that the 570 - 630 nm absorption band results from the overlap of separate absorption bands from a high and low-spin MetMbOH. The spin-state sensitive Raman band reflecting the high-spin species at 1607 cm^{-1} shows an excitation profile maximum at about 610 nm while the low-spin Raman band occurring at 1644 cm^{-1} shows an excitation profile maximum at 580 nm. The Fe-O stretch at 492 cm^{-1} has an excitation profile maximum at about 600 nm. The relationship between the resonance Raman spectra of MetMbOH and other hemoglobin and myoglobin derivatives will be discussed. This work was supported by NSF grants DMR-76-22452 (to P. Pershan) and PCM-76-20041 and NIH grant HL-17494 (T.M.S.)

T-AM-A10 NANOSECOND TRANSIENT RAMAN SPECTRA OF PHOTOLYZED CARBOXYHEMOGLOBIN. J. M. Friedman, K. B. Lyons and P. A. Fleury, Bell Laboratories, Murray Hill, N. J. 07974.

We have obtained resonance Raman spectra of an unligated hemoglobin transient occurring 5 to 10 nsec after photolyzing off CO ligands, using a pulsed Nd:YAG laser in conjunction with a Raman spectrograph-multichannel analyzer. From these spectra, we conclude that for the heme, the major electronic and structural changes associated with the transition from ligated to unligated hemoglobin are nearly complete within 5 nsec after photolysis. Although the Raman spectrum of the transient closely resembles that of deoxyhemoglobin, there are shifts of up to 5 cm^{-1} in comparing the two spectra. The recent results of a Raman Difference Spectroscopy study[1] of deoxyHb stabilized in both R and T quaternary structures, indicate that the shifts in frequencies of the Raman spectrum of the transient relative to T structure deoxyHb do not originate primarily from differences in the quaternary structure. Instead, it seems likely that the transient spectrum is derived from an unligated heme electronically perturbed by the as yet unrelaxed tertiary structure of the ligated Hb.

[1] J. A. Shelnutt, D. L. Rousseau, J. M. Friedman and S. Simon, submitted for publication.

T-AM-A11 THE RESONANCE RAMAN SPECTRUM OF OXIDIZED CYTOCHROME OXIDASE AND SOME OF ITS INHIBITOR COMPLEXES. G. T. Babcock† and I. Salmeen, Michigan State University, East Lansing, MI 48824, and Ford Motor Company, Dearborn, MI 48121.

Photoreduction of oxidized cytochrome oxidase, which occurs during laser illumination of static, liquid samples, has been circumvented with the use of a flowing sample cell. The high frequency resonance Raman spectrum of the oxidized oxidase, obtained with Soret band (λ_{ex} = 441.6 nm) laser excitation, shows prominent bands at 1375, 1599 and 1654 cm^{-1} and shoulders at 1340 and 1580 cm^{-1}. Ligand binding to cytochrome a_3^{3+} to form either the high-spin $a_3^{3+}\cdot HCOOH$ or the low-spin $a_3^{3+}\cdot CN^-$ species causes no alteration in the oxidase spectrum other than removal of the 1580 cm^{-1} shoulder. These observations suggest that the Raman spectrum of oxidized cytochrome oxidase obtained with 4416 Å excitation is dominated by vibrations of the low-spin cytochrome a^{3+} chromophore. The Raman spectra of low- and high-spin heme a model compounds are in agreement with this conclusion: bands in the 1580-1650 cm^{-1} region show spin state dependent differences of 7-12 cm^{-1}. The selective enhancement of cytochrome a^{3+} vibrational modes in the oxidized protein can be explained by a consideration of the laser frequency in relation to the Soret absorption properties of cytochromes a^{3+} (absorption maximum = 427 nm) and a_3^{3+} (absorption maximum = 414 nm) calculated by Vanneste (Biochemistry 5, 838 (1966)). (†Research supported by a Cottrell grant from the Research Corporation and an MSU Biomedical Research Support Grant.)

T-AM-A12 INCLUSION OF EXCITED STATES IN EPR ANALYSIS FOR LOW-SPIN FERRIC CYTOCHROME P-450. M. Sharrock, Department of Physics, Gustavus Adolphus College, St. Peter, MN 56082

Electron paramagnetic resonance (EPR) data for low-spin ferric heme complexes are usually analyzed in terms of two crystal-field parameters, Δ/λ and V/Δ, and the so-called "orbital reduction factor", k. The factor k, expected to be less than unity because of covalency, frequently exceeds unity. This observation has been explained by Griffith (1) as being due to admixture of excited quartet (S=3/2) states. In cytochrome P-450 complexes, k is especially large (2), reaching the maximum known value of 1.94 in substrate-bound low-spin ferric P-450 (g= 1.97,2.24,2.42) from Pseudomonas putida (3). In view of this pronounced departure from expected behavior, it seems preferable to take account explicitly of quartet states.

This procedure leads to an alternate three-parameter fit, in terms of Δ/λ, V/Δ, and a third parameter that is related to the energies of the excited states and therefore to the cubic crystal-field strength. Substrate-bound P-450 is seen to have a larger tetragonal crystal field (Δ/λ), and lower-lying quartet states, than the substrate-free P-450 (g=1.91, 2.26, 2.45). Other classes of heme proteins (4) have weaker tetragonal fields and higher quartet states than either of these P-450 complexes.

1) J.S. Griffith, Mol. Phys. 21, 135 (1971)
2) M. Chevion, et al., J. Biol. Chem. 252, 3637 (1977) and references therein.
3) M. Sharrock, et al. Biochim. Biophys. Acta 420 8 (1976)
4) W. E. Blumberg and J. Peisach, in Probes of Struct. and Func. of Macromol. and Membranes, Vol. 2 (B. Chance et al., eds.) 1971

The author thanks Prof. I. C. Gunsalus for support and encouragement and Prof. P.G. Debrunner for helpful discussions.

T-AM-A13 TIME DEPENDENT CHANGES IN THE ESR SPECTRUM OF SPIN-LABELED HEMOGLOBIN.
A.G. Beaudoin, H. Mizukami, Dept. of Biology, and A. Romero-Herrara,* Dept. of Anatomy, Wayne State University, Detroit, MI 48202.

The attachment of 4-isothiocyanate-2,2',6,6'-tetramethyl-1-piperidinyl-N-oxyl (CAS Registry no. 36410-81-8) to human hemoglobin increases the oxygen affinity ($P_{\frac{1}{2}}$ = 2.1 mm Hg) and decreases cooperativity (n = 1.6 to 1.8; values determined at pH 7.15 in 0.05M phosphate buffer). The spin-labeled protein has a five line ESR spectrum, consisting of a narrow-banded (mobile) triplet superimposed upon a broad-banded (immobile) triplet. A temporal dependence of the line shape is evident immediately after isolation of spin-labeled protein from the unreacted spin label by elution on a column of Sephadex G-25. The amplitude of the mobile triplet increases relative to the immobile triplet over a period of several hours; after 24 to 48 hours, the spectral amplitude ratio returns to nearly the original levels. Although isothiocyanate preferentially binds to the amino terminal end of a peptide, the exact sites of attachment for this spin label in hemoglobin have not been verified. A binding study has indicated that there are three spin labels per tetramer, however Scatchard analysis has raised the possibility that four sites may exist. It would appear that removal of the unreacted spin label alters the equilibrium of a heterogeneous population of spin-labeled hemoglobin, possibly involving the dimer-tetramer equilibrium. Until equilibrium is reached, the conformational constraints upon the mobility of at least certain of the bound spin label(s) is altered and, if this is the case, would explain the observed spectral time dependence. Work is currently in progress to identify the sites of attachment and the results of these efforts will be presented.

T-AM-A14 PHOTOCHEMICAL ACTION SPECTROSCOPY OF THE HEME PROTEIN P-450 IN SOLUBLE AND MEMBRANE-BOUND MONOOXYGENATION SYSTEMS.
Heinz Schleyer, David Y. Cooper[X], Otto Rosenthal[X], and Pamela Cheung[X]. Harrison Dept. of Surg. Res. and Johnson Res. Fdn., Univ. of Pennsylvania, Philadelphia, Pa., 19104.

In monooxygenation reactions the heme protein P-450 undergoes one-electron reduction to an unliganded Fe^{2+}(S=2) form. This form combines with O_2 to P-450(Fe^{2+})·O_2, the reactive species which leads to product formation. Carbon monoxide (CO) competes with O_2 for this Fe^{2+} form and yields the catalytically inactive Fe^{2+}·CO complex which, like other Fe^{2+} - ligand complexes, can be photodissociated with high quantum yield. In a functional monooxygenation system binding of CO causes inhibition by decreasing the concentration of active enzyme. Photodissociation of the inactive Fe^{2+}·CO complex in presence of O_2, on the other hand, leads to the formation of additional reactive Fe^{2+}·O_2 and thus to at least partial restoration of the CO-inhibited enzyme activity. A combination of measurements of monooxygenase activity, its CO inhibition, and the spectral dependence of the photodissociation of Fe^{2+}·CO allows unequivocal spectral characterization of the light-absorbing key enzyme responsible for the observed phenomena. We have applied this technique to studies of a variety of chemical compounds, analyzed the ongoing processes, and developed a theoretical model to account for the underlying events in these complex reaction systems, and, in the case of microsomal preparations, the observed formation of more than one reaction product in parallel pathways. A description is given and the model is applied to the analysis of the results of a study of N-dealkylation reactions in comparison with steroid hydroxylation as catalyzed by the heme protein P-450.

T-AM-B1 INTRINSIC MOLECULES IN LIPID BILAYER MEMBRANES: A LATTIC MODEL. D.A. Pink and D. Chapman*, St. Francis Xavier University, Antigonish, N.S., Canada, and University of London, London, England.

A lattice model of lipid bilayer membranes which contain intrinsic molecules has been developed, cluster approximations have been used to calculate the change of transition temperatures and transition enthalpies as functions of intrinsic molecule concentration. The average values of lipid chain areas (the order parameter of the system) as well as probabilities for lipid-lipid, lipid-molecule and molecule-molecule "contacts" were also calculated. We have modelled cases where the portion of a protein surface which interacts with the lipid chains via the Van der Waal's interaction is "smooth" (cholesterol-like) or "rougher," and we have considered cases where a protein may bend a lipid tightly in either a rigid or a number of excited chain states. Our results show that, in general, lipids adjacent to proteins are by no means immobilized, that there can be significant numbers of protein-protein "contacts" and that a case occurs wherein a protein can actually make the fluid phase more fluid with a "boundary layer" of lipid differing little from the average lipid.

T-AM-B2 BINDING OF IMMUNOGLOBULIN G TO PHOSPHOLIPID VESICLES BY SONICATION. Leaf Huang, Dept. of Biochemistry, Univ. of Tenn., Knoxville, TN 37916 and Stephen J. Kennel,* Biology Division, Oak Ridge National Laboratory, Oak Ridge, TN 37830.

Purified goat immunoglobulin G (IgG) does not bind to sonicated phospholipid vesicles. However, when IgG is sonicated together with phospholipids, 4 to 40% of IgG can be bound to the vesicles. The extent of binding depends on the period and power of sonication, the IgG to lipid ratio, and the lipid composition. Anionic phospholipids such as phosphatidylglycerol and phosphatidylserine, but not cholesterol, enhance binding about 50% over that obtained using the neutral phosphatidylcholine. Binding of IgG causes extensive aggregation of vesicles, as shown by electron microscopy, and aggregates can be separated from unbound IgG by chromatography on Sepharose 4B. The IgG-vesicle aggregates remain stable in either phosphate-buffered saline or 50% fetal calf serum (fcs) up to 20 hours at 37°C, although substantial lipid degradation in 50% fcs was observed. The use of goat IgG containing antibody to a purified protein antigen allowed quantitation of antibody activity of these preparations. Immune IgG sonicated alone shows 100% of the original antigen binding capacity, while vesicle-bound IgG retains 30-50%. Antigen binding capacity of bound IgG is not increased when vesicles are lysed by 1.5% NP40, suggesting all of the bound IgG are exposed on the outer surfaces of the vesicles. Purified $F(ab')_2$ fragments also bind with vesicles by sonication. The potential usefulness of the IgG-bound vesicles for liposome targeting will be discussed. Supported by American Cancer Society grant IN-89J.

T-AM-B3 DETERGENT INDUCED DISRUPTION AND INACTIVATION OF Na^+,K^+-ATPase AS STUDIED BY FLUORESCENCE ENERGY TRANSFER. Gupte,S., Johnson, J.David, Schwartz, Arnold. Dept of Pharmacology and Cell Biophysics, Univ. of Cincinnati College of Med. Cincinnati, Ohio 45267

The integral proteins of membranes are sensitive to inactivation by various detergents because of the delipidation process. As an attempt to monitor protein-lipid interactions and to relate these processes to the enzymatic function of a membrane-bound enzyme, efficient fluorescence energy transfer was established from the tryptophans of Na^+,K^+-ATPase (NKA) to lipid-bound fluorescence probes [either dansyl phosphatidyl ethanolamine (DPE) or 12-(9-anthroyl) stearate (12-AS)] incorporated into the bilayer. The efficiency of this energy transfer was used to monitor the changes in lipid-protein interactions as a function of varying concentrations of detergents and was correlated to the hydrolytic activity of NKA. Sodium dodecyl sulfate (SDS) was selected due to its universal application for delipidation and deoxycholate:sodium cholate (DOC:NaC) in 3:1 ratio because of its use in the purification of NKA. Stepwise additions of SDS for concentrations ranging from 0.0005% to 1% with NKA-DPE and NKA-12-AS (100μg/ml), produced stepwise reductions in the energy transfer; 50% decrease occured at 0.019%. The ATPase activity of NKA paralleled the decrease in energy transfer at low concentrations of SDS; 50% decrease in activity occured at 0.013% SDS. Stepwise addition of DOC:NaC to NKA-DPE (100μg/ml) showed a 40% increase in the energy transfer at 0.3% detergent concentration followed by a decrease; 50% decrease occured at 0.7% DOC:NaC. The 50% decrease in NKA activity occured at much lower concentrations, 0.2%. Detergent produced decrease in scattering was monitored in both cases as an additional measure of the solubilization of the membrane. Fluorescence energy transfer from protein to lipids is a promising approach to investigate the interactions between membrane-bound proteins and their boundary lipids. Supported by HL22619, HL22039, and MDAA.

T-AM-B4 P-31 NMR STUDIES OF PHOSPHOLIPID HEAD GROUP - RHODOPSIN INTERACTIONS. N. Zumbulyadis and D. F. O'Brien, Research Laboratories, Eastman Kodak Company, Rochester, N.Y. 14540.

The interaction of phospholipid head groups with rhodopsin in recombinants with different lipids has been studied by phosphorus-31 NMR, both at conventional (21 kGauss) and high (63 kGauss) magnetic field strength. The magnetic field dependence of the phosphorus linewidths, spin-lattice relaxation times and nuclear Overhauser enhancements is analyzed in terms of anisotropic head group motion and fast chemical exchange between bulk and protein associated lipid. In rhodopsin:asolectin recombinants, a preferential broadening of the phosphatidylcholine (PC) resonance is observed, with considerably less change in the width of the phosphatidylethanolamine (PE) signal. This observation could be interpreted as a selective enrichment of the PC in the boundary lipid region. It has recently been reported that unlike PE, PC is not hydrogen bonded; therefore, the observed preferential interaction could possibly be due to hydrogen bonding between PC and the rhodopsin incorporated in the bilayer. The phosphorus spin-lattice relaxation times decrease with increasing field strength. Chemical shift anisotropy relaxation becomes a major T_1 mechanism at 63 kG. We have developed a novel spin-lattice relaxation theory to interpret the T_1 data in terms of fast restricted motions. Results describing the head group motion and the effects of incorporated rhodopsin will be presented.

T-AM-B5 ^2H AND ^{31}P NMR OF PROTEIN LIPID INTERACTIONS IN MODEL AND BIOLOGICAL MEMBRANES. E. Oldfield, School of Chemical Sciences, University of Illinois at Urbana, Urbana, IL 61801.

High-field ^2H and ^{31}P NMR spectra of a variety of specifically deuterated protein-lipid complexes and intact biological membranes have been obtained. We find no evidence for rigid, ordered or immobilized boundary lipid in any of the systems investigated. Instead, we find that proteins disorder the hydrocarbon chain organization of lipid membranes. We find no evidence for an immobilized "boundary lipid", "annulus" or "halo" structure in any system studied. Exchange between free lipid and lipid associated with protein is in many cases fast ($>10^3$ s^{-1}). The disordering effects of proteins are manifested in decreases in both ^2H NMR quadrupole splittings and ^{31}P chemical shielding anisotropies. However, in some cases these changes are linked to decreases in T_2 indicating (perhaps) a decrease in the rates of motion. Our results may be made to be consistent with the EPR view of boundary lipid by invoking either timescale or specific protein-nitroxide interactions. New results with deuterated spin-labels relevant to the latter possibility will be presented.

T-AM-B6 ON THE MECHANISM OF PALMITYL CARNITINE INACTIVATION OF NA^+,K^+-ATPASE. J. David Johnson, S. Gupte and Arnold Schwartz, Dept. of Pharmacology and Cell Biophysics, Univ. of Cincinnati College of Medicine, Cincinnati, Ohio 45267.

Recently much attention has been focused on determining the role of fatty acids in the degradation of membrane function. Of particular importance is the mechanism of action of palmityl carnitine (p. carn). Concentrations of p. carn are thought to increase during ischemia and it has been shown to inhibit ATP hydrolysis in both Ca^{2+}-ATPase and Na^+,K^+-ATPase (NKA). The inhibition of NKA (100µg/ml) activity and the clearing of the slight turbidity of NKA suspensions was observed to be maximal near 160-200µM p. carn. The fluorescent lipid DPE (dansyl phosphatidyl ethanolamine) was incorporated into vesicles of NKA and phosphatidyl choline to form DPE-NKA and DPE-PC. Addition of p. carn to both DPE-NKA and DPE-PC produced 40% and 100% enhancements in DPE fluorescence which were maximal near 120 and 160µM, respectively. These observations provide direct evidence of p. carn induced perturbation of the lipid phase of the membrane. Centrifugation studies revealed that increasing amounts of DPE, phospholipid and solubilized protein were found in the supernatant and the pellet size decreased as increasing amounts of p. carn were added to NKA-DPE. Efficient fluorescence energy transfer was observed between the tryptophyl residues of NKA and DPE incorporated into its bilayer. This energy transfer allows us to monitor directly changes in protein-lipid interactions and the delipidation of membrane bound proteins produced by detergents (Gupte et al. This Volume). This energy transfer in NKA-DPE is abolished by 200µM p. carn in a manner analogous to the effect of detergents (SDS) on the disruption of energy transfer. These studies suggest that p. carn may act much like a detergent to disrupt the NKA membrane, reduce the turbidity, increase DPE fluorescence, disrupt energy transfer and inactivate this enzyme. SUPPORT, HL22619, HL22039, MDAA.

T-AM-B7 ACTIVATION FOR ACCESS TO THE HYDROPHOBIC INTERIOR BINDING REGION OF HUMAN SERUM ALBUMIN IS ENTROPY CONTROLLED. W. Scheider, University of Michigan, Ann Arbor, MI 48109.

Reaction rate studies of the complexation of long-chain fatty acid (FA) with human serum albumin (HSA) provide evidence that such complexation occurs in two sequential steps. In the first step, the ligand rapidly associates in a non-specific way with the exterior, so-called tertiary binding sites on HSA. The second step, during which it is postulated that the loosely bound FA gains access to the primary organic binding region normally interior to the protein, is a slower process (∿300 msec), and is rate limited by a negative entropy of activation of approximately (-16 Kcal/M). The enthalpy of this activation is negligible, suggesting that the opening up of the molecule for access to the interior requires little in the way of bond breaking. These results have been confirmed by dissociation activation studies as well. These rate experiments were done by stopped-flow dielectric technique (W. Scheider, 1977. Ann. N. Y. Acad. Sci 303:47-58).

T-AM-B8 CO-PRECIPITATION OF SOLUBLE PROTEINS WITH BILE SALTS. R. Fielding,* and S. S. Rothman. University of California, San Francisco, California 94143.

Co-precipitation of a variety of soluble proteins with bile salts occured when bile salts (Na cholate and its conjugates) were precipitated from aqueous solution by titration to their insoluble conjugate acids [or after the addition of metal ions (Cu^{++}, Fe^{++}) which form insoluble bile salts]. The % of protein precipitated increased with the amount of bile salt precipitated and approached 100% for some proteins. For α-amylase the % precipitated for a given amount of bile salt precipitate was constant at low protein concentrations, but began to fall off above 1 mg/ml. This suggests saturable equilibrium-dependent binding between protein and bile acid or salt. Amylase precipitated in this manner is not denatured and full activity can be recovered from the precipitate, which can be solubilized in base, glycocholate or ethanol. Increasing ionic strength from 0 to 1.5 M NaCl caused a slight (20-25%) reduction in co-precipitation. At neutral pH soluble bile salts did not form precipitates with proteins and binding was not observed by diafiltration. Proteins did not precipitate in the presence of already precipitated bile acids. Thus, it appears that individual molecules or small aggregates of uncharged bile acids/salts are responsible for co-precipitation. The insoluble amphipathic bile acids may precipitate hydrophilic proteins in a manner opposite, but analogous, to that by which soluble amphipathic bile salts (e.g., DOC) remove "hydrophobic" (insoluble) proteins from membranes into solution. The bile acid-protein interaction would be hydrophilic and act to exclude water from the protein's surface. We have reported a similar phenomenon with phosphatidyl inositol. Since biological amphiphiles can remove "soluble" proteins from solution, the removal of solvent water from proteins may not represent a significant energy barrier to their insertion into membranes under appropriate conditions in vivo. (Supported by NIH grants AM16990 and GM00927).

T-AM-B9 NON-RANDOM DISTRIBUTION OF PM2 RECEPTORS ON THE HOST CELL OUTER MEMBRANE. Paul Wanda, A. D. Keith*, and W. Snipes, The Pennsylvania State University, University Park, PA 16802.

The distribution of PM2 receptors on the host cell surface was investigated by measuring cell survival upon exposure to large multiplicies of virus. A temperature-sensitive cell mutant, designated RH12, was isolated which has normal amounts of receptor when grown at 25°C but no functional receptors when grown at 32°C. Cultures of RH12 grown at 25°C rapidly lose their sensitivity to PM2 upon subsequent growth at 32°, giving survival values of 24% and 67% after one and two mass doublings, respectively. These results are discussed in relation to various models for the synthesis and insertion of cell membrane components. A model is proposed in which PM2 receptors, independent of their mode of insertion, tend to aggregate and form patches on the cell surface. Reasonable agreement between this model and the data is obtained if the PM2 receptor molecules form, on the average, about two patches per cell, and these patches segregate at random during cell division. This work was supported by the U. S. Department of Energy.

T-AM-B10 PERTURBATION OF PROTEIN-LIPID INTERACTIONS IN BACTERIOPHAGE φ6. Neal DeLuca*, A. D. Keith* and W. Snipes, The Pennsylvania State University, University Park, PA 16802.

Certain quasi-spherical, hydrophobic molecules inactivate enveloped viruses such as φ6, PM2, HSV-1 and HSV-2, without harming the host cell. One of these molecules is the spin label 1,3-diphenyl-2,4',4'-dimethyloxazolidine-N-oxyl-propane, designated BPN. Partitioning of BPN into the membrane of φ6 results in the loss of a membrane protein necessary for infection. Experiments with radioactively labeled virus showed that BPN-treated virions are unable to attach to the host cell. Spin label studies were also carried out with BPN in preparations of φ6, φ6 phospholipids, and the host cell, Pseudomonas phaseolicola HB10Y. These studies showed a much greater restriction of rotational motion for BPN in the virus as compared to viral lipids and host cells. Considerations of the physical and chemical properties of the φ6 membrane suggest that the antiviral spin label is localized in the boundary lipid surrounding membrane proteins. This work was supported by the U. S. Department of Energy.

T-AM-B11 CARBON-13 NMR OF GANGLIOSIDES G_{M2} AND G_{D1a} AND GANGLIOSIDE SUGARS. L.O. Sillerud,* D.E. Schafer, J.H. Prestegard, R.K. Yu,* and W.H. Konigsberg* (Intr. by R.J. Barrnett), Yale University, New Haven CT 06510, and VA Medical Center, West Haven CT 06516.

High-resolution ^{13}C NMR spectra of gangliosides G_{M2} and G_{D1a}, as well as their constituent sugars and the oligosaccharide portion of ganglioside G_{M1}, have been obtained at 67.89 MHz and pH 7.0. These high-field spectra reveal several features of the monomeric sugars previously unreported. For example, changes in anomeric configuration perturb every carbon in galactose, including the exocyclic C_6. The glucose moiety of lactose shows similar behavior, with alterations in configuration giving rise to distinct peaks for α and β anomers, even for the ring carbon C_4, which participates in the linkage to the galactosyl residue. The same phenomena are found in neuraminyllactose and in the oligosaccharide portion of ganglioside G_{M1}. The observation of resonances from the α configuration of sialic acid in a solution of predominantly β anomer has enabled us to establish hydrogen bonding of C_8 to the carboxyl C_1 oxygen in only the α form. Titration of the ^{13}C shifts with pH in α sialic acid and in the oligosaccharide portion of G_{M1} showed that a similar hydrogen bonding occurs in G_{M1}. We observe distinct resonances from the anomeric carbons of the two sialic acids in G_{D1a}, indicating non-equivalence of these anionic residues. The assignments for the spectrum of ganglioside G_{M2} provide a good test for the understanding of ^{13}C shifts accompanying complex oligosaccharide formation.

T-AM-B12 STABILIZATION OF CHOLERA ENTEROTOXIN BY BINDING TO GANGLIOSIDE G_{M1}. L.O. Sillerud,* D.E. Schafer, R.K. Yu,* and W.H. Konigsberg,* Yale University, New Haven CT 06510, and VA Medical Center, West Haven CT 06516.

Differential scanning calorimetry (DSC) of intact cholera enterotoxin in solution at pH 7.5 revealed two transitions, an endothermic transition at about 51°C and an exothermic transition at 75°C. In general, exothermic transitions are seen in DSC only if they are kinetically limited--that is, if their rate at room temperature is so low as to render the reaction essentially static. Addition of ganglioside G_{M1} to the toxin results in the formation of a complex. When we added G_{M1} to the toxin and ran DSC scans on the complex the temperature of the exothermic peak was very sensitive to the presence of G_{M1}. This peak shifted from 75°C for the unliganded toxin to 48°C for toxin saturated with G_{M1}, suggesting that G_{M1} increases the rate of toxin aggregation. The denaturation temperatures of the toxin subunits were also perturbed by the interaction with G_{M1}. The transition temperature of the B subunit was raised from 51°C to 53.5°C on saturation with G_{M1}. When the mole ratio of G_{M1} to toxin reached 5, two transitions suddenly appeared, at 81°C and 93°C. As the ratio of G_{M1} to toxin was further increased, the 81°C transition diminished and the 93°C transition grew. We have also observed a transition at 93°C for the isolated A subunit free in solution. These results are consistent with the possibility that when five sites on the toxin, presumably corresponding to the five B subunits, are all occupied by G_{M1} molecules, a rearrangement may ensue, resulting in release of the A subunit from its association with the rest of the toxin molecule.

T-AM-B13 EFFECTS OF CROSSLINKING ON THE ATTACHMENT OF MEMBRANE PROTEINS TO THE CYTOSKELETON. N. D. Gershon, Physical Sciences Laboratory, Division of Computer Research and Technology, National Institutes of Health, Bethesda, MD 20014.

Processes that might lead to attachment of membrane proteins to submembranous filaments after crosslinking are considered. Because of their size, patches formed by crosslinking proteins might be entangled or interact with the filamentous network to a greater extent than a single protein. In addition, microfilaments might be sensitive to mechanical disturbances and to their rate of change. Areas under patches and caps are likely to be more static and less mechanically disturbed than areas under the rest of the cell surface and thus such delicate filaments can be polymerized more extensively under patches and caps. Also patches might serve as nucleation centers for filament polymerization.

T-AM-B14 NICOTINIC RECEPTOR CONTROL OF Ca UPTAKE BY SPERM CELL FRACTIONS. L. Nelson, Department of Physiology, Medical College of Ohio, Toledo, Ohio 43699.

Electron microscopic cytochemistry and autoradiography of bull sperm cells plasmolyzed by incubation in hypotonic KCl (15mM) show that the major site of calcium binding is the cytoplasmic surface of the plasma membrane. $LaCl_3$ has a strong affinity for these sites while showing no tendency to bind either with the external surface of the membrane or with demembranated fragments of midpiece or principal piece. Furthermore, pretreatment of suspensions of sperm cell fractions with La^{3+} increases the uptake of radioactively-labeled calcium ion. It had previously been shown that agents which depolarize nicotinic receptors tend to decrease the sperm cell membrane's binding of calcium. Millimolar amounts of nicotine, decamethonium and succinylcholine decrease the acetylcholinesterase activity of isolated sperm cell plasma membranes. Calcium ions cause a partial reversal, while La^{3+} strongly restores the activity of the enzyme. These data suggest a high degree of interaction between the sperm cell's cholinergic receptors and Ca^{2+} uptake.

T-AM-C1 EFFECT OF USE-DEPENDENT INHIBITION BY YOHIMBINE ON SODIUM INACTIVATION. G. Ehrenstein, R.J. Lipicky and D.L. Gilbert, NINCDS, NIH, Bethesda, Md. 20014 and Dept. of Pharmacology, Univ. of Cincinnati, Cincinnati, Ohio 45267.

Yohimbine is a drug that inhibits current through sodium channels in a use-dependent manner. We have determined the effect of use-dependent inhibition by yohimbine on the voltage dependence of the sodium inactivation parameter h_∞ in the squid giant axon. The conventional method of measuring h_∞ is to apply a long step voltage prepulse of variable amplitude followed by a command depolarizing step voltage pulse. For each prepulse voltage, h_∞ is proportional to the peak sodium current of the command pulse. The voltage dependence of h_∞ can thus be described by plotting the peak sodium current of the command pulse as a function of prepulse potential. If, in order to determine h_∞ under use-dependent conditions, a repetitive sequence of identical pulse pairs, each pair consisting of a prepulse and a depolarizing command pulse, were used to make the measurement of h_∞, ambiguity results. Any change in peak sodium current during a command pulse could be caused either by the effect of prepulse amplitude on use-dependent inhibition and/or by a change in $h_\infty(V)$. To avoid this ambiguity, we applied a series of depolarizing pulses with no prepulse followed by a single depolarizing command pulse with a long prepulse. This protocol was then repeated with different prepulse voltage amplitudes and constant command pulse voltage amplitude. Using this procedure, we found that use-dependent inhibition by yohimbine causes a shift of the inactivation curve $h_\infty(V)$ in the hyperpolarizing direction.

T-AM-C2 FORM AND SITE OF ACTION OF DIPHENYLHYDANTOIN ON THE SODIUM CHANNEL OF SQUID AXONS. R.S. Morello and T. Begenisich, Department of Physiology, University of Rochester, Rochester, N.Y. 14642.

The effects of the antiepileptic drug, diphenylhydantoin, (DPH, Dilantin, Penytoin) on the sodium channel currents of perfused, voltage clamped squid giant axons were studied. 100 uM DPH was applied either internally or externally at various internal or external pH values. Since it is a weak acid (pK=8.3), DPH can exist in either the neutral or anionic form. Externally applied DPH blocks sodium currents more effectively at lower external pH. Thus DPH either acts externally in the neutral form or the neutral form crosses the membrane and is effective internally. Internally applied DPH is more potent at lower internal pH. Further, internal DPH is unaffected by changes in external pH. These results suggest that the drug acts internally in the uncharged form. We found little effect of the drug on potassium currents.

Conditioning pulses of up to 2 seconds in duration do not alter the action of DPH. Its activity is reduced by hyperpolarized holding potentials suggesting that DPH interacts with the long term inactivation process. (Supported by USPHS 1K04 NS00322-01 and 1 R01 NS14138-01)

T-AM-C3 CURRENT-DEPENDENT BLOCK OF NERVE MEMBRANE SODIUM CHANNELS BY PARAGRACINE. C. H. Wu, I. Seyama,* and T. Narahashi. Dept. of Pharmacol., Northwestern Univ. Med. Sch., Chicago, IL 60611, U.S.A. and Dept. of Physiol., Hiroshima Univ. Sch. Med., Hiroshima 734, Japan.

Paragracine, isolated from the coelenterate species Parazoanthus gracilis, selectively blocks sodium channels in a current-dependent manner. When it is applied internally to the squid axons at a concentration of 0.20-0.25 mM, the inward sodium current (I_{Na}) remains unchanged while the outward I_{Na} shows progressive depression when pulsed at a frequency of 1 Hz. This block may be reversed by generating inward I_{Na}. The frequency-dependent blocking action depends on the direction of current flow rather than the membrane potential. When the external sodium concentration is reduced from 445 mM to 111 mM, the direction of I_{Na} is changed from inward to outward at E_m = 30 mV. Under this condition, the frequency-dependent block occurs. As the outward I_{Na} at large depolarizations is increased by such a maneuver, the extent of blockage is increased proportionally. In axons in which sodium inactivation has been removed by pronase, paragracine induces a time-dependent block in addition to the frequency-dependent block. It has no effect on sodium channels when applied externally. Potassium channels are not affected by paragracine applied either internally or externally. The drug will become a useful tool in characterizing the conformation of sodium channels. Supported by NIH grant NS 14144.

T-AM-C4 INTERACTION BETWEEN QX 314 AND BATRACHOTOXIN IN CULTURED NEUROBLASTOMA CELLS. L.M. Huang and G. Ehrenstein, NINCDS, NIH, Bethesda, Maryland, 20014

There are two possible mechanisms for local anesthetics to reduce the conductance of sodium channels. The drug may enter the channel and occlude it, thus impeding the transport of Na^+. Another possible mechanism is that the drug may bind to regulatory or gating molecules of the channel, and tend to keep the gate in the closed conformation. In order to distinguish between these two possibilities, we have studied the interaction of a quaternary derivative of lidocaine, QX 314, with a channel opener, batrachotoxin. Batrachotoxin causes a persistent activation of Na^+ channels in neuroblastoma cells. QX 314 was found to reduce this batrachotoxin-induced Na^+ uptake. In the presence of an excess of batrachotoxin, the apparent dissociation constant for QX 314 is 3 - 4 mM. By varying the batrachotoxin concentration, we found that QX 314 is a competitive inhibitor of batrachotoxin. This strongly suggests that QX 314 acts at the same site as does batrachotoxin. Since batrachotoxin is a channel-opener and thus cannot occlude Na channels, it is likely that QX 314 also does not occlude Na channels, but instead blocks the channel by acting on the regulatory component or the gating molecules in the membrane.

T-AM-C5 VOLTAGE- AND FREQUENCY-DEPENDENT BLOCK OF NA CHANNELS BY STEREOISOMERS OF LOCAL ANESTHETICS. J.Z. Yeh, Dept. of Pharmacology, Northwestern University Medical School, Chicago, ILL 60611.

Optically active tertiary amine local anesthetic RAC 109-I has been found to be at least two-fold more potent than its enantiomer RAC 109-II in blocking Na channels of voltage-clamped nodes of Ranvier. Similar results were observed with their corresponding quaternary derivatives RAC 421-I and RAC 421-II. These compounds also exhibited the accumulated frequency-dependent block (Hille, 1975, 1976). We further investigated the kinetics of blocking Na channels by internally applied drug to voltage-clamped giant axons of squid. At 0.5 mM, both RAC 109-I and RAC 109-II produced an initial resting block of 32%. Repetitive depolarization to -20 mv at 1 Hz increased RAC 109-I block to 69% and RAC 109-II to 42%. Repetitive depolarizations to +80 mv further enhanced the block, reaching 93% block for RAC 109-I and 66% for RAC 109-II, respectively. This difference in frequency- and voltage-dependent block between RAC 109 enantiomers was also observed with RAC 421 enantiomers. Longer pulses were more effective than shorter ones in enhancing the accumulated frequency-dependent block caused by RAC 109-I and RAC 421-I. Recovery from block was observed to be slower for these two compounds. Thus the difference in the kinetics of channel block among these enantiomers could account for the observed difference in potency in suppressing Na currents and nerve block. Since the initial resting block exhibits little or no stereospecificity and this block probably represents the initial drug entry into open channels, then the subsequent difference in dynamics of block between enantiomers suggests that the dissociation of drug molecule from channels is stereospecific.
Supported by NIH grants ROI GM-24866 and KO4 GM-442.

T-AM-C6 LIKE A LOCAL ANESTHETIC ? OCTANOL IMMOBILIZES GATING CHARGE. R.P.Swenson Jr. Dept. of Physiology,Univ. of Pennsylvania,Philadelphia,Pa.

Octanol-induced block of sodium channels closely resembles block by local anesthetics. A brief list of the similarities includes:voltage-dependent block of the sodium channel (crayfish),a small hyperpolarizing shift of the steady-state inactivation curve(crayfish and squid),a speeding of τ_h(measured from the falling phase)at most membrane potentials (crayfish and squid),a partial relief of block by hyperpolarizing prepulses or more negative holding potentials(crayfish).Unlike most local anesthetics octanol fails to exhibit frequency dependence(crayfish and squid). Among the local anesthetics only the neutral anesthetic benzocaine does not show frequency dependence(Hille,J.Gen.Physiol.69:497,1977). If local anesthetics increase the probability of the inactive state as hypothesized by Schwarz et al.(Biophys.J. 20:343,1977), then an effect on gating current similar to that produced by inactivation could be anticipated-i.e.-an immobilization of gating charge (Armstrong & Bezanilla, J.Gen.Physiol.70:567,1977). Gating current measurements reveal that 1mM octanol decreases the "on" gating charge in a voltage-dependent manner. A small decrease in the charge was seen at low depolarizations; this effect increased to a maximum of 50% at larger depolarizations. When the membrane was returned to -140 mV following a brief depolarization, an additional slow component of the "off" gating current was observed in the presence of octanol. The results may mean that octanol increases the population of sodium channels in the inactive state, and that hyperpolarization relieves block by returning these channels to their normal resting state.
Supported by NIH NS14144 and NS1254.

T-AM-C7 SODIUM CHANNEL INACTIVATION IN CRAYFISH GIANT AXONS AND MODIFICATION BY DIETHYL ETHER. B.P. Bean, P. Shrager, and D.A. Goldstein, Dept. of Radiation Biology and Biophysics and Dept. of Physiology, Univ. of Rochester Medical Center, Rochester, N.Y. 14642

Kinetics of sodium currents under voltage-clamp were investigated in normal and ether-treated crayfish giant axons. Sodium currents were separated from potassium and leak currents by using TTX-subtraction and/or using 1 mM 4-aminopyridine to block potassium currents. During a single voltage-step, sodium currents decay with a time-course which is well described by a single exponential. Currents inactivate completely, within experimental error, at all potentials at which there is measurable activation. As in squid and frog nerve, the time-constant of inactivation is strongly dependent on membrane potential, increasing from about 1 msec. at 0 mv. to 5 msec. at -40 mv (2°C). Inactivation is faster when diethyl ether is present in the bathing solution. 30-80 mM ether decreased τ_h by 10-40%. τ_h was decreased at all membrane potentials. When inactivation was produced with 50 msec prepulses to various potentials, the curve of inactivation vs. membrane potential was shifted slightly (2-6 mv.) in the hyperpolarizing direction by 50-100 mM ether. In addition to affecting inactivation kinetics, 30-120 mM ether decreased peak sodium currents by 10-50% without significantly changing the reversal potential. In experiments in which externally-stimulated, propagated action potentials were recorded (20°C), the only observed effect of clinical concentrations (10-25 mM) of diethyl ether was a decrease in the refractory period. This is consistent with more rapid inactivation kinetics.

Supported by NIH grant NS 10500. Work performed in part under contract with the U.S. Dept. of Energy and assigned Report No. UR-3490-1506.

T-AM-C8 DIFFERENTIAL EFFECTS OF DEUTERIUM OXIDE AND TEMPERATURE ON IONIC AND ASYMMETRY CURRENTS IN MYXICOLA GIANT AXONS. J.O. Bullock and C.L. Schauf. Department of Physiology, Rush University, Chicago, Illinois 60612.

In dialyzed Myxicola axons substitution of heavy water (D_2O) externally and internally slows both the sodium and potassium kinetics and decreases the maximum conductances. Furthermore, this effect is strongly temperature dependent in that the magnitude of the slowing produced by D_2O substitution decreases with increasing temperature over the range 3°C to 14°C. At 3°C the time constants for Na^+ activation and inactivation and K^+ activation are increased by 50-60%, while at 14°C the increase is only 15-25%, yielding a Q_{10} of approximately 1.4. The relatively small magnitude of the D_2O effect, combined with its strong temperature dependence suggest that the rate limiting process producing a conducting channel involves appreciable local changes in solvent structure. Maximum conductances in the presence of D_2O were decreased by approximately 30% while the voltage dependence of both g_{Na} and g_K was not appreciably changed by D_2O substitution. In contrast to the effects of heavy water substitution on the ionic currents, membrane asymmetry currents were not altered by D_2O, suggesting that gating charge movement may preceed by several steps the final transformation of the Na^+ channel to a conducting state. In Myxicola axons the effect of temperature alone on asymmetry current kinetics can be well described via a simple temporal expansion equivalent to a Q_{10} of 2.2 which is somewhat less than the Q_{10} of g_{Na} activation. The integral of membrane asymmetry current, representing maximum charge movement, is, however, not appreciably altered by temperature.

T-AM-C9 MODULATION OF AMINOPYRIDINE BLOCK OF POTASSIUM CHANNELS BY MEMBRANE POTENTIAL, H^+, AND Cs^+. G.E. Kirsch*, G.S. Oxford, J.Z. Yeh, and T. Narahashi, Dept. of Pharmacology, Northwestern Univ. Medical School, Chicago, IL 60611 and Dept. of Physiology, University of North Carolina, Chapel Hill, NC 27514.

The block of potassium channels by aminopyridine derivatives (2-AP, 3-AP, 4-AP, 2,3-DAP, and 3,4-DAP) in nerve membranes is relieved by depolarizing pulses. We investigated the unique blocking characteristics of this group of compounds applied internally to voltage-clamped squid axons under four experimental conditions: varying internal pH, varying holding potential, internal addition of TEA and its phenylpropyl derivative ($\emptyset$-C_3), and external replacement of Na^+ with Cs^+. The time course of block re-establishment was determined with a constant test pulse at varying intervals following either a single 8 ms conditioning pulse or trains of conditioning pulses. Decreasing the internal pH (which increases the charged form of aminopyridines) speeded the rate of block re-establishment. For example, 2,3-DAP (pK_a 7.0) at a concentration of 0.5mM, had average time constants of 1.5 sec at pH 6.3, where 17% of the drug molecules are in the neutral form, and 31.1 sec at pH 8.6 where the neutral form predominates (98%). Increasingly more positive holding potentials (range=-100 to -50 mv) also speeded block re-establishment. This effect of membrane potential was evident at both high and low pH. TEA (0.01-3mM) and $\emptyset$-C_3 (0.1mM) were observed to have no effect upon the rate of block re-establishment, whereas external Cs^+ (200mM) significantly prolonged block re-establishment with most aminopyridine derivitives. These data suggest that the affinity of the charged form of aminopyridine for the blocking site(s) is greater than the neutral form and are consistent with a model for the blocking site(s) in which Cs^+ can modulate AP binding affinity while TEA derivatives directly exclude access of AP molecules. Supported by NIH grant NS 14144 and by NSF grant BNS 77-14702.

T-AM-C10 Cholesterol Movement and Loading in Perfused Squid Axon, J. Steele*, M.J. Poznansky, G. Redman, M.S. Brodwick and D.C. Eaton, Department of Physiology, University of Alberta, Edmonton, Canada, and Department of Physiology and Biophysics, University of Texas Medical Branch, Galveston, Texas.

Cholesterol has been shown to play an important role in membrane structure and function (Demel & de Kruyff, BBA *457*: 259, 1976) and to exchange between bilayers. As a prerequisite to studying the effect of altered membrane cholesterol on electrical properties of the squid axon, we have demonstrated that it is possible to change membrane cholesterol levels by including sonicated lipid vesicles in either the external or internal perfusates. We monitored cholesterol movement by using vesicles composed of ^{3}H-cholesterol, egg lecithin and trace amounts of ^{14}C-cholesterol oleate as a non-exchangeable marker. Cholesterol loading was achieved by perfusing the axon with vesicles with a 2:1 mole ratio of cholesterol to egg lecithin. The axon was then perfused with standard perfusate and the amounts of ^{3}H and ^{14}C contained in the preparation were determined. If we assume equilibration of ^{3}H-cholesterol throughout the axonal and glial membranes, then an average of 0.54 µg of cholesterol was added in three separate axons, or in other words a 1:1 cholesterol to phospholipid mole ratio was attained. Only trace amounts of ^{14}C-cholesterol oleate were found. We also were able to demonstrate that cholesterol introduced on one side of the membrane could be depleted from the opposite side. Labelled cholesterol-egg lecithin vesicles were included in the external perfusate and cholesterol-free sphingomyelin vesicles were included in the internal perfusate. In one experiment typical of three, ^{3}H-cholesterol appeared in the internal perfusate at a rate of 4.1 µg/2 hr, suggesting a turnover rate of under 2 min for axon membrane cholesterol. None of the ^{14}C-cholesterol oleate appeared in the internal perfusate, indicating that there was no contamination of the internal perfusate with externally applied vesicles.

T-AM-C11 LIPOSOME MEDIATED LIPID EXCHANGE EFFECTS ON SQUID AXON MEMBRANE CURRENTS. **G. A. Redmann, M. S. Brodwick, D. C. Eaton, J. Steele* and M. Poznansky, Department of Physiology and Biophysics, University of Texas Medical Branch, Galveston, Texas 77550; University of Alberta, Edmonton Alberta T6G 2E2, Canada.**

Liposome mediated cholesterol addition and depletion in Aplysia ganglion respectively decreases and increases action potential frequency (Stephens and Shinitzsky, Nature 270: 267). We have studied the effects of liposome mediated cholesterol addition via dipalmityl phosphatidylcholine:cholesterol and dioeoylecithin:cholesterol (4:1 or 1:1) vesicles and cholesterol depletion via lecithin and sphingomyelin vesicles on voltage clamped and internally perfused squid axon. To monitor the alteration in lipid composition we used tritiated cholesterol and C^{14} labeled phospholipid containing vesicles. The liposomes were added to either side of the membrane, with the radioactive vesicles being placed on one side. (See Steele et al., this volume). Cholesterol addition on either side of the membrane resulted in 1) an increase in time to peak Na inward current for the potentials tested 2) reduced peak inward current 3) an increase in inactivation time constant 4) a slight reduction in K steady-state outward current 5) an approximately 10 mV depolarizing shift in the peak transient current-voltage relationship. Internal sphingomyelin vesicle perfusion reduced inward Na current time to peak. These effects were accompanied by negligible effects on leakage. Cholesterol addition apparently decreases the rate of movement of the Na gating molecule, possibly by alterations of the adjacent lipid environment. These effects may reflect membrane viscosity, thickness or surface potential influences on Na gating particle mobility. The current-voltage shift is consistent with a negative surface charge dilution mechanism.
Supported by DHEW grant NS-11963.

T-AM-C12 LANTHANUM EFFECTS ON SQUID GIANT AXON CONDUCTANCES. Stewart W. Jaslove and John W. Moore, Duke Univ., Durham, N.C. 27710.

Lanthanum ions were applied to the outside of intact giant axons of the squid (Loligo pealii) in the sucrose gap voltage clamp. All test solutions were maintained at constant ionic strength, pH and osmolarity, and contained either calcium (50 mM) or lanthanum (0.2-10 mM) as the only polyvalent cation. In spite of considerable variability, the results were similar to the finding in lobster axon that lanthanum at low concentration mimics the effects of calcium in maintaining low leakage and "normal" ionic currents[1]. However, while all concentrations of lanthanum tested slowed and blocked the potassium conductance, only the higher concentrations had this effect on the sodium system. The lowest test concentration (0.2 mM) appeared to mimic low calcium, in increasing the leakage and shifting the sodium conductances in the depolarizing direction.

[1]Takata, M., W. F. Pickard, J. Y. Lettvin, and J. W. Moore. (1966). J. Gen. Physiol. 50: 461-471.

T-AM-C13 NODE OF RANVIER MEMBRANE PROBED BY ALAMETHICIN

Michael D. Cahalan and James E. Hall Department of Physiology, University of California, Irvine, California 92717

The object of this study is to probe the membrane environment of the node of Ranvier. Alamethicin, a peptide antibiotic, induces a strongly voltage-dependent conductance, well studied in planar bilayers of many different lipid compositions. By studying alamethicin in the node of Ranvier and comparing the results obtained in bilayers, we can say something about the environment presented by the node to its native conductance mechanisms.

We have compared the alamethicin conductance in voltage-clamped bullfrog nodes of Ranvier bathed in 120 mM CsCl Ringer with alamethicin conductance in phosphatidyl ethanolamine-decane planar bilayers. In planar bilayers, a 4 mV increase in potential increases the conductance e-fold, but in node a 9 mV potential increase is required for an e-fold conductance increase. The variance of the conductance divided by the mean conductance in node is 0.9 0.14 nanomho. In planar films this number calculated from single channel distributions obtained in Ringer identical to that used for the node experiments is 0.66 0.07 nanomho. Because of uncertainty in current calibration for the node, these values can be regarded as essentially equivalent.

We conclude that, while the alamethicin single channel properties in node and planar bilayers are very similar, the voltage-gating properties are not.

T-AM-D1 OPTICAL PROBE ANALYSIS OF MEMBRANE ELECTRICAL FUNCTION IN SKELETAL MUSCLE. J. A. Heiny*, R. Valle* and S. H. Bryant, Department of Pharmacology and Cell Biophysics, U. of Cincinnati College of Medicine, Cincinnati, Ohio 45267.

Fluorescence signals have been recorded from bundles of normal and myotonic goat intercostal fibers stained with the penetrating dye Nile Blue A. The bundles were stimulated extracellularly and immersed in hypertonic sodium chloride ringer to block movement. Normal fibers produce a fluorescence change similar to that reported in frog muscle (Bezanilla & Horowicz, 1975) and purported to monitor events in excitation-contraction coupling, possibly depolarization of the sarcoplasmic reticulum. Mean time-to-peak of the fluorescence change was 25 msec and mean signal duration 180 msec, at 24°C. Myotonic fibers produced similar responses but with repetitive peaks.

Several non-penetrating dyes, M-540, WW-781 and Dye XVII (Cohen et al.,1977), have been reported to monitor potential changes across tubular membranes. We have verified this and made further controls, including glycerol detubulation. The ability to record T-system action potentials in an intact cell allowed us to test the finding of Eisenberg & Gage (1969) that frog tubular membranes lack chloride conductance. We have recorded tubular action potentials from bundles of frog semitendonosus fibers, in the presence and absence of chloride in the medium, below 9°C. Preliminary results with Dye XVII suggest that the rate of fall of the tubular action potential decreases in chloride-free medium by 10-15%. This is consistent with tubular membranes having chloride conductance comparable to surface membranes.

(This work supported by NIH Grant NS-03178 and an MDA postdoctoral fellowship to R. Valle. The authors thank A. Waggoner for the gift of some dyes.)

T-AM-D2 OPTICAL ABSORPTION CHANGES IN SKINNED MUSCLE FIBERS DURING CALCIUM RELEASE. Philip M. Best,* Jun Asayama,* and Lincoln E. Ford. University of Chicago,Chicago,Ill.60637

To look for possible voltage changes in the sarcoplasmic reticulum of muscle during calcium release, optical absorption was recorded in skinned fibers stained with the membrane-bound, voltage sensitive dye, NK2367 (Nippon Kanoh Co., Okayama). Skinned semitendinosus fibers from Xenopus laevis were stained for 20 minutes in solutions containing 0.2 mg/ml dye. All solutions contained 100 mM major ions (K-methanesulfonate or choline Cl), 5 mM Na_2ATP, 6 mM $MgCl_2$, and 20 mM carnosine at pH 7.0 and 6°C. After staining, fibers were placed in EGTA buffered Ca solutions to load internal stores and then stimulated to release the stored Ca by substituting choline-Cl for K-methanesulfonate, maintaining a constant KxCl product. Tension was monitored continuously and changes in absorption were recorded at 720 nm and 650 nm during and following this ionic stimulation. Wavelength independent noise and artifacts were much reduced by subtracting the 650 nm from the 720 nm signal. This difference signal showed a rapid decrease in absorption which reached a maximum of about 4% of dye dependent absorption at approximately 0.5 sec after stimulation and returned to near zero over the next 1-2 seconds. Tension rose to a maximum over 2-4 seconds. The optical response required both staining and Ca release; unstained fibers gave no change in the difference signal, and the magnitudes of both the optical and the tension responses in stained fibers were directly related to the duration of Ca loading. Free Ca (1 mM) was applied to unloaded, stained fibers. Tension rose rapidly, but no decrease in the optical signal was recorded. This control experiment shows that the optical signal is not due to a direct effect of Ca on the dye, to an optical change in the contractile proteins, or to a pH change produced by Ca binding. We tentatively conclude that the signal reflects an internal membrane voltage change associated with Ca release.

T-AM-D3 DIFFERENTIAL HOLOGRAPHIC RECORDING OF PRECONTRACTILE EVENTS IN NEURALLY STIMULATED STRIATED SKELETAL MUSCLE. M. Sharnoff and H. A. Kunkel, III*, Department of Physics, University of Delaware, Newark, DE 19711

We have followed the optical concomitants of latency elongation and relaxation in whole vertebrate twitch muscle excited by a single volley of neural impulses. Sartorii of Rana pipiens were dissected, stretched to 1.2 times their resting lengths, and trans-illuminated with 5147 Å light from an argon ion laser. Light scattered through an angle of 15-20° was collected by a dissecting microscope and directed to the holographic plate. Isometric muscle response was monitored by doubly exposing the holographic plate, one exposure flash (1.3 msec long) occuring just before, and the other just after, a 25 μsec stimulus delivered to the muscle's nerve. Between these exposures the length of the object path was shortened by ½ wavelength. Images reconstructed from these holograms display only the changes which occur during the time between exposures. A small number of muscle fibers become brightly visible within 5 msec of neural stimulation (22° C); the remaining fibers are recruited within the 5 msec space thereafter. The latency effects are not uniform along individual fibers nor across any section of the muscle. They are largest and earliest in the end-plate regions and, within individual fibers, may propagate at speeds exceeding 15 M/sec. Thus the mechanical components of latency response are conveyed along the fibers significantly more rapidly than is the action potential.

T-AM-D4 INFLUENCE OF EGTA ON STIMULATED ^{45}Ca EFFLUX FROM SKINNED MUSCLE FIBERS. Elizabeth W. Stephenson, Lab. Physical Biology, Natl. Inst. Health, Bethesda, MD 20014

Chloride stimulation of ^{45}Ca efflux from the SR of skinned muscle fibers is prevented by the Ca chelator EGTA (J. Gen. Physiol. 71:411, 1978). The basis of this Ca-dependence, which may be important in intact fibers, is not known. The present report describes the effects of EGTA on stimulation by low Mg or caffeine. Fibers from frog semitendinosus muscle, skinned by microdissection, were loaded with ^{45}Ca, rinsed, and stimulated by Mg reduction (20 μM to 4 μM Mg^{++}) or by addition of 5 mM caffeine (20 μM Mg^{++}). Isometric force and ^{45}Ca efflux from fiber to bath were measured simultaneously, as described previously. Myofilament space (MFS) Ca was chelated by addition of 5 mM EGTA before or after the stimulus; responses were followed for about 1 min, and residual ^{45}Ca was extracted with Triton-EGTA solution. Both stimuli were highly effective when applied shortly before EGTA: total loss of initial ^{45}Ca content was about 60% with low Mg and 68% with caffeine, compared to < 10% loss in EGTA with no stimulus. When EGTA addition preceded Mg reduction, total ^{45}Ca loss was reduced to control level, although a small immediate increase in efflux was detectable. When EGTA was added before caffeine, ^{45}Ca loss was reduced to about 40% fiber tracer; corrected for control loss in EGTA, stimulated loss was about half that when caffeine was applied before EGTA. The EGTA-resistant stimulation of efflux by caffeine was transient; the peak rate was < 1/3 the initial net flux in caffeine alone, occurred later, and declined rapidly. These results indicate that the stimulated Ca efflux is highly Ca-dependent after Mg reduction or caffeine as well as Cl. If a common pathway through the SR membrane mediates these stimulated fluxes, then the residual caffeine stimulation in EGTA suggests that either Ca is not an absolute requirement, or caffeine can initiate efflux through membrane sites that are not accessible to MFS EGTA.

T-AM-D5 CALCIUM TRANSIENTS IN SKELETAL MUSCLE: EFFECTS OF HYPERTONIC SOLUTIONS ON AEQUORIN LUMINESCENCE. H.H. Shlevin and S.R. Taylor, Mayo Foundation, Rochester, MN 55901.

It has been inferred that hypertonicity has little effect on Ca^{++} release in vertebrate skeletal muscle, and preliminary studies (Fedn.Proc. 34:1379,1975) did in fact suggest that Ca^{++} release was not abolished in response to single, brief electrical stimuli in hypertonic solutions. But the changes during high frequency tetanic stimulation were not reported. When a single frog skeletal muscle fiber that had been microinjected with aequorin was immersed in Ringer solution made hypertonic with sucrose, and when the fiber's response was measured at the same initial sarcomere length, both peak tetanic force and total light emission during the tetanus declined. The figure illustrates the average of three responses from a typical fiber (Rana temporaria-tibialis anterior, tetanus frequency 80 Hz, 14.1°C, sarcomere length, 2.5 μm) in normal Ringer and in Ringer solution made 1.5x and 2.0x hypertonic with sucrose. Peak tetanic force declined to approximately 71% of its normal value in 1.5x and to 20% of its normal value in 2.0x hypertonic Ringer solution. Concommitantly, the total light emission during the tetanus decreased to 84% of its normal value in 1.5x and to 67% of its normal value in 2.0x hypertonic Ringer solution. When the fiber was returned to either 1.5x hypertonic Ringer or to normal Ringer solution, peak tetanic force returned in less than 5 min. Force development and relaxation are dramatically slowed in hypertonic solutions. But the initial rate of decline of the aequorin response in 2.0x hypertonic Ringer is slowed by only 34% ($P < .06$) relative to control measurements in normal Ringer solution. (Supported by NS 05840 to HHS and by NS 14268 & AHA 77-983 to SRT).

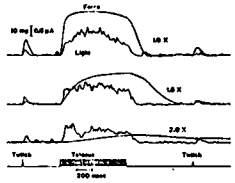

T-AM-D6 ARSENAZO III SIGNALS IN FROG MUSCLE. S.M. Baylor, W.K. Chandler and M.W. Marshall. Department of Physiology, Yale Medical School, New Haven and Department of Physiology, Newcastle Medical School, Newcastle-upon-Tyne.

The aim of the experiments was to measure calcium transients in singly dissected frog twitch fibers using purified Arsenazo III. Since the dye's color depends on pH and Mg, as well as Ca, experiments were first done using phenol red for pH and Arsenazo I for Mg. Changes in absorbance of these dyes, injected into highly stretched fibers (sarcomere spacing 3.8-4.3 μm), indicated that the internal pH changes by no more than 0.01 units and Mg by no more than 0.1 mM during a twitch. Arsenazo III signals were measured using light polarized at 0° and at 90° with respect to the fiber axis. The changes in 90° absorbance, measured at different wavelengths, were temporally similar and had spectral characteristics consistent with changes in myoplasmic free Ca (Miledi, Parker & Schalow, 1977). Absorbance signals measured with 0° light showed the Ca signal plus another, later component. The dichroic component (0° minus 90°) slightly preceded tension and the amplitude at different wavelengths scaled approximately as resting dye absorbance. The relative contributions of the dichroic and Ca components depended on dye concentration in the fiber. At low concentrations (0.1-0.2 mM) both components were present in approximately equal amounts whereas at higher concentrations the Ca component predominated. Calcium signals were also recorded under voltage clamp conditions using TTX to block Na currents and TEA to block K currents. Near mechanical threshold the amplitude of the signals changed e-fold for 3-4 mV, indicating that Ca release is strongly voltage dependent.

T-AM-D7 CALCIUM TRANSIENTS IN CUT SINGLE MUSCLE FIBERS. P. Palade* (Intr. by F. Bezanilla) Dept. Physiol., UCLA Med. Sch., Los Angeles, CA 90024.

Single twitch muscle fibers of Rana catesbiana were mounted in a vaseline gap apparatus modified for optical studies (Vergara and Bezanilla (1977), Biophys. J. 17:5a) either with ends left long enough to pin and stretch to ∿3.6 μ sarcomere length in a relaxing solution containing .02 mM EGTA or with ends cut short in the same solution with 1 mM EGTA instead. Both methods abolish or nearly abolish (respectively) movement elicited by action potentials and severely reduce that elicited by step depolarizations under voltage clamp. Fibers were iontophoretically injected with purified Arsenazo III and illuminated at wavelengths of 532, 600 and 660 nm to obtain differential absorbance traces reflecting changes in free intracellular calcium concentration and setting limits on possible ΔpH_i contributions. Signal-to-noise ratio was better than 40 dB, obviating any need for signal averaging. Membrane action potentials under current clamp conditions give rise to signals of $\Delta A_{660} - \Delta A_{532}/A_{532} = .02-.03$ whose rise lags behind the peak of the action potential by 1.2-1.5 msec and whose peak follows 5-8 msec later, at 21-23°C, under both sets of immobilization conditions. Under voltage clamp conditions with $V_H = -100$ mV, small depolarizations of ∿ 40 mV produce a signal with a long delay and slow rise which is not maintained during a 50 ms pulse. At intermediate depolarizations the signal gets larger with a shorter delay and lesser decline during the pulse. Finally, at high depolarizations the signal reaches a minimum lag of ∿ 2 msec and continues to rise throughout the pulse, reaching amplitudes several times higher than those elicited by action potentials. These studies demonstrate that sarcoplasmic reticulum function in the cut fiber preparation,as measured by calcium release,is intact. Supported by MDA and USPHS Grant No. RRO-5354.

T-AM-D8 LASER RAMAN INVESTIGATION OF SINGLE MUSCLE FIBERS. EFFECT OF ATP, Mg AND Ca. M. Pézolet*, J. Nadeau*, and M. Pigeon-Gosselin*, Dép. de Chimie, Université Laval, Québec, P.Q., and J.-P. Caillé, Dép. de Biophysique, Université de Sherbrooke, Sherbrooke, P.Q.

Raman spectra, in the frequency region of the protein vibrations, of single muscle fibers contained in glass capillary tubes will be presented. Each fiber, was isolated from the depressor muscle of the giant barnacle, was rinsed in an isotonic sucrose solution and introduced in the lumen of a glass capillary tube at least 24 hrs before recording the spectrum. During this period, the fiber-filled capillaries, 5 mm to 8 mm long, were incubated at approximately 2°C in an electrolyte solution containing 100 mM KCl, 25 mM THAM neutralysed at pH 7.4 with HCl, and 0.5 mM EGTA. Raman spectra obtained in these conditions are identical to those previously published (Pézolet et al., Biochim. Biophys. Acta 533, 263, 1978). With the addition of ATP, Ca^{+2} and Mg^{+2}, which are known to induce contraction in this type of preparation (Caillé, Can.J.Physiol.Pharmacol. 55, 888, 1977), modifications of the Raman spectrum of the fiber proteins occur. For example the intensity of the tryptophan hands at 760 and at 1340 cm^{-1}, and of the peak due to the symmetrical stretching vibration of the COO^- groups is reduced. On the other hand, both the amide I (1600 to 1700 cm^{-1}) and amide III (1230 to 1320 cm^{-1}) regions remained unchanged. From these results, the effects of ATP, Ca^{+2} and Mg^{+2} on the structure of the fiber proteins will be discussed.

This research received the financial support of the National Research Council and of the Medical Research Council of Canada.

T-AM-D9 EXTRACTION OF CALCIUM FROM SINGLE ISOLATED BARNACLE MUSCLE FIBERS BY INTERNAL DIALYSIS. J. Teresa Tiffert, and F.J. Brinley, Jr. Dept. of Physiology, University of Maryland School of Medicine, Baltimore, Md. 21201.

Fibers were soaked in 0 Ca saline for periods of 0-5 hr. and then analyzed for total calcium. The initial concentration was 0.90 mmol/kg and decreased 0.02 mmol/kg-hr. during soaking. The net loss of calcium was less than half of that calculated from the rate constant for tracer loss in Ca free solutions (Blaustein and Russell, 1974, J. Gen. Physiol. 63, 144; Ashley et al, 1977, J. Physiol. 269, 421). This result is consistent with previous work which indicated that less than half of the intracellular calcium in barnacle fibers was isotopically exchangeable (Brinley and Spangler, 1975, Biophys. J. 15, 281). In the present experiments, the ability of internal dialysis with EDTA to mobilize and remove intracellular calcium was investigated. A double porous capillary system was used. One capillary, acting as a guard, contained two porous regions located on either side of the single centrally located porous region of the second capillary. This system minimized longitudinal diffusion of calcium from the ends of the fiber into the center region. The internal dialysis solution was (mM):KEDTA 240, KTES 80, pH 7.3. The external bathing solution was (mM): K 10, Na 460, Mg 32, Ca 0, Cl 534, NaEDTA 0.1, NaTES 10, pH 7.6. Samples of effluent dialysate were analyzed for calcium during 4-6 hrs. of continuous dialysis to give the amount extracted. After dialysis the central region of the fiber was analyzed for residual calcium. The results were (mmole/kg):residual calcium, 0.35 ± 0.04 (n=14); dialyzable calcium 1.0 ± 0.2 (n=9). The residual calcium was not released by addition of 10 mM caffeine to the bathing solution. These results, together with earlier work, show that about 30-40% of intracellular calcium is firmly bound inside the fiber and apparently is neither ionizable nor exchangeable. Supported by PCN 77-03916, NS 13420-03.

T-AM-D10 MEASUREMENT OF THE FREE CALCIUM ION CONCENTRATION IN SHEEP CARDIAC PURKINJE FIBERS WITH NEUTRAL CARRIER Ca^{++}-SELECTIVE MICROELECTRODES. J. H. Sokol, *C. O. Lee, and F. J. Lupo* (Intr. by E. E. Windhager). Dept. of Physiology, Cornell Univ. Med. Coll., N. Y., N.Y. 10021 and Dept. of Elec. Engineering, Polytechnic Inst. of N.Y., Brooklyn, N.Y. 11201.

Ca^{++}-selective microelectrodes were made with a neutral ion carrier (obtaind from W. Simon) and some of their properties were investigated to see the feasibility of their intracellular application. The Nernst slope (S_{Ca}) and the selectivity of the microelectrodes varied inversely with their resistance (R_e), which was mainly dependent on their tip diameter. For microelectrodes with a tip diameter less than 1μ, R_e was very high (5 x 10^{10}-$10^{11}\Omega$), and S_{Ca} and selectivity were poor. Upon breaking the tip to about 1-2μ, R_e was drastically decreased, and S_{Ca} and the selectivity were markedly improved. Some of the microelectrodes with a tip diameter of about 1μ had a S_{Ca} between 5 and 9 mV/log a_{CaCl_2} for a pCa between 6 and 7 (with 150 mM K^+ and 1 mM Mg^{++}) and a selectivity coefficient, k_{CaK}, of approximately 3 x 10^{-4} for a mixture solution of 10^{-7} M Ca^{++} + 150 mM K^+. With this type of microelectrode, the intracellular free Ca ion concentration $(Ca^{++})_i$, of the fibers was determined. The $(Ca^{++})_i$ of fibers in the resting state was found to be (2.1 ± 1.2) x 10^{-7}M (mean ± S.D., n=7). In 2 fibers from different hearts the $(Ca^{++})_i$ was 1.0 and 2.6 x 10^{-7} M; exposure of these fibers to 5 x 10^{-7} M dihydro-ouabain led to a 3 and 4.5 fold increase in $(Ca^{++})_i$, respectively.

(Supported by USPHS HL 21136).

T-AM-D11 EFFECTS OF pH AND INOTROPIC AGENTS ON CALCIUM BINDING TO CARDIAC SARCOLEMMA. David C. Pang, Medical College of Virginia, Virginia Commonwealth Univ., Richmond, Va.23298

To test the relationship between the calcium bound to cardiac sarcolemma and cardiac contractility, the effects of pH and agents like caffeine, ouabain, epinephrine, propranolol and papaverine on calcium binding to isolated cardiac sarcolemma were investigated. At pH 7, cardiac sarcolemma exhibited two classes of calcium binding sites with dissociation constants of 4.2 x 10^{-5}M and 1.2 x 10^{-3}M. The maximum number of high and low affinity sites were 65 and 467 nmoles/mg respectively. On increasing the pH from 7.0 to 7.6, the amount of calcium bound increased to more than 150% of the control. On decreasing the pH from 7.0 to 6.2, calcium binding was inhibited to a great extent. The effects of the agents (10^{-6}- 10^{-2}M) on calcium binding was tested in the presence of 0.1 mM $CaCl_2$ and 10 mM imidazole, pH 7.0. Caffeine (10^{-2}M) had little or no effect on the calcium binding. Ouabain (10^{-6}-10^{-5}M) increased the amount of calcium bound to 2-fold. Epinehprine (10^{-4}-10^{-3}M) increased calcium binding slightly to 120% of the control. Propranolol (10^{-6}-10^{-3}M) decreased the amount of calcium bound to 50% of the control. Finally papaverine (10^{-4}M) inhibited calcium binding to a great extent. (This investigation was supported by research grant from USPHS, HL21493 and a Research Career Development Award from the National Institute of Heart, Lung and Blood 1 K04 HL00488).

T-AM-D12 VOLTAGE CLAMP EVIDENCE FOR DELAYED RECTIFIER CURRENTS IN THE T-TUBULES OF FROG STRIATED MUSCLE FIBERS. C. Lynch, Dept. of Physiology, Univ. of Rochester, Rochester, N.Y. (Present address: Dept. of Anesthesiology, Univ. of Virginia, Charlottesville, VA 22904)

Toe muscle fibers of Rana pipiens 1.0 to 1.4 mm in length were voltage clamped. According to terminated cable analysis, the conductance of these fibers was simply calculated as I/V since the voltage sensing electrode was placed 0.18-0.19 times fiber length from a current passing electrode placed near the center of the fiber. Experiments performed in hypertonic Ringer at 5°C gave calculated average G_m = 239 $\mu S/cm^2$ for a 30 mV depolarization and G_m = 743 $\mu S/cm^2$ for a 40 mV hyperpolarization (n = 26). This inward rectifier activated with a voltage dependent rate constant and was blocked by 5 mM Rb^+. An observed slow decline in inward current with maintained hyperpolarization is consistent with T-tubular K^+ depletion. Increasing the $[K^+]_o$ resulted in increased inward and outward conductance. Depolarization led to "cross-over" of the I-V relations for the varied $[K^+]_o$. Sustained depolarizations led to a positive shift in the inward rectifier reversal potential, consistent with K^+ accumulation. Following depolarizations of increasing duration, repolarization revealed increasing positive shift of the inward rectifier reversal potential with "cross-over" of the I-V relations. The delayed rectifier reversal potential shifted much less (or not at all) compared to that of the inward rectifier suggesting spatial separation of the majority of these two components. From the reversal potential shift, the amount of K^+ accumulation in the T-tubular space was calculated assuming a T-tubular volume of 1% fiber volume (increased due to hypertonicity). The conductance required for the estimated $\Delta[K^+]$ is 4 to 8 times the resting G_K. The presence of 20 to 30% of the delayed rectifier in the T-tubules would account for the observed degree of accumulation.

This work supported by NIH Grant AM01004-12.

T-AM-D13 INTRACELLULAR K AND NA ACTIVITIES IN PAPILLARY MUSCLE DURING INOTROPIC INTERVENtions. S.J. Cohen and H.A. Fozzard (Intro. by S. Glagov), Univ. of Chicago, Chicao, Ill.

Intracellular activities of Na and K [$(Na)_i$ and $(k)_i$] have been measured with liquid ion exchange (LIE) microelectrodes in guinea pig right ventricular papillary muscle. K LIE electrodes were made with Corning 477317 ion exchanger. LIE electrodes for Na contained 2.3% (W/V) potassium tetrakis(p-chlorophenyl)borate and 13% (W/V) tri (n-octyl) phosphine oxide in tri(ethyl-hexyl)phosphate, and had a selectivity of about 3.5:1 for Na over K. At 36°C, quiescent muscles had E_m = -87.9± 0.6mV (±S.E.M.; 9 muscles); $(K)_i$ = 116.1 ± 2.4mM (6 muscles); E_K = -94.5mV; $(Na)_i$ = 5.8 ± 3.4mM (4 muscles); E_{Na} = +80.0mV. In 7 of 9 experiments, initiation of increase in rate of stimulation caused a decrease in $(K)_i$ by only a few mM. Increases in $(Na)_i$ of 1-2 mM were measured in additional experiments. Exposure to ouabain (0.3μM) during 0.2 hz stimulation demonstrated a tension increase of 80% in 10 minutes. No fall in $(K)_i$ could be detected, but $(Na)_i$ was elevated by up to 2mM. In an effort to produce a comparable alteration in the sodium gradient, $(Na)_o$ was decreased. An equivalent increase in tension was produced when $(Na)_o$ was reduced by 25-30%, which was the same extent to which $(Na)_i$ was increased by ouabain.

T-AM-D14 THE INFLUENCE OF TEMPERATURE ON THE ACTIVITY OF THE SARCOLEMMAL Na-K PUMP IN CANINE VENTRICULAR MUSCLE. J.M. Jaeger*, S.R. Houser*, and A.R. Freeman, (Intr. by R. Carey). Dept. of Physiol., Temple Univ. Sch. of Med., Philadelphia, Pa. 19140.

The influence of temperature on sarcolemmal Na-K pump activity (A_{pump}) was studied using a novel electrophysiological technique. Canine right ventricular papillary muscles, superfused with an oxygenated Tyrode's solution (K_{bath} = 5.4 mM) and maintained at the desired temperature (+ 0.5°C), were externally driven at various rates and allowed to return to quiescence. Standard microelectrode techniques were employed to measure transmembrane potentials. During the drive period the series of maximum diastolic potentials (E_{max}) demonstrated a biphasic response. The initial linear depolarization phase $(dE_{max}/(dt)_o)$ is attributed to K^+ accumulation outside the membrane and the subsequent hyperpolarization to an increase in A_{pump}. Since E_{max} approximates the K^+ equilibrium potential and assuming a constant internal K^+ concentration, the Nernst equation can be utilized to calculate K^+ loss (ΔK_{out}) from the absolute change in E_{max} during the drive. Defining A_{pump} as millimoles of K^+ pumped per second, it is possible to calculate A_{pump} as $A_{pump} = [K_{bath}(\exp(dE_{max} F/RT)-1]/(dt)_o$. A phenomenological rate constant (α) may be calculated as $\alpha = [(dK_{out})/(dt)_o] \cdot 1/\Delta K_{out}$. Experiments performed at various temperatures (27°-37°C) reveal the extent of the influence of this temperature range on A_{pump} and offer electrophysiological evidence that as it functions in the intact cardiac cell membrane, the Na^+-K^+ pump and (Na-K) ATPase are identical. (Supported in part by NIH IT 32HL07198).

T-AM-E1 CIRCULAR DICHROISM SPECTRA OF ALLOPHYCOCYANIN FORMS. O. D. Canaani,* and E. Gantt,* Radiation Biology Laboratory, Smithsonian Institution, 12441 Parklawn Drive, Rockville, MD 20852. Introduced by W. Shropshire, Jr.

Allophycocyanin from dissociated phycobilisomes of Nostoc sp. was fractionated on calcium phosphate columns into three forms: APC I, APC II and APC III. These forms had absorption maxima at 654, 649 and 650 nm with relative absorbance at 620/650 nm of 0.39, 0.63 and 0.45 respectively (B.A. Zilinskas et al., 1978, Photochem. Photobiol. 27: 587). The circular dichroism (CD) spectra of the three forms were compared at 22°C. The CD spectrum of APC I_5 consisted of a large positive peak at 668 nm with a molecular ellipticity θ max = 7.3 x 10^5 deg cm^2 $dmole^{-1}$ and troughs at 643, 595 and 340 nm. APC II displayed positive ellipticity bands at 656 and 632 nm and troughs at 587 and 348 nm. APC III showed a major positive CD peak at 656 nm, a very small positive peak at 633 nm and troughs at 593 and 347 nm. The CD spectra of APC II and APC III appear to be similar to one another in their shape differing only in magnitude. In the chromophore absorption range, the CD spectrum of APC I differed from those of APC II and APC III in shape, sign and magnitude of ellipticity bands. Varying protein concentration over a six fold range showed no effect, suggesting the absence of aggregation and disaggregation. APC I was sensitive to chaotropic agents such as LiCl which caused a shift of the positive ellipticity band from 668 to 661 nm, a decrease in the magnitude of 643 and 595 nm bands and the appearance of a new positive CD band at 620 nm. Concomitantly, the absorption maximum shifted from 654 to 649 nm with an increase in the ratio of 620/650 nm from 0.39 to 0.63. This absorption spectrum then resembled that of APC II. The spectral properties of APC I are of potential significance because it probably serves as the bridging pigment in energy transfer from the phycobilisomes to chlorophyll.

T-AM-E2 ENERGY TRANSFER IN PHOTOSYNTHESIS. RELAXED EXCITON STATES AND FÖRSTER TRANSFER RATE CONSTANTS FOR CHLOROPHYLL A.* Lester L. Shipman, Chemistry Division, Argonne National Laboratory, Argonne, Illinois 60439.

After the very fast (10^{12}-10^{13} sec^{-1}) vibrational relaxation process which follows photon absorption by an array of interacting chromophore molecules, relaxed exciton states are populated. These relaxed exciton states are responsible for energy transfer, intersystem crossing, fluorescence, and singlet photochemistry. A procedure for the calculation of relaxed exciton states will be presented along with an example application to chlorophyll a arrays at 10^{-5} to 10^{-1} M concentrations. In the limit that the relaxed exciton states are each localized on a single molecule, then the Förster transfer mechanism is an appropriate description of the energy migration process. A formula has been derived for the calculation of Förster transfer rate constants for chlorophyll a; this formula is applicable over wide ranges of absorption maxima positions, solvents, relative orientations, and intermolecular distances.

* This work was performed under the auspices of the Division of Basic Energy Sciences of the United States Department of Energy.

T-AM-E3 ANALYSIS OF PHOTOSYSTEM I ANTENNAE. J. E. Mullet,* J. J. Burke,* and C. J. Arntzen, USDA, Dept. of Botany, University of Illinois, Urbana, IL 61801.

The purpose of this investigation was to analyze the size, fluorescence emission characteristics, and polypeptides associated with the Photosystem I (PSI) light-harvesting pigment complex. PSI particles isolated by mild detergent techniques from peas, cucumber or barley contained 110 ± 10 Chl/P700, 11 polypeptides, and had a major 77°K fluorescence emission peak at 736 nm. This emission was identical to the long-wavelength peak of intact chloroplast membranes. Treatment of the PSI particles with Triton-X-100 removed 50-70 Chl/P700, 3-4 polypeptides of molecular weight 21,500, 22,500, 25,000 and 26,000 and shifted the 77°K fluorescence emission peak to 724 nm, but had no effect on photochemical properties of the reaction center complex. Chloroplasts from a chlorophyll b-less barley mutant emitted long wavelength 77°K fluorescence at 724 nm compared to 736 nm for intact chloroplasts or PSI particles isolated from wild type barley. The chl b-less barley mutant was deficient in PSI polypeptides of 22.5, 25 and 26 Kdaltons. PSI particles were also isolated from barley mutant N-34 which lacks an active P700. These particles retained PSI polypeptides of 22.5, 25 and 26 Kdaltons but were deficient in the 65-68 Kdaltons species. They displayed a 77°K fluorescence emission at 731 nm. Chloroplasts from cucumbers grown under intermittent-light emit 77°K long wavelength fluorescence at 724 nm. A shift in emission to 735 nm occurred concomittant with synthesis of polypeptides of 21.5 and 26 Kdaltons. We conclude that intrinsic PSI complexes contain reaction center chlorophylls, 40-50 tightly associated antennae chlorophylls, plus a light-harvesting pigment complex of 50-70 chlorophyll a molecules. The light-harvesting chlorophylls emit fluorescence at 732-736 nm at 77°K. Their presence is correlated to specific polypeptides (21.5-26 Kdaltons).

T-AM-E4 IMMOBILIZATION AND CHEMICAL MODIFICATION OF PHOTOSYSTEM I. P. M. Abdella*, K. Burkey*, and E. L. Gross, Dept. of Biochemistry, The Ohio State University, 484 W. 12th Ave., Columbus, OH 43210

Photosystem I subchloroplast particles from spinach [Shiozawa, J. A., et al. (1974), Arch. Biochem. Biophys., 165, 388] in 0.04% Triton X-100 (PSI monomers) were immobilized by coupling to ethylenediamine-Sepharose CL-4B, with 1-ethyl-3-(3-dimethylaminopropyl) -carbodiimide (EDC). Chlorophyll-protein coupling efficiency was typically 20%. The immobilized particles retained full P700 photoreactivity. Successive washings with 0.2 and 1.0% Triton removed 50% of the chlorophyll, but failed to diminish [P700]. The rate of $P700^+$ reduction of immobilized PSI was 7-8 fold faster than that of the free particles.

A similar effect is seen with the PSI complex modified by carbodiimide-promoted amide formation between the carboxyl groups of the complex and ethylenediamine. The modification does not change the total P700 activity, but does increase the rate of $P700^+$ reduction by 10 fold compared to controls. The effects on $P700^+$ reduction seen in both cases are analogous to the effects of Mg^{2+} on PSI particles.

T-AM-E5 PROPERTIES OF THE IRON-SULFUR CENTERS OF PHOTOSYSTEM I IN SPINACH CHLOROPLASTS. C. Dismukes*, Department of Chemistry, Princeton University, Princeton, N.J. 08540. V. Petrouleas, Nuclear Research Center "Democritos", Aghia Paraskevi Attikis, Athens, Greece.

Illumination of green plants and algae results in the photoreduction of two iron-sulfur centers designated centers A and B which are associated with the acceptor side of Photosystem I. EPR spectroscopy reveals evidence of coupling between the centers, which along with the known stoichiometry implicates a single 8Fe8S protein involving two 4Fe4S clusters, similar to those found in bacteria. Curiously, the orientation dependence of the EPR spectra of these highly anisotropic centers are remarkably different when observed in aligned chloroplasts. The g tensor of center A shows no dependence on orientation of the thylakoid membranes in the EPR magnetic field, while center B is oriented with g_y predominantly normal to the plane of the membrane. This seemingly inconsistent observation for what is considered a single 8Fe8S protein may be reconciled by assuming different electron delocalization within the reduced centers. One-electron reduction of center A is thought to involve the localization of an electron in an orbital predominantly one Fe, with all Fe atoms in one 4Fe4S cluster having equal probability of becoming reduced. By contrast, upon reduction of center B the electron centers a fixed molecular orbital of the 4Fe4S cluster and only this orbital is involved. The EPR temperature dependence also serves to characterize these centers.

An unidentified acceptor, designated X, forms upon illumination of reduced samples. The characteristic EPR spectrum indicates rhombic symmetry with principal g values outside the range of known iron-sulfur proteins. Simple crystal field calculations suggest that this large g anisotropy can arise in iron-sulfur centers with highly asymmetric coordination about iron. This center is aligned in the membranes with g_x predominantly normal to the membrane plane. EPR temperature depdendence suggests that this can be a 4Fe4S center,not a 2Fe2S center.

T-AM-E6 CYCLIC ELECTRON FLOW IN INTACT CHLOROPLASTS. D. Crowther, J. D. Mills and G. Hind, Biology Department, Brookhaven National Laboratory, Upton, L.I., N.Y. 11973.

Coupled electron flow around photosystem I seems to contribute to the ATP-producing capacity of the chloroplast. The activity of this cycle in isolated intact chloroplasts depends on the redox poise of the cycle components. Here it is shown that such cyclic activity may be regenerated in isolated intact chloroplasts poisoned with 20 μM DCMU if suitable concentrations of dithionite are subsequently added. The activity so restored could form a transmembrane pH gradient (as shown by light-induced quenching of 9-aminoacridine or chlorophyll-a fluorescence) and a transmembrane electrical potential (as shown by flash induced absorbance changes in the 518nm region). The former effects were sensitive to nigericin and the latter to valinomycin as expected from chemiosmotic theory. Neither were regenerated in chloroplasts previously subjected to osmotic shock. The regenerated flash induced 518nm change in intact chloroplasts showed a slow ($t_{1/2}$ 5-10 msec) phase of equal amplitude to the fast ($t_{1/2}$ < 200 μsec) phase. This slow phase was blocked by antimycin A or by DBMIB, both of which also inhibited pH gradient formation. The system resembles that of cyclic electron flow in the purple non-sulphur photosynthetic bacteria. (Supported by U.S. Department of Energy).

T-AM-E7 THE KINETICS AND EXTENT OF THE DARK REDUCTION OF CYTOCHROME f IN SPINACH CHLOROPLASTS. J. Whitmarsh and W. A. Cramer. Purdue University, W. Lafayette, Indiana.

The questions of whether the stoichiometry of the turnover of cytochrome f, and the time course of its reduction subsequent to a light flash, are consistent with efficient function in non-cyclic electron transport have been investigated. Measurements were made of the absorbance change at the 553 nm α-band maximum relative to a reference wavelength. In the dark cytochrome f is initially fully reduced and is oxidized by a 0.3s flash, and reduced again in the dark period following the flash. In the presence of gramicidin at 18°C the dark reduction was characterized by a half-time of 25-30 ms, stoichiometries of cyt f:chlorophyll and P700:chlorophyll of 1:670 and 1:640, respectively, and a short time delay. The time delay in the dark reduction of cytochrome f, which is expected for a component in an intermediate position in the chain, becomes more apparent using chloroplasts in the presence of valinomycin and K^+. Under these conditions the half-time for cytochrome f dark reduction was 130-150 ms, and the delay was approximately 20 ms. A sigmoidal time course for the reduction of cytochrome f has been calculated for an irreversible, linear electron transport chain. The kinetics for reduction of cytochrome f predicted by the calculation in the presence of valinomycin and K^+ are in reasonably good agreement with the experimental data. Preliminary calculations for the time course of the oxidation of plastoquinone and the reduction of cytochrome f, plastocyanin, and P700 also agree well with the experimental kinetic data. The measured value for the activation energy of the dark reduction of cytochrome f (11 ± 1 kcal/mol) is the same as that for non-cyclic electron transport in steady state light. The observation of one cytochrome f reduced per P700, with kinetics that are in agreement with those predicted for a component in the linear chain, imply that cytochrome f functions in non-cyclic electron transport between plastoquinone and P700. (This research was supported by a grant from NSF (BMS 75-16037X).)

T-AM-E8 NMR AND ESR STUDIES OF CHLOROPLAST MANGANESE. Rita Khanna, S. Rajan*, Govindjee, and H.S. Gutowsky*, Departments of Chemistry, Physiology and Biophysics, University of Illinois, Urbana, Illinois 61801.

Indirect evidence suggests that membrane bound manganese plays an important role in oxygen evolution. The unpaired electron spin of manganese can lead to a large increase in magnetic relaxation rates of water proton nuclei bound near the ion. Water proton relaxation rate (PRR) measurements can be used to monitor the abundance and oxidation state of bound manganese.[1] Release of the bound manganese pool results in the appearance of ESR detectable 6-line pattern typical for $Mn^{2+}(H_2O)_6$. We have used NMR and ESR techniques to correlate the amount of bound and free manganese with the rate of oxygen evolution. Treatment of chloroplast membranes with compounds such as tetraphenylboron (TPB) and hydroxylamine (NH_2OH) affect the manganese pool and the rate of oxygen evolution. TPB reduces manganese to the more efficient relaxer species Mn(II), whereas NH_2OH has multiple effects. Addition of low concentration of NH_2OH reduces the oxidizing equivalents leading to an increase in Mn(II) concentration thereby enhancing the PRR. Incubation of chloroplast membranes with high concentration of NH_2OH leads to an initial rise followed by a progressive decline in PRR due to the release of bound manganese. This release of manganese was independently detected by ESR measurements. Supported by research grants from the National Science Foundation to Govindjee (PCM 76-11657) and to H.S. Gutowsky (MPS 73-0498 and CHE 77-04585).

[1] T. Wydrzynski, S.B. Marks, P.G. Schmidt, Govindjee, and H.S. Gutowsky, Biochemistry, 17, 2155-2162 (1978).

T-AM-E9 CATIONS DO NOT INACTIVATE REACTION CENTER 2 CHARGE SEPARATION IN A SATURATING FLASH BUT INCREASE ENERGY TRANSFER FROM CHLOROPHYLL b TO CHLOROPHYLL a OF PHOTOSYSTEM II ANTENNA COMPLEX. D. Wong, S. Saphon*, and Govindjee, Department of Physiology and Biophysics, University of Illinois, Urbana, IL 61801.

Divalent cations affect several processes in the photosynthetic apparatus, e.g. regulation of excitation energy distribution and re-distribution between the 2 photosystems, and activity of system II reactions. Reported below are experiments performed in sucrose-washed broken chloroplasts. The amplitude of the flash-induced absorbance change at 515 nm, ΔA, was measured in the presence of 5 mM ferricyanide (to minimize the contribution from photosystem I) and used here as an indicator of photosystem II activity. It was found that: (1) in a single short flash, after 2-3 minutes dark-incubation, ΔA was not affected by prior addition of 10 mM Mg^{2+} both in the absence and presence of diuron (DCMU); (2) under the repetitive flashing conditions used, ΔA per flash was 20x smaller, but was enhanced ~2x by the addition of Mg^{2+}. These results show that divalent cations do not alter the total number of photosystem II reaction centers and capacity for charge separation, but may affect their recovery rates. The intensities and polarizations of chl a fluorescence at 730 or 760 nm were also measured as a function of the excitation wavelength in the presence of DCMU. The ratio of the fluorescence intensitites in the presence of Mg^{2+} to that in its absence showed relative maxima at 650 (chl b) and ~675 nm (chl a). Correspondingly, the Mg^{2+}-induced increase in depolarization of chl a fluorescence (normalized to that of the sample in the absence of Mg^{2+}) showed relative maxima at 650, 675, and ~685 nm. These results provide the first experimental evidence that Mg^{2+} increases the energy coupling between chl b and chl a in photosystem II in thylakoid membranes.

T-AM-E10 LIGATED CHLOROPHYLLS AS PRIMARY DONORS IN PHOTOSYNTHETIC OXYGEN EVOLUTION.† M. S. Davis,* A. Forman,* L. K. Hanson,* and J. Fajer, Brookhaven National Laboratory, Upton, N. Y. 11973.

Magnesium and zinc tetraphenyl chlorins, synthetic models for chlorophyll, exhibit significant variations in the unpaired spin densities of their cation radicals with concomitant changes in oxidation potentials, as a function of solvent and axial ligand. Similar effects are observed for chlorophyll a and its cation radicals. Oxidation potentials for Chl → Chl^+ as high as +0.9V (vs NHE) are observed in nonaqueous solvents with linewidths of the ESR signals of monomeric Chl^+ ranging between 9.2 and 7.8 G in solution. Clearly, the narrowing of ESR linewidths cannot be used as the sole criteria for establishing the existence of dimeric chlorophyll cations in vivo: ENDOR measurements must complement the ESR data. The changes in electronic configuration and ease of oxidation are attributed to mixing of two nearly degenerate ground states of the radicals independently predicted by self-consistent field and extended Huckel molecular orbital calculations.

Comparison of the properties of chlorophyll in vitro with the optical, redox and magnetic characteristics attributed to P680, the primary donor of photosystem II, which mediates oxygen evolution in plant photosynthesis, leads us to suggest that P680 may be a ligated chlorophyll monomer whose function as a phototrap is determined by interactions with its immediate (protein?) environment.

---

†This work was performed under the auspices of the Division of Chemical Sciences, U. S. Department of Energy, Washington, D. C., under Contract #EY76-C-02-0016.

T-AM-E11 ELECTRONIC STRUCTURE AND HYPERFINE INTERACTIONS IN Chla MONOMER CATION AND ANION. S. K. Mun, Jane C. Chang and T. P. Das, Department of Physics, State University of New York, Albany, New York 12222

We have investigated the electronic structures and proton hyperfine interactions in Chla cation and anion using the procedure we have employed in earlier work[1] on Bchla and BPha cations and anions including the fifth ring and both π and σ electrons. Experimental data are available on the proton hyperfine interactions in Chla cation[2] with which we can compare our theoretical results. Theory is able to explain the fact that the methyl proton hyperfine interaction is larger for ring III than ring I, although the theoretical ratio is close to 1.5 while the experimental ratio is closer to 2. In addition our results in $Chla^+$ ion explain the smaller values of the ring I and ring III methyl proton and methine proton hyperfine interaction constants compared to $BChla^+$ ion and the comparable hyperfine constants for the ring IV protons. These results indicate that a satisfactory description of the overall spin distribution in $Chla^+$ ion has been obtained. Results will also be presented for the Chla anion. (Grant support NIH : GM2523001)

1. Jane C. Chang and T. P. Das, Biochim. Biophys. Acta, 502, 61(1978); Biophys. J. 21, 107a (1978)
2. J. R. Norris, et. al. Ann. N.Y. Acad. Sci., 244, 260(1975); G. Feher et. al. Ann. N.Y. Acad. Sci., 244, 239 (1975)

T-AM-E12 CALCULATION OF THE EPR SPECTRUM FROM PARTIALLY ORDERED ENSEMBLES APPLIED TO A PHOTOSYNTHETIC SYSTEM. Richard Friesner, John A. Nairn* and Kenneth Sauer, University of California, Berkeley, California 94720.

We have developed a general method for calculating the EPR spectrum of partially ordered ensembles of paramagnetic species. The method involves direct determination of the probability density of magnetic field orientation in the principal magnetic axis system of the paramagnetic spin system from considerations of the symmetry properties of the ensemble. We have successfully applied the theory to a polarized triplet signal arising from reaction centers of photosynthetic bacteria, whole cells of which have been aligned by magnetic field orientation.

T-AM-E13 CHLOROPHYLL PHOTOPHYSICS.† R. Kugel,* J. J. Katz,* and J. C. Hindman, Chemistry Division, Argonne National Laboratory, Argonne, Illinois 60439.

A series of rate equations has been developed describing the time evolution of the ground and excited state populations for in vitro chlorophyll solutions under conditions of intense optical pumping. It is shown that the predictions of the rate equations with respect to the photon fluxes required to produce population inversion (lasing) and the effect of pump power on the fluorescence quantum yield and fluorescence lifetime are in reasonable agreement with experiment. The application of the rate equations to the prediction of the effects of various annihilation processes that may be important in in vivo chlorophyll is discussed.

†Work performed under the auspices of the Division of Basic Energy Sciences of the Department of Energy.

T-AM-E14 RESONANCE RAMAN SPECTROSCOPY OF COPPER TETRAPHENYL PORPHYRIN ISOLATED IN A NITROGEN MATRIX. D. C. O'Shea, J.L. Yang*, School of Physics, Georgia Institute of Technology. Atlanta, Georgia 30332 and J. A. Shelnutt, Bell Telephone Laboratories, Murray Hill, New Jersey 07749.

Matrix isolation techniques have been used to study vibronic coupling effects in copper tetraphenyl porphyrin (CuTPP). The absorption spectrum of CuTPP in a nitrogen matrix shows stronger relative absorption at the Q(0-0) transition, the lower energy electronic state with no vibrational quanta excited, than at the B (or Soret) transition compared to this same ratio, Q(0-0)/B, for CuTPP in CS_2 solution at room temperature. Raman excitation profiles for the matrix isolated samples generated from the resonance Raman spectra of a number of vibrational lines appear to show an enhanced peak at the Q(0-0) wavelength over the spectra in the CS_2 solution. These results also show evidence of reduced vibronic coupling in the nitrogen matrix. The unexplained correlation between weak Q(0-0) absorption (relative to the Soret band) and strong vibronic coupling effects is seen here as it has been in CrTPPCl, an intermediate case, and NiEtio, a converse example (strong Q(0-0) and no evidence of strong coupling).[1] This study gives yet another indication of the importance of environmental effects on the electronic states of porphyrins.

[1] J. A. Shelnutt et al J. Chem Phys, 66, 3387 (1977)

T-AM-F1 Na^+K^+ATPase IS VERY SENSITIVE TO MgATP at 37°C. Edward S. Hyman, Touro Research Institute, New Orleans, La. 70115.

At 0°C dephosphorylation of NaKATPase (E) from rabbit outer renal medulla (Jorgensen) can be studied using either a chase of "cold" ATP or by using 10 to 30 mM EDTA to bind Mg^{++} and thus stop phosphorylation of E. At 37°C a chase of unlabeled ATP gives good results, but when EDTA (or CDTA) is used to stop phosphorylation, the apparent dephosphorylation of E even in the presence of K^+ is trivial or incomplete, depending on the concentration of K^+, Mg^{++}, and ATP used. EDTA or CDTA requires about 0.2 sec. to exert its full effect. Since Pi formation continues after adding EDTA, phosphorylation is not completely stopped. The different results with EDTA at 0°C and at 37°C was found to be due to a hundred fold increase in sensitivity of E to MgATP at 37°C. Whereas at 0°C E does not phosphorylate when less than 1×10^{-6} M MgATP is present, at 37°C E phosphorylated 40% on adding ATP without adding Mg^{++}. This phosphorylation increased to 58% on adding 1×10^{-4} M EGTA, and it fell to 0 with 1×10^{-3} M EDTA or $(NaPO_3)_6$. These chelating agents demonstrate that E prepared with ultra pure reagents was significantly contaminated with Mg^{++} and with a calcium like (interfering) ion. Using metal buffer systems, E was found to begin phosphorylating at 1×10^{-8} M MgATP at 37°C. If phosphorylation of E could be equated to binding of MgATP, then a Hill plot shows N = 0.92 and $K_a = 2.2 \times 10^{-6}$ M^{-1} at 37°C, about one-half of the reported association K for E and ATP at 0°C. The calculated MgATP in solution after adding EDTA to stop phosphorylation was still sufficient to continue phosphorylation at 37°C. These data point out the extreme and selective sensitivity of this mamalian E to MgATP at 37°C, and they explain the erratic effect of EDTA (or CDTA) at 37°C. NIH Grant # AM 12718-08

T-AM-F2 Na^+,K^+-ATPase: EFFECTS OF TRITON X-100 AND DIGITONIN ON THE CROSS-LINKING OF SUBUNITS IN THE PRESENCE OF Cu^{2+}. A. Askari and W. Huang*, Dept. of Pharmacology, Med. College of Ohio, Toledo, OH. 43699.

When purified Na^+,K^+-ATPase is incubated with Cu^{2+} (or with Cu^{2+}-phenanthroline complex), its two subunits, α and β, are cross-linked (Huang and Askari, BBRC, 82,1314,1978). In experiments of short duration the major products (detected by SDS-polyacrylamide gel electrophoresis) are an α,β-dimer that dissociates in EDTA, and α,α-dimer that is stable in EDTA. Both can be dissociated by mercaptoethanol. The following identical effects of Triton X-100 and digitonin on cross-linking reactions have been observed: 1. When the enzyme is solubilized in detergent and then exposed to Cu^{2+}, the formation of α,α-dimer is inhibited and that of α,β-dimer is enhanced. Here, the α,β-dimer is resistant to EDTA. 2. If the native enzyme is reacted with Cu^{2+}, and the cross-linked products are then exposed to detergent, the unstable α,β-dimer is rapidly converted to one that is resistant to EDTA. These findings indicate that the rate of conversion of α-Cu^{2+}-β to α-S-S-β is enhanced by detergent. Formation of related α,β-dimers from the native and the solubilized enzymes strongly suggests the existence of a non-covalent α,β-dimer in the native state. Because the nature of cross-linked α,α-dimer is not known, and because the inhibitory effect of detergent on its formation can be accounted for by the activating effect of detergent on α,β-dimer formation, the possibility that α,α-dimer is a collision complex can not be ruled out. Therefore, while the presence of a native α-oligomer is suggested by molecular weight and kinetic studies, its existence is not established by cross-linking experiments. (Supported by NIH grants ES-01599 and HL-19129.)

T-AM-F3 POTASSIUM INFLUXES IN SEVERAL RED CELL POPULATIONS OF NEWBORN,GENETICALLY LK SHEEP SEPARATED BY COUNTER CURRENT CENTRIFUGATION. P.K.Lauf, and G. Valet+, Dept. Physiology, Duke Univ. Med. Ctr., Durham, N.C. 27710, U.S.A.and Max Planck Institute of Biochemistry, 8033 Martinsried, W. Germany.

In previous studies (J.Cell.Physiol.94:1978,215)we proposed that the high potassium (HK)-low potassium (LK) transition occurring in red cells of genotypically LK lambs during the first 3 months after birth is due to a gradual replacement of the large fetal HK type red cell population by two consecutive populations of different cellular volume of which the final red cell population exhibited the typical LK character. Here we report on cation fluxes in each of the 3 red cell populations separated from whole blood at various times after birth by counter current centrifugation (CCC),and on the effect of anti-L. The volume of the erythrocytes separated by CCC in isotonic media was monitored by electric sizing. Cellular cations were analyzed and K-influxes (using ^{86}Rubidium as tracer) were determined in presence and absence of anti-L, and with or without ouabain. The large (36 um^3) fetal HK type red cells had HK type fluxes unaffected by anti-L. The transitional second population contained small (28 um^3)red cells with LK cation steady state composition and LK pump and leak fluxes stimulated by anti-L_p and reduced by anti-L_1,respectively. The third (30 um^3) cell population progressively assumed LK cation status with LK cation fluxes susceptible to the effect of anti-L_p and anti-L_1 Hence cellular replacement is the primary determinant of the HK/LK transition in newborn, genetically LK sheep. (Supported in part by USPHS 2 PO1-12,157 & in part by the German Academic Exchange Service)

T-AM-F4 *ANOMALOUS AEROBIC GLYCOLYSIS IN VASCULAR SMOOTH MUSCLE (VSM) IS COUPLED TO Na-K TRANSPORT PROCESSES.* *W. Pease*, M. Bauer* and R.J. Paul. Department of Physiology, University of Cincinnati, College of Medicine, Cincinnati, Ohio 45267.*

Under aerobic conditions, lactate is the predominant end product of glucose catabolism in vascular smooth muscle. While a characteristic of vascular metabolism, there is no obvious survival value for this inefficient use of glucose. As such, aerobic glycolysis in VSM is sometimes considered to be an artifact. Our results, however, indicate that the rate of lactate production (J_{lac}) is closely coupled to Na-K transport related processes. The rate of O_2 consumption (J_{O_2}), on the other hand, is more strongly related to contractile processes. Porcine coronary vessels were studied in a muscle chamber which allowed for simultaneous measurements of isometric force, polarographic determination of J_{O_2} and sampling of the bathing medium for lactate content. Unstimulated values of J_{O_2} and J_{lac} were 81.4 ± 2.9 (n=6) and 134.4 ± 6.9 (n=57) nanomol/(min·g blot). Under the following conditions designed to stimulate or inhibit Na-K transport, the steady state values normalized to the unstimulated rates and KCl stimulated active isometric force (ΔP_o) are:

Condition	J_{lac}	$\sigma_{\bar{x}}(n)$	J_{O_2}	$\sigma_{\bar{x}}(n)$	ΔP_o	$\sigma_{\bar{x}}(n)$
10^{-5}M Ouabain	.52	.05(12)	1.24	.05(5)	.50	.04(5)
No external K^+	.55	.04(10)	1.06	.06(5)	.14	.04(5)
K_2SO_4 for NaCl	.43	.06 (3)	1.70	.04(3)	1.41	.01(3)
80mM added KCl	1.67	.08(28)	1.80	.05(8)	1.00	

J_{lac} reflects changes in transport conditions while J_{O_2} was found to only increase, paralleling increases in isometric force. While the mechanisms underlying this functional separation of glycolytic and oxidative metabolism is unknown, it may reflect the localization of mitochondria within the cell. *Supported by the American Heart Association.*

T-AM-F5 STUDIES ON THE STIMULATION BY HIGH K^+-ARTIFICIAL SEAWATER OF SODIUM EFFLUX IN BARNACLE MUSCLE FIBERS. Drusilla Mason Sharp*, Ronald G. Schultz* and E.E. Bittar. Dept. of Physiology, University of Wisconsin, Madison, WI 53706.

Depolarization of ouabain-treated and untreated barnacle muscle fibers with high K^+-artificial seawater (ASW) causes a stimulation of the Na efflux. Omission of external Ca^{2+} virtually abolishes the response of the ouabain-insensitive efflux. A sigmoidal concentration-response curve is obtained when external Ca^{2+} is varied prior to depolarization with 200mM-K^+-ASW. Stimulation of the ouabain-insensitive sodium efflux with 100mM-K^+-ASW is reduced by about 40% in fibers preinjected with 250mM-EGTA: 324.0±58.9%,n=3 vs 545.3±38.8%,n=3 ($p<.05$). External application of 10^{-4}M-verapamil practically abolishes the response: 7.0±3.8%,n=3 stimulation compared with a value of 738.7±31.3%,n=3 ($p<<.001$) obtained for controls. The ouabain-insensitive Na efflux is stimulated by injection of $CaCl_2$ e.g. 0.1M-$CaCl_2$ causes a stimulation of 186.3±9.7%,n=7. Both cAMP and cGMP are also found to stimulate sodium efflux when injected into barnacle muscle fibers: 10^{-4}M-cAMP and 10^{-3}M-cGMP cause stimulations measuring 530.3±103.9%,n=3 and 184.3±23.6%,n=10 respectively. Fibers injected with a pure inhibitor of cAMP-dependent protein kinase (PKI) show a reduced response of the ouabain-insensitive Na efflux to subsequent injection of 0.1M-$CaCl_2$ (124.1±9.7%,n=8, $p<.001$), 10^{-4}M-cAMP (76.7±26.1%,n=3, $p<.02$) and 10^{-3}M-cGMP (43.4±11.9%,n=11, $p<.001$). The response of the ouabain-insensitive Na efflux to 100mM-K^+-ASW is also markedly reduced by preinjecting PKI: 429.0±40.1%,n=11 stimulation vs 834.9±76.3%,n=12 ($p<.001$). This finding and the observation that the response is abolished by verapamil suggest that the stimulation caused by high K^+ is the result of activation of a cAMP-dependent protein kinase via a mechanism involving entry of external Ca^{2+} into the fiber.

T-AM-F6 RELATION BETWEEN STATE OF RED CELL CATION PUMP AND GLYCERALDEHYDE 3-PHOSPHATE DEHYDROGENASE ^{31}P NMR RESONANCE. E. T. Fossel and A. K. Solomon, Biophysical Laboratory, Harvard Medical School, Boston, MA 02115.

One of the most convincing arguments that Na,K-ATPase in human red cells is coupled to cation transport was the demonstration by Glynn and Lew (J. Physiol. 207, 393, 1970), among others, that application of a Na gradient much steeper than normal would cause the cell to synthesize ATP from ADP, in contrast to normal conditions when ATP is consumed to pump Na out of the cell. We had previously suggested (J. Cell Biol., 79, 235a, 1978) that intracellular glyceraldehyde 3-phosphate dehydrogenase (G3PDH) might be connected with cation transport. Using glyceraldehyde 3-phosphate (G3P) as a ^{31}P nuclear magnetic resonance probe of G3PDH conformation we had shown that, at constant ionic strength, the conformation of G3PDH was dependent upon intracellular Na conc (with a half-value of 20-30 mM Na) and extracellular K conc (with a half value of about 2 mM K), concentrations similar to the values effective for activation of the red cell alkali cation transport system. We have now studied the conformation of G3PDH using inside out red cell vesicles under conditions modeled on those used by Glynn and Lew to drive the pump backwards in whole cells at constant ionic strength. Glynn and Lew found that increasing extracellular Na from 0 to 100 mM increased ATP production by a factor of 1.4; we found that a similar Na conc change increased the G3P resonance shift from 1.4 Hz to 2.0 Hz, a factor of 1.4 also. At 150 mM extracellular Na, an increase of K conc from 0 to 1.3 mM inhibits the ATP synthesis by 50%; the half value for inhibition of the G3P resonance shift is 1.5 mM K. These results strengthen the view that there is a relation between the conformation of G3PDH and the state of the cation transport system. (Supported in part by NIH Grant 5 R01 GM 15692).

T-AM-F7 CALCIUM CARRYING SYSTEM IN THE GIANT MUSCLE FIBER OF THE BARNACLE SPECIES, Balanus nubilus. P. S. Beirao* and N. Lakshminarayanaiah, Department of Pharmacology, Thomas Jefferson University, Philadelphia, Pa. 19107.

Single barnacle muscle fibers from Balanus nubilus were internally perfused with an isotonic solution containing 180 mM tetraethylammonium acetate and the effects of calcium concentration in the external solution on the voltage clamp currents, especially the initial inward current, were examined. Muscle fiber in external solution containing no added Ca (concentration $< 10^{-5}$ M) gave a current-voltage curve that showed a small inward current followed by a small outward current. An identical curve was realised when the chloride in the external solution was replaced by acetate. The peak inward current increased with increase in Ca concentration in the external solution, but the increase in peak current for equal increments of Ca concentration was reduced and attained saturation conforming to an adsorption regime which was described by the Langmuir equation. A double reciprocal plot of the data of peak inward current due to Ca realised as a function of Ca concentration gave values of 20.7 mM and 200% (the current due to 20 mM Ca normalized to 100%) for the dissociation constant and the maximum current respectively. These values were found to depend on the concentration of Mg used in the external solutions. The peak inward Ca currents measured at two Ca concentrations as a function of pH were unaffected in the pH range 6.1 - 8.8; however when the pH was reduced below 6.1, the currents were depressed.

T-AM-F8 THE EFFECT OF LIPOSOMES ON THYROIDAL IODIDE UPTAKE. G.L. Jendrasiak* and A. Zaleski* (Intr. by A. Veis), V.A. Lakeside Hospital and Northwestern University Medical School, Chicago, IL 60611.

The presence of liposomes in the bathing medium of porcine thyroid slices has a strong effect on the accumulation of iodide by the slices as given by the T/M, i.e., the ratio of the iodide concentration in the slice to that present in the surrounding medium. The liposomes lower the T/M and the lowering depends on the amount of cholesterol present in the phospholipid liposomes being greater for greater amounts of cholesterol. The effect also depends on the size of the liposomes, being greater for the smaller liposomes. The effect of propranolol and liposomes together was also studied with interesting results. The results obtained could be due to the alteration of cholesterol content of the thyroid cell membrane or to an effect on the cell cholesterol metabolism, among others.

T-AM-F9 MAGNESIUM CONTENT AND NET FLUXES IN SQUID GIANT AXONS. M. Caldwell-Violich* and J. Requena, Centro de Biofísica y Bioquímica, IVIC, Apartado 1827, Caracas 101, Venezuela.

Mg content ($[Mg]_i$) of axoplasm of the tropical squid Doryteuthis plei was determined by atomic absorption to be 4.2 ± 0.2 mM/kg for fresh axons. This concentration does not change with the time if axons are stored in 15 mM Mg(Na) SeaWater. $[Mg]_i$ increases linearly with $[Mg]_o$ up to 250 mM Mg_o. The curve relating $[Mg]_i$ with external cation concentration ($[X]_o$), Na or Li substituted by Tris, is biphasic. Axons stored for 3 h. in 100 mM Mg_o, 0 Na (Tris) SW show a $[Mg]_i$ of 7.1 ± 0.5 mM/kg. In the range of 0 to 100 mM X_o irregardless of the nature of X_o, $[Mg]_i$ varies transitorily with a peak value of 9.3 mM at 40 mM X_o and falling to about 8 mM Mg_i at 100 mM X_o. In the range 100 to 385 mM X_o, however, the relation differs depending upon whether the external cation is Na or Li. For the latter, $[Mg]_i$ increases linearly with $[Li]_o$ reaching a maximum of 14.5 mM Mg_i at 385 mM Li_o after 3 h., while for the former, $[Mg]_i$ remains constant in this range of $[Na]_o$ at approximately 6.5 mM. If axons are poisoned with the inhibitors of mitochondria, FCCP and glicolisis, Iodoacetic Acid (IAA), $[Mg]_i$ shows the same behaviour in response to changes in $[X]_o$ as it does in control axons with the exception that Mg_i levels are ca. 40% higher. Nervous activity results in an extra influx of 0.95 fmol Mg/cm^2.imp.mM Mg_o). Axons whose $[Mg]_i$ has been increased ca. 4 fold by incubation in 333 mM Mg, 40 mM Li SW can recover physiological concentrations of Mg_i in 220 mM Na SW with a half time of 5 hours. Axons allowed to recover in 0 Na (Tris) SW, fail to lose this imposed load of Mg_i. Poisoning with FCCP + IAA does not affect the axon's ability to expel the imposed load although it appears to increase the rate of extrusion approximately three fold. It is concluded that the Na electrochemical gradient is required to maintain a physiological $[Mg]_i$ and that metabolical poisoning does not impare this ability.
M.C-V. is a Vollmer Foundation scholar.

T-AM-F10 MEMBRANE PERMEABILITIES MEASURED IN THE PRESENCE AND ABSENCE OF A CONCENTRATION GRADIENT ARE DIFFERENT: A MEMBRANE STRUCTURE EFFECT? M. H. Friedman, R. A. Meyer* and E. C. Hills*, Applied Physics Laboratory, Johns Hopkins University, Laurel, MD 20810

Many artificial membranes and biological barriers to transport (e.g., epithelia) are heterogeneous structures comprised of numerous, often interconnecting pathways, each with its own transport properties. The solute flux driven by a concentration gradient across such membranes will generally differ from that predicted on the basis of tracer permeabilities which are measured in the absence of a concentration gradient. An interferometric technique is used to measure simultaneously the permeability, hydraulic conductivity, and reflection coefficient of Cuprophan 150PM in the presence of a sucrose concentration gradient. For this solute/membrane system, the permeability measured in the presence of a concentration gradient is significantly greater than the tracer permeability. Using an analysis which does not assume ideal dilute solutions and includes diffusion layers adjacent to the membrane, it is shown that the difference between the two permeabilities cannot be explained if the membrane consists of only one kind of pathway but can be explained if the membrane possesses a degree of parallel-path structure.

(Work supported by Contract N00024-78-C-5384, Department of the Navy)

T-AM-F11 MEMBRANE TRANSPORT: COMPARISON BETWEEN VARIOUS METHODS OF DETERMINING PHENOMENOLOGICAL COEFFICIENTS. A. Zelman, M. White* and D. Gisser*, Rensselaer Polytechnic Institute, Troy, N.Y. 12181.

In an apparatus which permits precise measurement of C(t) and V(t) on both sides of the membrane simultaneously and maintains $\bar{C}$ constant to $\pm 0.2\%$, a series of measurements were made with solution agitation (solution stirring rate) as the variable. These non-steady state experiments allow determination of any set of phenomenological coefficients as a function of $\bar{C}$ and solution agitation. The "practical" flux equations for J_s and J_v have been evaluated for L_p, σ and ω with the flux equations solved either simultaneously or independently for the following: 1) linear J_s and linear J_v, 2) exponential J_s and linear J_v and 3) integration of the linear J_s and J_v assuming constant $\bar{C}$. By comparing values of J_s and J_v calculated from the flux equations to experimental values of J_s and J_v, the form which fits the experimental data most precisely was determined. For NaAc, $\bar{C} = 0.15M$, $\Delta C/\bar{C} = 0.5 \rightarrow 0.002$, $\Delta P = 30$ torr, $T = 25^{\circ}C$ and Cuprophane PT-150 membrane, the linear flux equations solved simultaneously gave the best data fit over this range with

$R_{J_s} = \pm 5 \times 10^{-10} \frac{\text{mole}}{\text{cm}^2 \text{ sec}}$, $R_{J_v} = \pm 4 \times 10^{-7} \frac{\text{cm}}{\text{sec}}$ where R indicates error estimate by sum of squares method.

$\omega = 7.91 \times 10^{-9} \frac{\text{mole}}{\text{sec cm}^2 \text{ atm}}$, $L_p = 5.40 \times 10^{-5} \frac{\text{cm}}{\text{sec atm}}$, $\sigma = 0.0575$

T-AM-F12 DEPENDENCE OF SALT AND BUFFER ON PROTON TRANSPORT ACROSS MEMBRANE AND ON OSCILLATIONS. T. Ree Chay, University of Pittsburgh, Pittsburgh, PA 15260.

By using Eyring's multi-barrier kinetics, we have constructed a mathematical model to show the role of buffer and salt on the membrane transport. The model shows that salt and buffer (which play only a minor role in homogeneous media) play an important role in the membrane transport such that the proton transport is enhanced or inhibited depending on the location of isoelectric point of proteins in a membrane. When the model is applied to a system containing enzymes (in a membrane) which possess the autocatalytic character in pH and substrates (in a bath) whose product is proton, the model exhibits sustained oscillations in pH and substrate concentration. The theory also shows that the oscillation strongly depends on the buffer and salt concentrations.

This work is supported by NSF Grant PCM 76-81543.

T-AM-G1 MONOMERIZATION OF PYRIMIDINE DIMERS IN DNA BY LYS-TRP-LYS: ONLY SHORT WAVELENGTH ULTRAVIOLET RADIATION IS EFFECTIVE. John Clark Sutherland and Kathleen Pietruszka Griffin*, Biology Department, Brookhaven National Laboratory, Upton, N.Y. 11973.

Hélène and his associates (ref. 1 and references cited therein) have shown that tryptophan residues in tripeptides (such as Lys-Trp-Lys) or proteins (such as the gene 32 product from phage T-4) can monomerize pyrimidine dimers contained in DNA when exposed to broadband illumination (240-390 nm). These results have lead to speculation (2) that some of the photoreactivation observed in mammalian cells might be due to nonspecific, tryptophan containing proteins or peptides rather than a specific enzyme which has as a primary function the light mediated photoenzymatic monomerization of pyrimidine dimers i.e., a "true" photoreactivating enzyme.

To test this possibility, we have measured the ability of Lys-Trp-Lys plus light to monomerize dimers as a function of wavelength in the range normally used in photoreactivation experiments. We find 313 nm radiation slightly effective in monomerizing dimers in the presence of Lys-Trp-Lys. No monomerization was observed at longer wavelengths, (334, 365 and 405 nm) even at very high fluences -- up to one megaJoule/ m^2. These data suggest that it is unlikely that nonspecific tryptophan-containing proteins can be mistaken for photoreactivating enzymes since the wavelengths which are effective in driving the Lys-Trp-Lys mediated reaction are routinely excluded from photoreactivation experiments. (Supported by U.S. Dept. of Energy and a Research Career Development Award from the Nat. Cancer Inst. (CA05075) to JCS.

1. Hélène, C. and Charlier, M. (1977) Photochem. Photobiol. 25, 429-434.
2. Mortelsman, K., Cleaver, J. E., Friedberg, E. C., Paterson, M. C., Smith, B. P. and Thomas, G. H. (1977) Mutat. Res. 44, 433-446.

T-AM-G2 DNA REPAIR IN HUMAN CELLS TREATED WITH COMBINATIONS OF 7, 12 DIMETHYLBENZ-(A)ANTHRACENE EPOXIDE AND ULTRAVIOLET RADIATION. F. E. Ahmed, and R. B. Setlow, Biology Department, Brookhaven National Laboratory, Upton, N.Y. 11973.

We investigated excision repair in normal human cells treated with the DMBA-epoxide and compared it to excision repair of UV damage. Radioautography showed that unscheduled DNA synthesis (UDS) saturates at a dose of 9.2 μM and remains constant up to the highest concentration employed (37 μM). The magnitude of UDS, however, was 0.1-0.2 of the value obtained after a saturating UV dose (20 Jm^{-2} at 254 nm). Repair replication measurements gave a similar result. Perhaps the small amount of UDS and repair replication is a result of a small patch size as compared to UV. XP cells defective in UV repair were also defective in repair of the chemical damage. We also measured repair after the combined action of DMBA-epoxide and UV in both normal and XP-C cells by radioautography, repair replication and loss of sites sensitive to a UV endonuclease from M. luteus (the nuclease does not work on DNA treated with DMBA-epoxide). In normal human cells UDS and repair replication were additive or greater, and DMBA-epoxide did not inhibit loss of sites sensitive to UV-endonuclease. In XP-C, however, there was less UDS than for each treatment separately, and DMBA-epoxide inhibited dimer removal. There was no loss of viability measured by uptake of the vital dye trypan blue and no loss of radioactivity from treated cells in the time of the experiments ($\leq$ 24 hr). Therefore, we conclude that responses to the combined treatment of UV and DMBA-epoxide are similar to those of UV plus N-acetoxy-2-acetylaminofluorene (AAAF)[1]. In the later case we interpreted the results as indicating different pathways for repair of UV and chemical in normal cells and that the pathways for repair in XP cells are different from those of normal cells. (Supported by U.S. Dept. of Energy.)

1. F. E. Ahmed, and R. B. Setlow. Biophys. J. 21: 94a (1978).

T-AM-G3 KINETICS OF DNA REPAIR SYNTHESIS IN HUMAN FIBROBLASTS INDUCED BY CHEMICAL CARCINOGENS AND ULTRAVIOLET LIGHT.
J. W. Levinson, V. M. Maher*, and J. J. McCormick, Michigan State Univ., East Lansing, MI 48824.

We examined both DNA excision repair synthesis, using the BrdUrd-CsCl gradient centrifugation method, and semi-conservative DNA synthesis following treatment of normal and xeroderma pigmentosum (XP) fibroblasts (XP12BE) with 4 chemical carcinogens and ultraviolet (UV) light (predominately 254 nm). The chemicals, 4-nitroquinoline-1-oxide (4NQO), N-acetoxy-2-acetylaminofluorene (N-AcO-AAF), (-)-7α,8β-dihydroxy-9β,10β,-epoxy-7,8,9,10-tetrahydrobenzo(a)pyrene (BP diol epoxide I) and 4,5-dihydrobenzo(a)pyrene-4,5-epoxide (BP 4,5-oxide) and UV light induced excision repair in normal cells while only 4NQO did so in XP cells. In normal cells the induction of excision repair correlated with inhibition of semi-conservative DNA synthesis. In XP cells, inhibition of semi-conservative DNA synthesis was observed at doses several times lower than those required for normal cells. Excision repair synthesis measured over a 36 hr period reached a maximum at 50μM for 4NQO, 4.5μM for N-AcO-AAF, and 35μM for BP diol epoxide I but continued to increase for UV light (up to 40 J/m^2) and BP 4,5-oxide (up to 140μM). Minimal doses required to detect repair by this method were 1 J/m^2 for UV light, 4,5μM for BP diol epoxide I, and 70μM for BP 4,5-oxide. Repair was detected at the lowest doses tested for N-AcO-AAF and 4NQO (2.2μM). Experiments measuring the rate of excision repair indicated that repair was complete in 2 days for 6.5 J/m^2 UV light or 50μM 4NQO, 5 days for 4μM N-AcO-AAF and 3 days for 8.9μM BP diol epoxide I and 140μM BP 4,5-oxide. (Support by DHEW Grants CA 21247 and CA 21253 and by DOE Contract ER-78-S-02-4659.)

T-AM-G4 CORRELATION AMONG THE RATES OF DIMER EXCISION, DNA REPAIR REPLICATION AND RECOVERY OF HUMAN CELLS FROM POTENTIALLY LETHAL DAMAGE INDUCED BY ULTRAVIOLET RADIATION. B. Konze-Thomas*, J.W. Levinson, V.M. Maher*, and J.J. McCormick, Michigan State University, East Lansing, MI 48824.

We have investigated the kinetics of the removal of thymine-containing pyrimidine dimers from the acid-precipitable fraction of DNA isolated from ultraviolet (UV)-irradiated diploid human fibroplasts in the confluent (G_0) and in growing cultures. The results were compared with the kinetics of incorporation of ^{3}H-thymidine into parental DNA in similar UV-irradiated cultures and with the kinetics of biological recovery of UV-irradiated cells. The kinetics of repair replication is correlated with the rate of excision of dimers. A dose of 40 J/m^2 resulted in dimerization of 0.25% of the thymine in confluent and growing cultures. About 20% of the induced dimers were excised within 3 hr post-irradiation, 60% by 6 hr, 80% by 12 hr. Incubation of cells for an additional 12 hr resulted in the removal of only an additional 5 to 10%. The rate of biological recovery also reflects the kinetics of removal of dimers. Cells irradiated with 7 J/m^2 and prevented from replicating by density inhibition, but allowed to carry out excision repair for various times post-irradiation, exhibited low survival of colony-forming ability (18%) if released immediately, but a higher survival if released from confluence after 4, 8, 12, 16 hr. By 18 hr, survival reached 100%. Cells irradiated with 20 J/m^2 and maintained in a similar manner showed an initial survey of 5% and exhibited a gradual increase in survival, reaching 20% by 12 hr, 50% by 24 hr. The results demonstrate that normal human cells are very proficient at excision and support the hypothesis that pyrimidine dimers are responsible for the cytotoxic effect of UV radiation. (Supported by DHEW Grants CA 21247 & CA 21253 and by DOE Contract 4659, and by a Grant to B. Konze-Thomas from the Deutsche Forschungsgemeinschaft.)

T-AM-G5 DNA REPAIR IN XERODERMA PIGMENTOSUM HETEROZYGOTES. R. B. Setlow and Eleanor Grist* Brookhaven National Laboratory, Upton, New York 11973.

Normal human fibroblasts are able to repair effectively, by an excision process, DNA damage resulting from UV irradiation or from treatment with the proximate carcinogen N-acetoxy-2-acetylaminofluorene (AAAF). XP fibroblasts (with the exception of variants) are defective in the repair of both types of damage. If cells are treated with repair saturating doses of both UV (20 J/m^2 of 254 nm) and AAAF (20 μm, 20 min), the repair in normal cells is additive but in XP cells repair is strongly inhibited.[1] XP heterozygotes show normal amounts of UV repair but we guessed that they might fall in between normal and XP cells in their response to a combination of UV and AAAF. We used an endonuclease from M. luteus specific for pyrimidine dimers to measure UV-repair in the presence of damage from AAAF. Cells, with DNA labeled with ^{3}H, were irradiated with 20 J/m^2 and cells, with ^{14}C label, were treated with both UV and 20 μm AAAF. Twenty-four hours later, the cells were collected together, the DNA extracted and the numbers of breaks per dalton introduced by the nuclease determined by sedimentation in alkali. The differences between the latter numbers and the numbers of enzyme sensitive sites at zero time gives the amount of repair. We have investigated five XP heterozygote strains. Two showed a near normal response to the combined treatment (10-20% inhibition of dimer removal) and three showed an inhibition of ~ 50%. Thus in their response to a combined treatment of UV and AAAF some XP heterozygote strains act as if they had a mixture of repair systems. (Work supported by the U.S. Department of Energy.)

1. F. E. Ahmed and R. B. Setlow, Biophys. J. 21, 94a (1978).

T-AM-G6 RELATIVE CONTRIBUTION OF UNREPAIRED SINGLE STRAND AND DOUBLE STRAND DNA BREAKS TO BIOLOGICAL DAMAGE. A. Cole, R. E. Meyn, and R. Chen*, University of Texas System Cancer Center, M. D. Anderson Hospital and Tumor Institute, Texas Medical Center, Houston, TX 77030

Induction and repair of DNA strand breaks produced by low Linear Energy Transfer (LET) gamma radiation and high LET alpha radiation were studied using neutral sucrose sedimentation to measure double strand breaks (DSB) only and alkaline elution to measure total breaks including single strand breaks (SSB) and DSB. DSB contributions were subtracted from total breaks to determine SSB contributions. The following table lists the strand breaks calculated for gamma and alpha irradiations that produced the same biological effect, i.e. 50% lethality.

	250r γ	42r α		250r γ	42r α
Initial SSB	1000	56	Unrejoined SSB	7.5	5.6
Initial DSB	20	9	Unrejoined DSB	2.0	3.6
Initial SSB + DSB	1020	65	Unrejoined SSB + DSB	9.5	9.2

This data shows that the total number of unrejoined SSB plus unrejoined DSB were the same for the two doses which produced a similar biological effect. Thus, it appears that both SSB and DSB contribute to lethality. We propose that unrejoinable (lethal) breaks represent complex DNA damage containing multiple proximate lesions which may be assayed as either SSB or DSB or other DNA damage, depending on the location of the individual lesions.
Supported in part by Department of Energy Contract EY-76-S-05-2832

T-AM-G7 MULTIPLE PATHWAYS OF INTRAREPLICATION (POSTREPLICATION) REPAIR IN E. coli K-12. R. H. Rothman*[1] and A. J. Clark*[2] (Intr. by F. W. Studier), [1]Department of Biology, Brookhaven National Laboratory, Upton, N.Y. 11973 and [2]Department of Molecular Biology, University of California, Berkeley, Calif. 94720.

Postreplication repair (intrareplication repair to denote that it occurs during rather than subsequent to DNA replication) has been shown to be comprised of more than one pathway. We previously proposed recB- and recF-dependent pathways (1) and Sedgwick (2) has proposed polA-dependent and independent pathways. Youngs and Smith (3) found that intrareplication repair in a uvrB mutant depends upon recB, exrA, and uvrD, and interpreted their data to indicate that there are at least four pathways, one dependent upon each mutant and a fourth requiring all three wild type alleles. Since the uvrB uvrD recB exrA strain is more resistant than a uvrB recA strain they suggested a fifth pathway, possibly dependent upon recF. We find that a uvrB recB recF strain is as sensitive as a uvrB recA mutant and therefore suggest that there are only two major intrareplication repair pathways. The effects of other mutations on intrareplication repair may be interpreted as acting within either the recB- or recF- dependent pathways.

(1) Rothman, R. H., T. Kato, and A. J. Clark. In "Molecular Mechanisms for Repair of DNA" (P. C. Hanawalt and R. B. Setlow, eds.) pp. 283-291. Plenum Press, N.Y. 1975
(2) Sedgwick, S. G. J. Bacteriol. 123; 154-161 1975
(3) Youngs, D. A. and K. C. Smith. J. Bacteriol. 125; 102-110 1976

R.H.R. was supported by U.S. Public Health Service Training Grant GM367 to the Genetics Department, U.C. Berkeley, and N.I.H. National Research Service Award GM05643. This research was sponsored by U.S. Public Health Service Research Grant AI05371 from the National Institute of Allergy and Infectious Disease, and by the U.S. Department of Energy.

T-AM-G8 IS POST-REPLICATION REPAIR REAL? J.E. Cleaver, L. Kapp*, and S.D. Park*, Laboratory of Radiobiology, University of California, San Francisco, Calif. 94143

Post-replication repair has been operationally defined on the basis of the reduced sizes of DNA labeled with ^{3}HdThd at various times after irradiation with UV light (chase-pulse)and the subsequent increase in these sizes (pulse-chase). We have analyzed DNA sizes in chase-pulse and pulse-chase experiments in normal, excision defective and variant xeroderma pigmentosum cells. In chase-pulse experiments DNA sizes decrease for 1-2 hr, and then recover as exponential functions of time, allowing definition of a rate constant, k hr^{-1}. During recovery, excision breaks reduce the number of replicating domains; the recovery constant k, depends on (i) replicon size (ii) excision ability (iii) caffeine concentration (iv) the XP variant gene product. The mechanism of recovery appears to involve replication forks that stop completely or replicate uninterrupted past damaged sites; the probability of stopping decreases with time after irradiation as new replicons initiate and is altered in the XP variant. In pulse-chase experiments labeled DNA in control and irradiated cells increases with time at a constant rate, independent of dose, excision ability, caffeine and the XP variant gene product. If the initial labeled size is reduced by irradiation, then the maximum size reached during the chase is below control, indicating persistent blocks. The mechanism for these events appears to involve normal chain elongation; adjacent replicons being joined by a termination process that is only slightly slowed by a damaged site which behaves as a termination site in an abnormal place. If 2 or more damaged sites are between approaching replication forks termination is blocked for many hours. These phenomena involve normal replication and termination mechanisms, blocked forks, and excision repair; no distinct replication-specific events can or need be identified as a unique "post-replication repair mechanism". Work supported by the U.S. Dept. of Energy and Seoul National University, Korea.

T-AM-G9 INHIBITION OF DNA EXCISION REPAIR IN HUMAN CELLS BY ARABINOFURANOSYL CYTOSINE: EFFECT ON NORMAL AND XERODERMA PIGMENTOSUM CELLS.† W. C. Dunn,* and J. D. Regan*(Intr. by J. S. Cook), Biology Division, Oak Ridge National Laboratory, Oak Ridge, TN 37830.

A 10 μM concentration of the antineoplastic agent arabinofuranosyl cytosine (ara-C), in the presence of 2 mM hydroxyurea, inhibits DNA excision repair in normal human skin fibroblasts by preventing closure of incised, pyrimidine dimer-containing regions in the DNA following 20 J/m^2 of ultraviolet (254 nm) radiation. This inhibition results in the accumulation of single-strand breaks in the DNA of irradiated cells (7.39 breaks/10^8 daltons in 18 hours) as determined by alkaline sucrose sedimentation. Cells from complementation groups of xeroderma pigmentosum, defective in early steps of excision repair, show reduced numbers of DNA single-strand breaks/10^8 daltons when compared with normal cells. CsCl gradient analysis of [^{3}H] thymidine incorporation during repair replication indicates that ara-C causes a 6-56% reduction in the number of nucleotide bases inserted in the DNA at concentrations of 1 and 10 μM, respectively. These concentrations result in the substitution for deoxycytidine (dCyd) by ara-C of 40 and 100%, respectively, in repaired regions. Repair inhibition is reversed by 50% upon removal of ara-C and by >95% with the addition of 100 μM dCyd. Chromatography of digested DNA shows that incorporated ara-C is not removed during dCyd reversal, suggesting that ara-C incorporation per se does not play a significant role in repair inhibition. The dependence on hydroxyurea for ara-C repair inhibition is presumably due to a subsequent reduction in the intracellular pool of dCyd. The total results suggest that ara-C is a weak competitive inhibitor of DNA polymerases associated with ultraviolet-induced excision repair. (†Research sponsored jointly by NCI under Interagency Agreement # 40-5-63 and by the Division of Biomedical and Environmental Research, U.S. Department of Energy, under contract W-7405-eng-26 with the Union Carbide Corporation.)

T-AM-G10 INHIBITION OF SEMICONSERVATIVE AND REPAIR DNA SYNTHESIS IN MAMMALIAN CELLS BY NOVOBIOCIN. M. Mattern and D. Scudiero*, National Cancer Institute, Bldg. 37, Rm. #3C-21, Bethesda, Maryland 20014.

Novobiocin inhibits semiconservative DNA synthesis and, to a lesser extent, RNA and protein synthesis in prokaryotes, presumably by blocking the formation of supercoils in DNA by the enzyme gyrase. There are conflicting reports concerning the effect of novobiocin upon the repair of damaged DNA. In mammalian cells, novobiocin was found to inhibit semiconservative DNA synthesis and, as in bacteria, RNA and protein synthesis to a lesser extent. In a human skin fibroblast cell strain (CRL 1187) 1.7 mM novobiocin completely abolished ultraviolet light-induced DNA repair synthesis as measured by the BND cellulose method. An ultraviolet dose of 15 J/m^2 induced a specific activity of repair synthesis of 200 CPM/ug of DNA in cells not treated with novobiocin. Cells treated with 1.7 mM novobiocin had a specific activity of repair of 0.7 CPM/ug of DNA. This concentration of novobiocin results in approximately 50 % cell survival and 10 % semiconservative DNA synthesis in Chinese Hamster ovary cells. Novobiocin alone did not appear to induce repair synthesis.

T-AM-G11 DOSE RESPONSE RELATIONS FOR UV INDUCTION OF PROTEIN X IN E.COLI STRAIN AB1157. Deno Kazanis*, Ernest C.Pollard and D.J.Fluke. Zoology Department, Duke University, Durham, N.C. 27706.

The phenomenon of induced repair in E.coli strains which are not recA$^-$ nor lex$^-$ involves a number of observed responses, including mutagenesis, inhibition of post radiation DNA degradation, septum inhibition, radioresistance and the induction of prophage. Protein X, an inducible protein, has been identified as the recA gene product. Its induction by UV light should therefore parallel the induction of other induced repair phenomena, a parallelism we refer to as coordinate induction. In order to make valid comparisons the UV dosimetry must be absolute and the light of one wavelength. The monochromator in the Duke Zoology department has been employed to give light at 265nm with the intensity monitored through the sample during exposure and with a field lateral average measured by thermopile and galvanometer. The observation of protein X was made in SDS-polyacrylamide gels with an 8 - 20% gel gradient. The induced band is readily seen on staining. By introducing ^{35}S during the post-induction incubation period the bands are radioactively labeled. They are then excised, dissolved in 30% hydrogen peroxide and counted in Aquasol in a liquid scintillation counter. The dose response relation is found to be coordinate with induced inhibition of post radiation DNA degradation, induced radioresistance and very close to the dose-response relation for W-reactivation. It deviates from the dose-response relation for the induction of AB1157λ.

Support from a Hargitt Fellowship and D.O.E. grant EY-76- S-05-3631 is acknowledged.

T-AM-G12 DOSE RESPONSE RELATIONS FOR UV INDUCTION OF SEPTUM INHIBITION IN FOUR STRAINS OF E.COLI K12. Brian Robinson*, D.J.Fluke and Ernest C.Pollard, Duke University, Durham, N.C. 27706.

The strains and radiation-related mutations which they carry are as follows:

1. AB1157 uvr$^+$ lon$^+$. Carries excision repair;non filament forming.
2. AB1886 uvr$^+$ lon$^-$. No excision repair; non filament forming.
3. AB1899 uvr$^+$ lon$^-$. Carries excision repair; forms filaments.
4. AB1896 uvr$^-$ lon$^-$. No excision repair; forms filaments.

Using absolute dosimetry and monochromatic light of 265nm wavelength, we observed the dose response relations for these strains. To observe septum inhibition we allowed the cells to grow for 120 minutes after treatment with UV and took photographs of the cells as seen in a microscope in a Petroff-Hausser cell. These photographs were subsequently analyzed for the length of cell. Any cell which lay outside the normal range of the unirradiated cells was scored as septum inhibited. The strains which are lon$^-$, develop into long filamentous forms at longer incubation times. However, all four strains show septum inhibition. Strain AB1157 shows a dose response relation which is coordinate with other manifestations of induced repair. AB1886 behaves in the same way but at markedly (5 - 6 fold)less dose. This is believed to be because in the excision lacking strain daughter strand gaps are formed at lower doses. Strain AB1899 shows a dose response relation with considerably lower doses than for the uvr$^+$ lon$^+$ case, but not quite as sensitively as for the uvr$^-$ case. The double mutant AB1896 which is both lon$^-$ and uvr$^-$ shows a dose response relation rather closely like AB1886 (uvr$^-$). The spontaneous level of induction is 3.5% in AB1157, 4.5% in AB1886,and about 8% in the two lon$^-$ cases. Supported by D.O.E. Grant EY-76-S-05-3631.

T-AM-Po1 EVOLUTIONARY TREES FROM PROTEIN SEQUENCES: PROBABILITY OF CORRECT RECONSTRUCTION OF FOUR-BRANCH TOPOLOGIES. W. C. Barker and M. O. Dayhoff, National Biomed. Res. Fnd., Georgetown Univ. Med. Ctr., 3900 Reservoir Rd. N.W., Washington, D.C. 20007

We tested a corrected-matrix method of deriving evolutionary trees from protein sequences by reconstructing topologies from computer-evolved model sequences. Specified numbers of changes were made to a model sequence 100 residues long of average amino acid composition to generate five new sequences related to each other as shown, where α represents the number of changes from a node to an exterior sequence and β is the number of changes between sequences at the interior nodes. Values of α varied from 8 to 64 changes and the ratio of $\beta:\alpha$ varied from 4:1 to 1:8. A set of ten independent simulations was run for each evolutionary history considered. Matrices of percent difference between the generated exterior sequences were corrected for parallel and superimposed mutations. These matrices were used in a computer program that calculates best-fitting branch lengths for the three possible topological connections of the four sequences. The topology with the smallest absolute overall length was correct for all cases with $\beta:\alpha$ between 4:1 and 1:2, for 87% of cases with $\beta:\alpha$ of 1:4, and for 67% of cases with $\beta:\alpha$ of 1:8. Using the matrices of estimated mutations produced more correct topologies than using matrices of percent differences. (Supported by NIH Grants HD 09547 and GM 08710.)

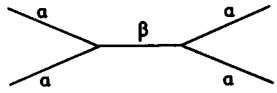

T-AM-Po2 BIFURCATING KINETIC MODELS OF POLYPEPTIDE ADAPTORS AND THE ORIGIN OF THE GENETIC CODE. V. Bedian, SUNY/buffalo, Dept. of Biophysical Sc., 118 Cary Hall, Buffalo, N.Y. 14214.

Differential equations representing the kinetics of template directed polypeptide production are derived from a detailed description of the polymerization process. The assumptions are:1)stable polynucleotide replication;2)energy rich monomers;3)irreversible amino acid polymerization catalyzed by synthetase-like proteins (adaptors);4)fixed codon frame, and start/stop positions;5)localization of components. The system of adaptors is characterized by: kinetic parameters (production and decay rates); a specific activity matrix S (catalytic rates); and a structural genetics matrix M (relationship of adaptor critical sites to template codons). For a given codon and amino acid alphabet, all possible assignments (codon-amino acid pairs) are represented by adaptors in the system, so that only special subsets of adaptors can execute an unambiguous code. A coding subset of adaptors that can produce all its components by its collective catalytic action (i.e. coded M), is a self-coding system (SCS). For two letter alphabets, that define four assignments with two coding subsets, reduction of a four adaptor system yields two components representing the two competing codes. Linear analysis and numerical integration indicate, that this system can have 1, 2, or 3 asymptotically stable steady states, depending on the kinetic, S, and M parameters. These states can be interpreted as:1)a single SCS;2)a single non-coding system (NCS);3)a pair of SCS's;4)one SCS and one NCS; and 5)under very symmetrical conditions, one NCS and two SCS's. The model also suggests a plausible selection function: the nonlinear term in each equation is the efficiency (Q) of selfreproduction of the component. Steady state values of Q indicate an evolutionary pathway connecting a NCS of nonspecific, noncoded adaptors (Q minimum) to a SCS of specific, coded adaptors (Q maximum). The model also predicts behavior similar to suppression mutants, and can be extended to larger alphabets and code evolution problems.

T-AM-Po3 SOME THEORETICAL ASPECTS OF THE INTERACTION BETWEEN ELECTRICALLY EXCITABLE CELLS AND MAGNETIC FIELDS. Eric Jakobsson, Department of Physiology and Biophysics and Program in Bioengineering, University of Illinois, Urbana, Illinois 61801.

It can be shown from Maxwell's Equations that the magnetic fields associated with currents in space-clamped membranes are zero. This follows from the fact that the curl of both the real and displacement current vectors is zero, and is true for cylindrical and spherical cells as well as for a flat membrane. For propagated electrical signals however, the curls of the real and displacement current vectors are not zero, so one expects propagated signals to generate and be affected by magnetic fields. This paper will consider the problems associated with calculating magnetic fields produced by electrical activity and also with calculating the effects on electrical activity of externally applied magnetic fields. Large magnetic forces may also be induced in nominally voltage-clamped membranes when the electric field is changing very rapidly, such as during the (almost) instantaneous step from one voltage to another during voltage clamp experiments. Possible effects of these forces on the results of voltage-clamp experiments will be considered.

This work was partially supported by the Bioengineering Program of the University of Illinois and partially by Grant #HL 21342 from the National Institutes of Health.

T-AM-Po4 DIFFUSION ON A DISK: SOLUTIONS TO LAPLACE'S EQUATION FOR DEVELOPMENTALLY RELEVANT GEOMETRIES. K. Conway*(Intr. by R.K. Hunt), Biophysics, Johns Hopkins U., Baltimore, MD 21218

Field-like properties are displayed by the digit pattern of a limb bud and the "map" of neural connections of retinal ganglion cells. The physical basis for such a morphogenetic field is probably a near-neighbor process like diffusion or cell-surface interactions. These and other possible mechanisms (electric fields or ion currents) can be represented by modifications of Laplace's equation. Previous efforts to quantify such patterns have been limited to very simple geometries, such as a line of cells (Crick, Nature, 225:420). I have solved a modified diffusion equation $DV^2M + S = dM/dT$, for several geometries and conditions. The geometries were disk, ring, and portions of a sphere. Both concentration dependent and independent sources and sinks (S) were used. Boundaries were impermeable. Analytical solutions to most of these problems are complex and do not converge at the edge of the surface. Numerical solutions were generated by repeatedly computing the change in the morphogen (M) for each locus over a small change in time. Results were presented numerically as contour plots, and as 3-dim plots. The resulting patterns are monotonic but non-linear gradients of M. The degree of nonlinearity is startling. I conclude that developmental gradients are distinctly non-linear, except for very simple geometries. Later events such as differentiation must be able to use non-linear gradients. Several types of source-sink functions (S) produce useful gradients that are still changing at long times. And, as expected, different geometries produce different patterns. Thus, in the growing, folding organ bud, the gradient pattern probably never stops changing. Later events must "pick off" the information at some time, and may be able to use the same gradient repetitively (Kauffman, Science, 199:259; Hunt et al., unpublished).

I thank S. Hardt for the initial version of this computer program. (NIH#GM 07231-03)

T-AM-Po5 "PSEUDOCHEMOTAXIS" - KINETIC RESPONSES OF MICROORGANISMS TO ATTRACTANT GRADIENTS. I. Richard Lapidus, Physics Department, Stevens Institute of Technology, Hoboken, New Jersey 07030.

Apparent chemotactic behavior by microorganisms moving in defined attractant gradients is exhibited if the "random motility" is a function of the attractant concentration. Computer techniques are used to solve the differential equations of motion for a population of microorganisms responding chemokinetically to variable attractant concentrations. The distinction between chemotactic (directed) responses and simple chemokinetic (random) responses which are modulated by a variable attractant concentration is discussed. The interpretation of experimental data on the behavior of microorganisms in attractant gradients may change at different times during an experiment. Several examples of such experiments and their interpretation are discussed.

T-AM-Po6 MODELS OF THE MOLECULAR STRUCTURE OF RECEPTORS FOR THE TUMOR-PROMOTING AGENTS PROSTAGLANDINS AND PMA. J. R. Smythies and J. Wright,* University of Alabama in Birmingham, Birmingham, Alabama 35294.

In 1975 the prediction was published, on stereochemical grounds, that prostaglandins (PGs) would be tumor promoters. This hypothesis was based in part on their molecular homomorphology with the known tumor promoter, anthralin. This hypothesis was confirmed experimentally by Lupulescu in 1978. PGs and related tumor promoters powerfully induce ornithine decarboxylase (ODC), the rate-limiting step in the synthesis of the polyamines, putrescine and spermidine, essential for cell growth. Spermine is a powerful inhibitor of ODC. A model receptor is presented complementary to 2 PGs + 2 Ca++ and other known and probable tumor promoters (as agonists) and to certain anti-tumor compounds (as antagonists). This consists simply of two anti-parallel polypeptide β-chains 12-13 Å apart, each of sequence - phosphoser - x - ile - x - his - x - phosphoser - . All tumor promoters have the molecular structural capacity to interact with this model receptor so as to align the 2 p-sers at each end to enable them to chelate one Ca++ ion between them. A series of anti-cancer drugs (such as maytansine) have the molecular structural capacity to bind to this receptor and fail to align the p-sers correctly to chelate Ca++. This model receptor also shows a high degree of molecular complementarity to one molecule of spermine. This receptor could therefore be on the control mechanism for synthesis of ODC at which spermine acts as the natural end-product feedback inhibitor and PG + Ca++ as the natural activators. Tumor-promoting phorbol esters such as PMA may act in part at another receptor. PMA is a close structural homologue of lysophosphatidylethanolamine (LPE), and it could be a competitive inhibitor of LPE at a postulated negative feedback receptor for LPE on phospholipase A2. CPK molecular models illustrating these various stereochemical relationships will be presented.

T-AM-Po7 A NEW METHOD TO MEASURE SHEAR STRESS AT THE WALL OF GLASS MODEL ARTERIAL BIFURCATIONS. S.L. Adamson* (Intr. by Margot R. Roach), Biophysics Dept., University of Western Ontario, London, Ontario, Canada.†

Shear stress at the arterial wall has been implicated in the etiology of atherosclerosis however no direct measurements of wall shear stresses have been made in vivo. A new method is presented which measures shear stress at the wall of glass models of arterial branchpoints. The model is connected to a water-filled pressure reservoir and to a flowmeter. The test section is filled with white latex paint, then flow from the pressure reservoir is started. The removal of liquid paint from the central region occurs quickly but a thin layer (less than 1 μm thick) is removed slowly from the wall at a rate which is proportional to the shear stress. The change in intensity of light reflected from the tube (as it goes from opaque to transparent) is recorded on tape with a videocamera. The shear stress can be determined from the rate of change in the recorded signal. Since the videotape can be played back repeatedly, a single run can be used to produce a continuous picture of shear stress as a function of position in the model artery. Experiments completed to date confirm the usefulness of this approach in assessing shear stress in straight cylindrical tubes ($r = 0.385$ cm, shear stress 0.80 to 1.80 dynes/cm^2, steady flow). That is, the time taken for intensity to fall from 50% to 20% of the initial value has been found to reliably measure shear stress to within 5% of the Poiseuille flow prediction. Experiments in progress examine a greater range of shear stresses in models of large arterial branch sites (origins of the renal, coeliac and intercostal arteries). Flows with Reynolds number from 100 to 1500 are being examined, as is the effect of altering the fraction of flow to the branch artery.

†Supported by a grant from the Ont. Heart Found. & a Studentship from Medical Res. Council.

T-AM-Po8 EFFECT OF BLOOD FLOW ON ORIENTATION OF ARTERIAL ENDOTHELIAL CELLS.† B.L. Langille* and M.A. Reidy* (Intr. by M. Sherebrin), Biophysics Department, University of Western Ontario, London, Ontario, Canada.

Current evidence suggests that fluid mechanical forces (particularly shear stresses) can injure the endothelial lining of arteries and that such injury is important in the initiation of atherosclerosis. Critical to this hypothesis is direct confirmation that the endothelium is sensitive to local blood flow patterns. Such confirmation is difficult because it is necessary to examine endothelium over areas large enough to include cells exposed to significantly different blood flow patterns. Recently developed techniques using the scanning electron microscope (SEM) provide the opportunity for such examination. We have used the SEM to observe the endothelium of the rabbit aorta in areas where changes in the direction of blood velocity can be established (particularly at arterial branch sites). In these areas endothelial cells are consistently aligned along the direction of blood flow. In addition, when normal flow patterns were chronically altered by surgical interventions, changes in endothelial cell orientation followed changes in flow direction. Such interventions included constriction of the abdominal aorta, in which case endothelial cells ultimately become organized into swirling, vortex-like patterns downstream from the constriction. Also, ligation of one renal artery caused realignment of cells around the orifice of this artery from the direction of normal renal artery flow to the direction of aortic flow. Our findings confirm that the endothelium is highly sensitive to local haemodynamic forces.

†Supported by the Ontario Heart Foundation.

T-AM-Po9 MORPHOLOGIC EVIDENCE FOR C-TYPE RNA VIRUSES IN ISOLATED RAT VENTRAL PROSTATE EPITHELIAL CELLS. K.M. Anderson, M. Rubenstein*, T.M. Seed*[1], Oncology Lab., Dept. of Biochemistry, Dept. of Medicine, Rush-Presbyterian-St. Luke's Medical Center, Chicago, IL, and Division Biol. Med. Res.[1], Argonne National Laboratory, Argonne, Illinois.

We are evaluating a method for separating epithelial and connective tissue cells from rat ventral prostate by mechanical disruption of the organ and centrifugation of cells through a Ficoll gradient. Characteristically, four cellular fractions are obtained, but most cells are in bands 2 and 4. Band 4, at the gradient-cushion interface, contains the highest percent of cells positive for prostate-specific acid phosphatase, binds the greatest amount of ^{3}H-testosterone or its metabolites *in vivo* or *in vitro*, and is enriched in nucleated cells with prominent endoplasmic reticulum, secretory vacoules, granules and microvilli.

When these epithelial cells from band 4 were examined by transmission electron microscopy, typical C-type viral particles were readily seen either budding from, or in close proximity to their plasma membranes. To our knowledge, observation of C-type viral particles in prostate cell fractions from Sprague-Dawley and Long-Evans rats has not been reported. Dissociation of prostatic tissue and sedimentation through a Ficoll gradient facilitated their detection. This may represent a general method for enhancing visualization of viruses in normal and cancerous parenchymatous tissues.

T-AM-Pol0 PLATELET AGGREGATION STUDIES BY COMPUTER IMAGE ANALYSIS.
J. A. Zeller*, R. E. Dayhoff, R. S. Ledley, Dept. of Pathology, George Washington University and Veterans Administration Medical Center and Dept. of Physiology and Biophysics, Georgetown University, Washington, D.C.

One of the problems in the study of thrombotic and embolic disease is the limitations of in vitro methodologies in measuring platelet aggregation. The most popular in vitro method, light transmission aggregometry, is insensitive to the earliest stages of aggregation and does not provide information about the size and number of free platelets and aggregates. Our image analysis methodology overcomes these limitations. The TEXAC Image Analyzer is faster than conventional computers and is well suited to the whole picture image analysis necessary for recognition and sizing of platelet aggregates. The TEXAC scans multiple microscope fields of formalin stabilized platelet rich plasma, identifies each point of the digitized image as either background or platelet, and determines the area of each free platelet or aggregate. Loose platelet aggregates can be distinguished from multiple free platelets by an algorithm of neighborhood averaging. Aggregates as small as doublets are recognized by this system. We have found doublets, small aggregates (three through eight platelets) and large aggregates (nine or more) in apparently unstimulated platelet suspensions of normal subjects; they are also found in platelet suspensions stimulated with low concentrations of adenosine diphosphate (0.16 uM), even in the absence of changes in light transmission by aggregometry. Our TEXAC image analysis method offers the prospect of providing a clinically useful tool for recognizing hyperaggregable platelet behavior.

T-AM-Pol1 BACTERIAL BIOLUMINESCENCE FROM SINGLE CELLS EXHIBIT NO OSCILLATIONS
Elisha Haas* and J.W. Hastings, Biological Labs., Harvard Univ., Cambridge, MA 02138

Since the usual measurements of light emission from marine bacteria involve a large number (10^6 to 10^{10}) of cells, the question has often been raised as to whether or not the individual cell's luminescence is truly continuous. To investigate this question we assembled a sensitive photon counting system with computerized data acquisition. Several luminous species were studied: Beneckea harveyi, Photobacterium belozerskii, P. fischeri and P. leiognathi. Isolated single cells gave count rates ranging from 2 to 10 times the background, depending on the brightness of the strain and the state of induction. No flashes, bursts or oscillations were evident from data collected in counting intervals of 100 msec. To detect possible low amplitude oscillations we used both photon autocorrelation and power spectral analysis using the fast Fourier transform, but none were found. Our algorithms can detect an oscillating component with an intensity as low as 0.3% of the average, as determined by the analysis of reference light sources. Finally, if the photons are emitted in a completely random fashion, the counts at low count rate should be Poisson distributed. The count distribution from the living cell match closely that of a radioactive light standard attenuated to the same average count rate, indicating that there are indeed no periodic or non-periodic bursts in the emission rate.

T-AM-Pol2 SEPARATION OF T AND B LYMPHOCYTES FROM HUMAN TONSILS BY DENSITY GRADIENT ELECTROPHORESIS.
C.D. Platsoucas, R.A. Good* and S. Gupta*, Memorial Sloan-Kettering Cancer Center, New York, N.Y. 10021.

T and B lymphocytes from human tonsils were separated by density gradient electrophoresis on the basis of their surface charge. The separated cell fractions were characterized by a panel of surface markers. The high mobility cells were T lymphocytes (E rosette positive cells) with minimal contamination of surface immunoglobulin-positive cells (B cells). The intermediate mobility fractions contained both T and B lymphocytes, whereas the low mobility cells were predominantly B lymphocytes (sIg-positive cells) with only 10% to 30% T cell contamination. Surface IgM-positive lymphocytes, and cells with IgG Fc or complement receptors were present only in the low and intermediate mobility fractions. The separation of T and B lymphocytes from tonsils, by density gradient electrophoresis, was of higher purity than that from peripheral blood. This investigation demonstrates that T lymphocytes are present predominantly in the high mobility fractions, whereas B lymphocytes are enriched in the low mobility fractions. Supported by grants T-32 CA-09149, CA-19267, CA-17404, AI-11843, NS-11457 and AG-00541 from the NIH and the Fund for the Advanced Study of Cancer.

T-AM-Pol3 HIGH PRESSURE LIQUID CHROMATOGRAPHY PROCEDURES FOR DETECTING NICOTINATE-AND HYPOXANTHINE/GUANINE PHOSPHORIBOSYLTRANSFERASE ACTIVITIES. L. Hanna, L. Ali, and D. L. Sloan, City College of N.Y., N.Y., N.Y. 10031.

High pressure liquid chromatography(HPLC) is a sensitive method for separating and characterizing purine and pyrimidine bases and nucleotides. Using 25mM $(NH_4)H_2PO_4$(pH8) as elution buffer, the substrates (nicotinate, ATP) and products (NaMN,ADP) of the reaction catalyzed by nicotinate phosphoribosyltransferase(NPRT) can be separated completely and their concentrations characterized. At a pressure of 800 psi (0.7 ml/min) the elution times of ATP, nicotinate, ADP, and NaMN from a μC-18 column (Waters/Assoc.) are 4.13, 5.88, 4.50, 3.25 min respectively. The ATP and nicotinate peaks are observed to decrease concomitant with ADP and NaMN peak appearances in the presence of NPRT, Mg^{+2} and phosphoribosyl pyrophosphate (PRPP). A fifth peak (AMP) also appears (5.0 min) as a result of this incubation suggesting that sizable AMP concentration results from this reaction. Using 100 mM $(NH_4)H_2PO_4$(pH6) and the same column at 1000 psi (1 ml/min) a complete separation of hypoxanthine (10 min) from IMP (6 min) and guanine (10 min) from GMP (6 min) can be achieved. In separate experiments it was determined that guanine is preferred over hypoxanthine as substrate by the criteria of nucleotide formed/min/mg in the presence of PRPP, Mg^{+2}, hypoxanthine/guanine phosphoribosyltransferase from yeast, and base. In all of the assay procedures, samples were heated and filtered through millipore filters (.025μM) to remove enzyme before HPLC injection. Buffers were eluted though small μC-18 beds prior to each HPLC run. This work was supported by grants BC-268(ACS), 20183(NIH).

T-AM-Pol4 THERMODYNAMICS OF CANCER ANALYTIC REACTIONS. L. Moffat* and D. Yourtee, Cancer Research Center, Columbia, Mo. 65205.

The need for a rapid, inexpensive, and accurate detection method from biological fluids continues to prevail in the field of cancer research. One recent concept of detection proposes the coordination of multiple biological markers capable of amplifying the existence of small tumors. The utilization of this concept requires some form of instrumentation that would produce a common measurement for the reactions involved. Calorimetry, because of the universal nature of heat change, is one possible method of demonstrating this combined marker amplification. This research investigates the thermodynamic properties of the fructose phosphates and their corresponding isoenzymes of aldolase. A change in the ratios of the components in this interaction has been considered by some as a cancer marker. This report deals with a means of obtaining those ratios through a simple additive process involving the heats of the involved reactions. This additive process could be applied to other cancer marker reactions, thus hopefully resulting in a combined marker signal from one basic form of instrumentation. In addition to the fructose system, other applications in the cancer analytic area will be presented.

T-AM-Pol5 ZERO PRESSURE GRADIENT STOPPED FLOW THERMAL APPARATUS. P. D. Bowen*, R. Paul*, B. Balko*, R. L. Berger, Laboratory of Technical Development, NHLBI, Bethesda, MD 20014, and H. A. Hopkins*, Department of Chemistry, Georgia State University, Atlanta, GA 30303.

A zero pressure gradient stopped flow thermal apparatus has been constructed which eliminates the 10 to 15 millidegree temperature pulse occuring at stopping due to the adiabatic compressibility of water (1). A time resolution of 3-5 milliseconds is achieved without the initial rise distorted by the pressure induced step function. Detectivity in this bandpass is 0.2 millidegrees.

(1) J. Pochobradsky, B. Balko, and R. L. Berger, Anal. Letters (In press, 1978).

T-AM-Po16 AC RESISTANCE MEASUREMENT OF SINGLE CELLS BY FLOW CYTOMETRY. R. A. Hoffman, Ortho Instruments, 410 University Ave., Westwood, MA 02090

The Coulter volume measurement has been extended to the use of high frequency A.C. currents. A flow system instrument described previously (R.A. Hoffman and W.B. Britt, J. Histochem. Cytochem., in Press) has been improved so that it is routinely possible to detect human erythrocytes and the larger human platelets traversing a 93μ diameter orifice. Briefly, cells in saline suspension are caused to flow through a sensing orifice. Changes in the DC and AC resistance of the orifice due to the entry of a cell are simultaneously detected. Under normal conditions the DC resistance change is a measure of cell volume while the AC resistance change depends additionally on the resistivity of the cell interior. The AC measurement has been made with frequencies from 1-9 MHz. The usual working frequency has been 4.5 MHz. The instrument will be described, and representative data on several mammalian cell types will be presented. I have observed two cell types in human blood that are indistinguishable on the basis of DC Coulter volume but which are easily distinguished on the basis of AC resistance measurements at 4.5 MHz. The cell type with the higher AC resistance is a small lymphocyte while that with the lower AC resistance seems to be some type of red cell. (This work was performed while the author was with the Biophysics and Instrumentation Group, Los Alamos Scientific Laboratory, University of California, Los Alamos, New Mexico, and it was supported under interagency agreement Y01-CM-40102 between the United States Department of Energy and the National Cancer Institute of the National Institutes of Health).

T-AM-Po17 DIPOLAR CORRELATION TIMES FOR DETERMINATION OF Mn^{2+}-SUBSTRATE DISTANCES ON ENZYMES. A.S. Mildvan, G.M. Smith* and R.K. Gupta, Inst. for Cancer Research, Philadelphia, PA 19111

For paramagnetic ions such as Co^{2+} with short electron-spin relaxation times (τ_s) the dipolar correlation time (τ_c) is dominated by τ_s. This permits an estimation of τ_c for calculating metal-substrate distances from the frequency dependence of the longitudinal relaxation time (T_{1p}) of water protons in the same complex. For macromolecular complexes of Mn^{2+} the similarity of τ_c values determined from T_{1p} of water protons and of substrate nuclei (^1H, ^{13}C, ^{31}P) at magnetic fields ranging from 2 - 52 K gauss (Table) indicates this to be a reasonable approximation as well. Hence a common mechanism (τ_s) may modulate all Mn^{2+}-nuclear dipolar interactions in macromolecular complexes. A 2-fold uncertainty in τ_c yields a 2-fold uncertainty in the number of water ligands but only a 12% uncertainty in the calculated Mn^{2+}-substrate distances.

Mn^{2+}-Complex	$\tau_c(H_2O)$(nsec)	τ_c(Substrate)(nsec)
Pyruvate Kinase-Mn^{2+}-Pyruvate-Pi	5.5 ± 1.0	3.5 ± 1.5 (^{13}C)
Pyruvate Carboxylase-Mn^{2+}-Pyruvate	6.5 ± 2.0	3.2 ± 1.0 (^1H), 4.5 ± 1.0 (^{13}C)
Phosphoglucomutase-Mn^{2+}-CH_3PO_3	3.6 ± 1.0	3.5 ± 1.0 (^1H)
Xylose Isomerase-Mn^{2+}-Xylose	0.35 ± 0.15	0.4 ± 0.2 (^1H)
RNA Polymerase-Mn^{2+}-ApU	2.9 ± 1.0	1.8 ± 1.2 (^1H)
Enolase-Mn^{2+}-CH_2PEP	0.8 ± 0.2	2.1 ± 1.7 (^1H)
Carbonic Anhydrase-Mn^{2+}-pNO_2phenol	3.8 ± 0.4	5.5 ± 0.6 (^1H)
Aldolase-Mn^{2+}-Acetol-P	2.1 ± 0.5	2.0 ± 0.6 (^{31}P), 0.9 ± 0.5 (^1H)

T-AM-Po18 DETECTION OF PREGNANCY RELATED HORMONES IN RAT BLOOD BY NMR METHOD. H.S. Sandhu,* G.B. Friedmann and N. Sherwood.*

Measurements of the spin-lattice relaxation time (T_1) and spin-spin relaxation time (T_2) were carried out in rat red blood cells and plasma samples at room temperature using NMR pulse techniques. The samples studied had hormones related to the reproductive cycle: leuteinizing hormone (up to 7000 times physiological level), human chorionic gonadotrophin (up to 60 times physiological level) and estradiol - 17β. The presence of these hormones in blood did not produce any measurable changes in T_1 or T_2. NMR Spectra of the sample containing these hormones showed no signals attributable to these hormones indicating that the hormones level in blood is too small to produce any significant changes in T_1 or T_2.

T-AM-Po19 SIDEBAND INTENSITIES FOR NMR SPECTRA OF SAMPLES SPUN AT THE MAGIC ANGLE. J. Herzfeld and A. E. Berger*, Biophysical Laboratory, Harvard Medical School, Boston, MA 02115 and Applied Mathematics Branch, Naval Surface Weapons Center, Silver Springs, MD 20910.

In liquids, NMR resonances are very narrow by virtue of rapid isotropic tumbling which averages anisotropic interactions. When molecules are hindered in their motion, as for example in membranes, the NMR resonances are broadened. In the absence of quadrapolar interactions, the line widths for decoupled spectra are generally dominated by the chemical shift anisotropy ($\Delta\sigma$). Spinning the sample rapidly about an axis at 54°44' (the "magic angle") with respect to the magnetic field, averages the chemical shift to its isotropic value and a single narrow line is obtained. At slower speeds, the isotropic line is flanked by sidebands spaced at the spinning frequency (w_r). The intensities (I_n) of these sidebands are of interest because they contain information concerning the chemical shift anisotropy, which in turn reflects the extent of molecular motion. Lippmaa et al.[1] have calculated the dependence of I_0 and $I_{\pm 1}$ on w_r, for axially symmetric chemical shift tensors. We have extended this calculation to include all the sidebands and asymmetric chemical shift tensors. I_n can be expressed as a double power series in $(\sigma_{11}+\sigma_{22}-2\sigma_{33})/w_r$ and $(\sigma_{11}-\sigma_{22})/w_r$, which converges rapidly for $w_r \gg \Delta\sigma$. For $w_r < \Delta\sigma$, it is more practical to evaluate I_n by numerical integration. We report both the coefficients of the power series and the calculated line intensities. These are compared with spectra obtained for barium diethylphosphate and brushite ($CaHPO_4$) at various $w_r < \Delta\sigma$. We also discuss methods for recovering the principal values of the chemical shift tensor from the sideband intensities. (Supported by NIH grant GM23316 and the NSWC Independent Research Fund.)

1. Proceedings of the XIXth Congress Ampere, Heidelberg, 1976, pp. 113-118.

T-AM-Po20 EFFECT OF MEMBRANE SUSPENSION TURBIDITY ON DPH FLUORESCENCE ANISOTROPY. B. R. Lentz, B. M. Moore*, and D. A. Barrow*, University of North Carolina, Chapel Hill, N. C. 27514.

Data are presented to demonstrate the depolarization of 1,6-diphenyl-1,3,5-hexatriene (DPH) fluorescence by light scattering in turbid membrane suspensions. This artificial decrease in fluorescence anisotropy caused by light scattering has been noted by Teale based on the polarized fluorescence of two different fluorophores in isotropic glycogen solutions. Teale developed approximate equations describing this effect (Teale, Photochemistry and Photobiology 10, 1969, 363). Our results, obtained with a variety of membrane systems, confirm the general applicability of Teale's equations to depolarization by membrane suspensions, although the depolarization constants differ from that predicted by Teale's theory. Indeed, the depolarization proportionality constants obtained with different membrane systems are not equal, but are shown to vary with a) the physical state of the membrane, b) the cholesterol content of the membrane, c) the protein content of the membrane, and d) the method of membrane preparation or isolation. We conclude that depolarization corrections must always be considered when using DPH fluorescence anisotropy to compare the fluidities within different membrane bilayers.

T-AM-Po21 RAPID AUTOMATIC MEASUREMENT OF RAYLEIGH INTERFEROGRAMS FROM THE ULTRACENTRIFUGE. T. M. Laue* and D. A. Yphantis, Biochemistry and Biophysics Section, Biological Sciences Group and Institute of Materials Science, University of Connecticut, Storrs, CT 06268.

Rayleigh interferograms from the ultracentrifuge can be measured accurately at rate of two radial points per second using a photodiode array to scan the photographic image and a modified Walsh transform to reduce the data. A 1024 element linear photodiode array is arranged perpendicular to the fringes, spanning about five fringes in the magnified photographic image. The center-to-center spacing of the photodiodes is 26 μm and the active area of each diode is 15 μm by 15 μm. The radial position of the image is chosen by stepping motor drive of the comparator stage under computer control. The light intensities impinging on the photodiodes are digitized and then buffered by a 1024 byte memory. These buffered intensities are reduced using a modified Walsh transform (essentially a square-wave Fourier transform) to yield the fringe phase and the transform magnitude. Fringe phase is simply related to the fringe displacement, hence to the total refractive index at the given radial position. The magnitude of the transform depends on the overall fringe image quality as well as the "goodness" of the transform fit, thus providing a convenient method of weighting the data. The computer system also provides data plotting and editing facilities. Radial position, fringe phase and transform magnitude are all output in a form compatible with existing ultracentrifugal data analysis programs. Using this system, fringe displacements routinely can be measured to better than 1 μm of fringe displacement, making the accuracy comparable to vidicon techniques and superior to manual approaches. The long term stability, the absence of demanding and expensive equipment and the increased reliability make this system superior to systems using vidicons.

T-AM-Po22 A LASER DOPPLER FLOW METER. R. W. Wunderlich,* R. L. Folger,* and B. R. Ware, Department of Chemistry, Harvard University, Cambridge, MA 02138 and D. B. Giddon,* College of Dentistry, New York University, New York, NY 10016

Blood flow rate has been studied non-invasively by measuring the Doppler broadening of laser light which has been scattered by the moving erythrocytes. Although a quantitative analysis of the Doppler shift spectrum is not tractable because of multiple scattering and geometric uncertainties, a frequency-weighted average of the spectrum does correlate with blood flow rate. We have constructed a portable apparatus for convenient laser Doppler analysis of blood flow. This device electronically computes the normalized second moment of the Doppler shift spectrum. Glass fiber optics are used to direct a low-power Helium-Neon laser onto the region of interest and to collect the light scattered by the specimen. The output of the photodiode detector consists of a DC component (< 0.5 Hz) proportional to the intensity of the incident light, a slowly varying component (0.5 Hz - 15 Hz) caused by the pulsatile cardiac cycle, and the higher-frequency Doppler signal (100 Hz - 8 kHz). By isolating the DC and low-frequency components, and amplifying the low-frequency component, the apparatus serves as an optical plethysmograph. The high-frequency component of the signal is passed through a bandpass filter, amplified, differentiated with respect to time, passed through a root-mean-square detector, and divided by the average signal power in the range of the bandpass filter. This sequence is equivalent to computing the normalized second moment of the Doppler shift spectrum. Design details and sample data will be presented.

T-AM-Po23 LIGHT SCATTERING FROM CELLS IN STREAM-IN-AIR FLOW CYTOMETERS. G. Salzman, M. Wilder* and J. Jett* Biophysics & Instrumentation Group, Los Alamos Scientific Laboratory, Los Alamos, NM 87545

Both forward angle and 90° light scattering measurements have been used with stream-in-air flow cytometers for cell sizing with little theoretical base for the measurements. Electromagnetic scattering theory calculations are compared with measurements on two commercial stream-in-air flow cytometers. Forward and 90° detector responses are shown to be nonlinear, (2) sensitive to particle position within the stream and (3) sensitive to particle refractive index. Effects of cell fixation and changes in nuclear-to-cytoplasmic diameter ratio are presented. This work is being done under the auspices of the United States Department of Energy.

T-AM-Po24 SMOOTHING OF DOPPLER SPECTRA LINE SHAPES BY VARIABLE PERIOD OSCILLATING ELECTRIC FIELDS. E.E. Uzgiris, General Electric Corporate Research and Development, P.O. Box 8, Schenectady, New York 12301; D.H. Cluxton*, Russell Sage College, Troy, New York 12180

The study of cell and particle electrophoresis by laser Doppler techniques requires the application of an electric field to a conducting solution. Steady d.c. electric fields are usually not possible because of electrode polarization and electrode surface reactions. Hence, it has been common practice to apply temporally varying electric fields, either pulses of alternating polarity or square-wave fields of constant amplitude. Oscillating particle motion leads to harmonic structure (multiples of the square-wave electric field frequency) in the scattered light spectra. This harmonic structure may be considerably smoothed by a suitable variation of the period of the applied square-wave field. We present experimental and theoretical conditions for achieving line smoothing. In practice, the application of a pseudo-random period oscillating electric field yields line shapes that approach the line shapes to be expected from the application of a continuous d.c. electric field.

T-AM-Po25 BIOMAGNETIC RESEARCH AT THE LAWRENCE BERKELEY LABORATORY. T. Tenforde, C. Gaffey, T. Yang, M. Raybourn, R. Roots,* R. Farinato,* S. Kronenberg,* C. Dols,* G. Meyer,* and M. Zaretsky,* Biology and Medicine Division, Lawrence Berkeley Laboratory, University of California, Berkeley, California 94720.

Facilities have been developed at LBL for large-scale experimentation on magnetic field effects in whole-animal, cellular, and molecular systems. Physiological studies on small mammals and organ systems exposed to fields of $\lesssim 20$ kilogauss strength include measurements of deep-body temperature via telemetry, cardiac activity, nerve impulse conduction, behavioral tests, and visual function. Results to date have shown a strong effect of DC magnetic fields on the electrocardiogram, with a six-fold increase in the T-wave amplitude occurring in a 20 kilogauss field. No magnetic effects have yet been observed for the other physiological parameters under investigation. Studies are also being carried out to assess magnetic field effects on the growth and development of cultured mammalian cells, Tribolium confusum beetles, and Zea mays corn seeds. The possibility that conformational changes occur in supercoiled double-helical DNA as a result of alignment in strong magnetic fields is being studied by gel electrophoresis and electrooptical birefringence techniques. Preliminary results in each of these research areas will be reported.

Research support received from the U.S. Department of Energy under contract W-7405-eng-48 with the Lawrence Berkeley Laboratory.

T-AM-Po26 EXTRACTION OF MEMBRANE PROTEINS WITH SHORT-CHAIN ALIPHATIC ACIDS. S. Szuchet and D.B. Wilde*, The University of Chicago, Chicago, Il., 60637

Short-chain carboxylic acids have proved to be good solvents for studying the quaternary structure of proteins (Szuchet & Yphantis, Biochemistry 12,5115,1973; Arch. Biochem. Biophys. 173,495,1976; Szuchet, ibid. 177,436,1976). Here we assess the potential of these acids--acetic, propionic, butyric and valeric--for extracting membrane proteins. Erythrocyte membranes have been chosen as a model system for these studies because their protein composition has been investigated extensively. We have adopted the extraction procedure and nomenclature of Yu et al., (J. Supramol. Struct. 1,233,1973). Components solubilized into the supernatant or retained in the pellet were identified by SDS-polyacrylamide gel electrophoresis. Our preliminary results indicate: a) at constant concentration of acid (0.1N) and in the absence of added neutral salts the selectivity of extraction increases with increasing length of the aliphatic chain. For example, acetic acid is the least selective solvent of the series tested, b) increasing the ionic strength of the acid solution by adding NaCl has the same effect as increasing the length of acid's carbon chain; c) at high ionic strength, e.g., 0.2M, stepping up the concentration of acid results in reduced selectivity. The observations suggest that these solvents can be usefull tools for the purification and characterization of membrane proteins.

Supported by a grant from the Muscular Dystrophy Association.

T-AM-Po27 EFFECTS OF CHOLESTEROL-PHOSPHOLIPID LIPOSOMES ON THE TRANSFORMATION OF MOUSE SPLENIC LYMPHOCYTES BY LECTINS. S.H.C. Ip, J. Abrahm*, R.A. Cooper*, Hematology-Oncology Section, University of Pennsylvania, Philadelphia, PA 19104.

Mouse splenic lymphocytes were preincubated for 18 hours with sonicated dispersions of cholesterol and lecithin in a normal culture medium containing RPMI 1640 and 5% rat serum. The presence of cholesterol was found to enhance lectin-stimulated transformation by 2-3 fold. Shortening the preincubation time decreased the stimulatory effect. Little or no effect was observed when liposomes were added 24 or more hours after addition of lectin. The response was linearly related to the cholesterol/phospholipid (C/P) molar ratio of added liposomes with maximal stimulation at C/P > 1.0, no effect at a C/P of 0.2-0.4 and 30% inhibition at a C/P of 0.0. In contrast, a 25-fold variation in cholesterol concentration of the incubation medium at a constant C/P did not affect the degree of stimulation of the lymphocyte transformation. In addition to the enhanced transformation, DNA synthesis was greater in the cells preincubated with cholesterol. The maximum level of ^{3}H-thymidine incorporation occurred 48 hours after the addition of concanavalin A in the samples preincubated with cholesterol-enriched liposomes. The maximum in the control samples occurred at 72 hours. Similar results were observed with two different phospholipid liposomes (dipalmitoyl and egg lecithin), with three lectins (conA, PHA and PWM) and with either ^{3}H-Leucine or ^{3}H-Thymidine incorporation as the measure of transformation. 7-Ketocholesterol (2 µg/ml) suppressed the transformation in the control samples but had no effect on samples preincubated with cholesterol-enriched liposomes. These studies demonstrate that the lymphocyte transformation can be strongly influenced by cholesterol liposomes. The added cholesterol may have its effect by serving as a substrate for membrane biosynthesis or by altering the cellular membrane fluidity as demonstrated in our earlier studies. Supp. by Grant AM15441.

T-AM-Po28 DIFFERENTIAL LABELING OF AMINO-LIPIDS ON LIPOSOMES WITH FLUORESCAMINE. H. C. Lee* and J. G. Forte, Dept. of Physiology-Anatomy, Univ. of Calif., Berkeley, Ca. 94720.

Chemical probes for amine groups, fluorescamine (FA) and trinitrobenzenesulfonate (TNBS), were used to differentially label amino phospholipids in liposomes. At low concentrations, FA reacts primarily with amino lipids on the external half of the bilayer. Further increase in [FA] resulted in linear increase of labeling indicating penetration and reaction with the internal half of the bilayer. Because of the pH requirements of the FA reaction, internal labeling can be eliminated with a H^{+} gradient: inside acidic/outside alkaline. Differential labeling was achieved with another reagent, TNBS, which is normally not permeable but which can be transported by valinomycin-K^{+} complex and react with internal amines. Thus, either half of the bilayer can be labeled with the same or different reagents. When liposomes were double-labeled, the fluorescence of FA was quenched by the TNBS label. This quenching was reversed by solubilizing the liposomes with acidic ethanol. No quenching occurred when FA labeled liposomes were mixed with TNBS reacted liposomes (or trinitrophenylated methylamine) suggesting close proximity of two labels is required for quenching. Conditions which promoted vesicular fusion promptly produced quenching. These differential labeling procedures can be usefully applied to (1) quantitate amino lipids on internal and external vesicular surfaces, (2) monitor vesicular fusion, and (3) assess liposomal structure. (Supported by USPHS grant AM 10141.)

T-AM-Po29 THE INFLUENCE OF SALINE GROWTH CONDITIONS ON BARLEY ROOT PLASMA MEMBRANE-BOUND ADENOSINE TRIPHOSPHATASE ACTIVITY: THE EFFECT OF LIPID "FLUIDITY" ON ENZYME ACTIVITY. C. R. Caldwell*, L. L. Yang, and A. Haug*, MSU-DOE Plant Research Laboratory, Michigan State University, E. Lansing, MI 48824.

There is considerable evidence to suggest that the plant plasma membrane plays a significant role in determining a plant's response to environmental stresses. In particular, it has been demonstrated that alterations in the ionic environment, as well as, growth temperature, can result in changes in the plasma membrane constituents and membrane-bound enzyme activities of certain plants. Therefore, it seems possible that a given plant's ability to alter its membrane components in response to environmental stresses may determine whether the plant survives the stress. In order to investigate the possible involvement of the root plasma membrane in the salt tolerance of barley, two varieties of Hordeum vulgare, having different relative salt tolerances, were grown in nutrient solutions containing up to 250 mM NaCl. A plasma membrane-enriched fraction was prepared from the barley roots using the standard procedures of differential centrifugation and sucrose gradient fractionation, with the addition of an aqueous two-phase partitioning of the gradient membrane fraction to improve purity. The temperatures at which lipid phase separations occur were determined by electron spin resonance spectroscopy, using the spin probe 5-nitroxide stearate. The temperature-dependance of the kinetic constants of the membrane-bound, ion-stimulated adenosine triphosphatase (ATPase) was also determined. The correlation between the lipid phase separations and alterations in ATPase activation energy will be discussed relative to the growth conditions of the barley. The physiological role of the lipid-ATPase interactions in barley salt tolerance will also be discussed.
Supported by US-DOE Contract No. EY-76-C-02-1338.

T-AM-Po30 VARIATION OF LIFETIME AND POLARIZATION ACROSS THE EMISSION BAND OF FLUORESCENT MEMBRANE PROBES. E. D. Matayoshi, A. M. Kleinfeld, and A. K. Solomon, Biophysical Laboratory, Harvard Medical School, Boston, MA 02115.

We have measured the lifetimes and steady state polarizations of fluorescent membrane probes which are thought to sample the hydrophobic region of the bilayer. Lifetimes were determined at 20 nm intervals by phase-modulation fluorometry at 10 and 30 MHZ, using an emission monochromator (8 nm bandpass); steady state polarizations were performed in the same instrument. The polarization (p) of both 12-(9-Anthroyl)stearic acid (12-AS) and N-phenyl-1-naphthylamine (NPN), bound to sonicated egg phosphatidylcholine vesicles, decreases monotonically from maximal values at the blue end of the emission. Between 0° and 40°C, p decreases by factors of 1.7 - 2.0 for 12-AS (400-530 nm), and 1.2 - 1.5 for NPN (370-500 nm). In parallel, the mean decay times (τ) increase monotonically from minimal values at the blue end. The same trends are also observed (although less dramatically) in triolein, but the wavelength dependence of τ is abolished in methanol or decane. In contrast, the probes 1,6-diphenyl-1,3,5-hexatriene and trans-parinaric acid exhibit constant p and τ across their emission band in either vesicles or triolein. Time-dependent spectral shifts, which have previously been observed in viscous polar solvents and at the membrane-water interface of lipid vesicles, were attributed to solvent dielectric relaxation (DeToma et. al., J. Am. Chem. Soc. 98:5001, 1976). This interpretation is clearly untenable in the present case because we have observed these effects when 12-AS and NPN are solvated in media of low dielectric constant. Possible explanations involving intramolecular relaxation of the fluorophore and solvent polarizability will be discussed.
(Supported in part by USPHS Grant R01 HL 14820).

T-AM-Po31 PHOTOBLEACHING RECOVERY STUDIES OF MEMBRANE EVENTS ACCOMPANYING LECTIN STIMULATION OF RABBIT LYMPHOCYTES. J.S. Peacock,* M.D. Leuther,* H. Krakauer,* and B.G. Barisas. St. Louis University School of Medicine, St. Louis, MO 63104.

This paper is a preliminary report on the use of fluorescence photobleaching recovery (FPR) techniques to examine the modulation of lymphocyte membrane component lateral mobilities by the events of lectin stimulation. Both the mitogens concanavalin A (con A) and succinyl con A (S con A) stimulate the proliferation of rabbit T lymphocytes. With tetravalent con A commitment to proliferation occurs after as brief an exposure to mitogen as 10 min. and is only partially reversible by treating the cells with α-methylmannoside. Divalent S con A on the other hand must be present on the cell surface until the onset of DNA synthesis which can occur as late as 72 hr. Removal of this lectin at any time prior to onset of DNA synthesis reverses stimulation. We examine by FPR the mobilities of various membrane molecules including con A receptors, insulin receptors, and the lipid probe 3,3'-dioctadecylindocarbocyanine diiodide throughout the time course of lectin stimulation and compare T cells with non-responding B cells in the presence and absence of mitogen. This work was supported by grants from Research Corporation, NSF, and NIH.

T-AM-Po32 FLUORESCENCE POLARIZATION STUDIES OF MEMBRANES FROM CULTURED SKIN FIBROBLASTS DERIVED FROM DUCHENNE DYSTROPHIC PATIENTS. J. Michael Shaw, Erica A. Schlag* and I.R. Konigsberg*, Depts. of Biochemistry and Biology, University of Virginia, Charlottesville, VA 22901, and Dept. of Biochemistry, Medical College of Virginia (MCV), Richmond, VA 23298.

Human skin fibroblasts from biopsies obtained from duchenne muscular dystrophy patients and normal individuals have been cultured to confluency. Plasma membranes were prepared by fractionation in a sucrose-step gradient, a two phase polymer system and a cell lysis procedure followed by flotation of the membranes over a sucrose pad. Membrane purity by these three different procedures have been compared. Fluorescent polarization experiments were carried out by incubating the plasma membrane enriched preparations (200-800 μg protein) with the fluorescent dye, diphenylhexatriene (DPH) normally in the range of one DPH molecule per 200-400 molecules of membrane lipid at 37°C. Steady-state fluorescent polarization measurements were performed while cooling the cuvette (≈15°C/hr) down to ≈7°C in a Perkin Elmer MPF-3 instrument. Results derived from these studies consistently revealed, at all temperatures, that fibroblast membranes derived from duchenne dystrophic patients have from 8 to 17% lower anisotropy values for the fluorescence depolarization of DPH when compared to control membrane preparations. The decreased anisotropy values suggest a more 'fluid-like' environment in the dystrophic membranes than the respective control. This trend was found to occur in all plasma membrane preparations. These experiments are presently being extended by examination of a larger number of duchenne and normal membrane samples and lipid extracts of the membranes with the use of an SLM-480 spectrofluorometer in which both lifetimes and depolarization measurements are being performed. Support of the majority of this work by a fellowship (GM05190) to JMS while a postdoctoral fellow in the laboratory of Dr. T. E. Thompson and a MDA center grant to the University of Virginia. JMS is presently at MCV.

T-AM-Po33 MEMBRANE FLUIDITY AS CHARACTERIZED BY PYRENE FLUORESCENCE KINETICS. B.M. Liu, K.-H. Chen*, M. Habercom*, and H.C. Cheung, Biophysics Section, Department of Biomathematics University of Alabama in Birmingham, Birmingham, AL 35294.

The fluorescence decay kinetics of pyrene has been used to monitor thermal transition of membrane vesicles using the single-photon detection technique. Both the monomer and excimer decays of this probe incorporated into sonicated liposomes (DPPC) and sarcoplasmic reticulum vesicles cannot be satisfactorily accounted for by the three-dimensional diffusion-dependent fluorescence quenching model (Vanderkooi, J.M. and Callis, J.B., Biochemistry 13: 4000, 1974). In addition, the corresponding two-dimensional diffusion-dependent quenching model (Owen, C.S., J. Chem. Phys. 62: 3204, 1975) does not appear to be compatible with our monomer data. A scheme based on excited state interaction is suggested for the observed decay patterns. The temperature dependence of the decay time of the excimer in both types of vesicles shows characteristic transitions at temperatures corresponding to the thermal transition temperatures reported in the literature. Preliminary studies indicate that the melting behavior of the bilayer can be described by the one-dimensional Ising model of nearest neighbor interactions.
(Supported in part by the Muscular Dystrophy Association.)

T-AM-Po34 MEMBRANE VISCOSITY: A SMALL LIPID-PHASE SPIN PROBE REPORTS THE SAME VISCOSITY AS TWO INTEGRAL MEMBRANE PROTEINS. C.L. Wey‡ P.L. Ahl‡ R.A. Cone, Dept. of Biophysics, and B.J. Gaffney, Dept. of Chemistry, Johns Hopkins University, Baltimore, MD 21218

We have used two methods to measure the "effective" viscosity of the membrane in DML (dimyristoylphosphatidylcholine) vesicles: (1) Bacteriorhodopsin was incorporated in the vesicles (by detergent solubilization followed by dialysis in the presence of DML), and its rate of rotational diffusion was determined from the rate of decay of photodichroism induced by a polarized flash. The effective viscosity of the membrane site of this integral membrane protein was calculated using the Stokes-Einstein's relation for a rotating cylinder (assuming r=18Å, h=30Å). (2) A spin probe small enough to tumble in the lipid phase (2,2,4,4-tetramethyl-1,2,3,4-tetrahydro-γ-carboline-3-oxyl:~5x8x11Å), was dissolved in the same vesicle preparation, and its EPR spectrum was compared to that of the same spin probe dissolved in a reference oil of known viscosity (American White Oil USP 35). We find that at 26°C, bacteriorhodopsin reported an effective viscosity of 2.1±1.1 poise (rotational relaxation time, τ=6μs). The spin probe reported an effective viscosity of 3.0±1.5 poise. This close correspondence was maintained as the temperature was varied over the range 23-36°C. We have applied essentially the same two methods to intact disk membranes of isolated frog rod outer segments, observing the rotational diffusion of rhodopsin (assuming r=23Å,h=30Å). We find that at 20°C, rhodopsin reported an effective viscosity of 4.0±2.0 poise(τ=20μs), while the small lipid phase spin probe reported an effective viscosity of 3.6±1.5 poise. Stubbs et al.(Biochem. 15,2766) using a small lipid phase fluorescent probe(DPH), observed an effective viscosity of 3.8±.5 p at 20°C for bovine disk membranes. Thus small lipid-phase probes report viscosities in good agreement with the viscosities experienced by rhodopsin and bacteriorhodopsin.
(Supported by NIH grant EY00520 and CA15997.)

T-AM-Po35 DEUTERIUM T_1 RELAXATION AND THE MICROVISCOSITY PROFILE OF LIPID BILAYERS. Michael F. Brown and Joachim Seelig*, Biocenter, University of Basel, CH-4056 Basel, Switzerland.

Spin-lattice (T_1) relaxation time measurements have been made using a number of selectively deuterated DPPC bilayers and have been interpreted in terms of the fatty acyl chain ordering and dynamics in these systems. Plots of the motional correlation times derived from the T_1 data as a function of the deuterated chain segment position generally resemble the order profiles determined previously. From a dynamic point of view, the primary result of the increased orientational order in the bilayer is not a large decrease in the rate of segmental motion compared to paraffinic liquids, but rather to favor coupled rotations of the fatty acyl chain segments which allow for parallel chain packing in the bilayer. Thus the rate of segmental motion is rapid, yet the motional correlations lead to the long range ordering characteristic of lipid membranes. By comparison of the deuterium T_1 data to that for n-alkanes it is possible to further interpret the results in terms of the bilayer microviscosity profile. In the "plateau" region of constant motion and order (chain segments C3 to C9) the microviscosity of the DPPC bilayer at 51°C is estimated to be about 14 c.p., dropping to about 2-4 c.p. in the central region of the bilayer. These results are compatible with previous estimates using spin label EPR, but not with studies employing fluorescent probes such as diphenylhexatriene (DPH) or pyrene, which lead to significantly higher microviscosity estimates. (Supported by the Swiss National Science Foundation (J.S.) and a postdoctoral fellowship from the US NIH (M.F.B.)

T-AM-Po36 RHODOPSIN-PHOSPHOLIPID INTERACTIONS: DEPENDENCE OF THE META I TO META II TRANSITION KINETICS ON THE LEVEL OF ASSOCIATED DISK PHOSPHOLIPIDS.
B.J. Litman, O. Kalinsky*, and M. Ottolenghi*, Biochemistry Department, University of Virginia, Charlottesville, Va. 22908; and Physical Chemistry Department, Hebrew University, Jerusalem, Israel.

Solubilization of ROS disk membranes in the non-ionic detergent octyl glucoside was employed to prepare rhodopsin samples with varying levels of associated phospholipid. Flash photolysis studies have been carried out on these samples to determine the effect of associated disk phospholipids on the meta I to meta II transition kinetics. As the level of associated phospholipid fell from 35 to 5 phospholipids per rhodopsin, the rate constant for the formation of meta II increased from 6.9×10^3 to 23.6×10^3 sec^{-1}, demonstrating an increased rate of meta II formation with decreasing levels of associated phospholipid. The activation free energy for this process was found to have a linear dependence on the level of rhodopsin-associated phospholipid over the range of phospholipid to rhodopsin ratio studied, with a slope of 24 cal per mole of rhodopsin-associated phospholipid. A variety of evidence suggests that rhodopsin undergoes a reversible conformation change during the meta I to meta II transition. The results reported here indicate that the activation free energy for this process increases in an incremental fashion for each additional mole of associated phospholipid. No evidence was found for an enhanced effect at the level of associated phospholipid which might correspond to a phospholipid boundary layerof rhodopsin. (Supported by grants from the National Science Foundation and the National Eye Institute).

T-AM-Po37 ROTATIONAL MOBILITY OF SOLUBLE AND RECONSTITUTED CYTOCHROME OXIDASE.
A. T. Quintanilha, M. S. Swanson* and D. D. Thomas, Membrane Bioenergetics Group, Lawrence Berkeley Laboratory, University of California, Berkeley, California 94720 and Department of Structural Biology, Stanford University School of Medicine, Stanford, California 94305.

The rotational mobility of bovine heart mitochondrial cytochrome oxidase in solution and incorporated into liposomes was studied by saturation transfer electron paramagnetic resonance. Two enzyme preparations were used containing different amounts of endogenous lipids (∿6% and ∿40% by weight). Liposomes, made from purified lipids, asolectin and mitochondrial lipids were prepared by sonication and maleimide spin labeled cytochrome oxidase was added to the preformed vesicles. The oxidase activity was not affected by spin labeling. At the highest lipid/protein molar ratios (∿300) electron microscopy showed vesicles mainly in the size range of 50-100 nm. Whereas the soluble oxidase showed rotational correlation times in the μsec range, the membranous oxidase consistently showed rotational correlation times in the msec range. The membranous oxidase activity was always greater than the soluble one. Our results indicate that rotational immobilization of the membranous cytochrome oxidase occurs for a large range of lipid/protein molar ratios: this suggests that cytochrome oxidase aggregates may occur in the lipid membrane.
(Research supported by the Department of Energy.)

T-AM-Po38 ADSORPTION OF Cd^{++}, Mn^{++}, Ca^{++}, Mg^{++}, Co^{++} and Ba^{++} TO DIFFERENT PHOSPHATIDYLCHOLINE BILAYERS. L.J. Lis, and R.P. Rand, Brock University, St. Catharines, Ontario, and V.A. Parsegian, N.I.H., Bethesda, MD 20014.

We have used osmotic stress (Biophys. J. (1977) 18:209) to measure the net repulsive force between phosphatidylcholine bilayers in chloride solutions of divalent metals. For bilayer separations between 30Å and 100Å, that repulsion is apparently the electrostatic interaction between bilayer surfaces charged by the adsorption of divalent cations. Ions of greater surface affinity produce a greater force. Using a non-linear Poisson-Boltzmann equation, we have learned to convert the measured force into an estimate of the adsorbed charge density and electrostatic potential at the locus of adsorption. As bilayers are brought together, the bound charge desorbs. The surface potential is not constant nor, surprisingly, is there a constant binding coefficient if one assumes a mass action law for ions interacting with binding sites. NaCl added to the medium decreases the repulsion, but increases the amount of charge apparently bound. The Ca^{++} adsorption per unit area to different phosphatidylcholines increases as: egg PC ≈ dioleyl < dilauroyl < dimyristoyl ≈ dipalmitoyl < distearoyl. (This sequence is in the same order as the molecular density of the phospholipids in the bilayer.) For dipalmitoyl PC at T=22°C, the avidity of ion binding goes as $Cd^{++} \approx Mn^{++} \approx Ca^{++} > Mg^{++} \approx Co^{++} > Ba^{++}$.

T-AM-Po39 MEASUREMENT OF ELECTROSTATIC FORCES ACROSS A SALT SOLUTION BETWEEN CHARGED PHOSPHOLIPID BILAYERS. M. Loosley-Millman, Physics Department, University of Guelph; R.P. Rand, Biological Sciences, Brock University.

The technique of X-ray diffraction coupled with an osmotic stress technique (LeNeveu et al. Biophys.J.(1977) 18:601) is used to measure the repulsive force between charged phospholipid bilayers (5% egg phosphatidyl glycerol (PG) in dioleoyl lecithin (DOL)), in various salt solutions, as a function of bilayer separation d_w. For d_w < 25 Å hydration repulsive forces dominate electrostatic repulsive forces as previously observed (Cowley et al. Biochemistry (1978) 17:3163). For d_w > 25 Å, and for a range of ionic strengths which shows indefinite swelling and complete shielding at the extremes, the results show good qualitative agreement with theory based on electric double-layer considerations, developed by Parsegian and Gingell (Biophys.J. (1972) 12:1192). However, quantitatively the measured electrostatic repulsion is always less than that predicted theoretically, suggesting an unexpectedly low dissociation of the PG lipid head groups in this multilamellar system.

T-AM-Po40 INFLUENCE OF TEMPERATURE AND HYDROCARBON CHAIN FLUIDITY ON Mn^{2+} BINDING TO PHOSPHOLIPID VESICLES. J. S. Puskin; Dept. Radiation Biology and Biophysics, University of Rochester, Rochester, NY 14642.

Mn^{2+} binding to phosphatidylserine and phosphatidylglycerol vesicles was measured as a function of temperature by EPR. Corresponding variations in lipid fluidity with temperature were monitored with nitroxide spin probes.

Calculations based on the Gouy-Chapman theory predict a 5-to 10-fold enhancement of Mn binding affinity when a bilayer composed of acidic phospholipids is cooled through its phase transition. However, such an enhancement was not observed. Mn binding to dipalmitoyl phosphatidylglycerol, under some conditions, exhibited large hysteresis effects as samples were cycled back and forth through the phase transition. Light scattering measurements on parallel samples indicated extensive Mn dependent aggregation in these cases, suggesting the formation of strong divalent cation bridges between vesicles.

(Supported by NIH grant GM21664 and by a contract from DOE: Rept. #UR-3490-1500)

T-AM-Po41 EVIDENCE FOR A METASTABLE CONFORMATION OF N-STEAROYL SPHINGOMYELIN. T.N. Estep, W.I. Calhoun, Y. Barenholz*, R.L. Biltonen, G.G. Shipley, and T.E. Thompson, Department of Biochemistry, University of Virginia School of Medicine, Charlottesville, Va. 22908, and Biophysics Division, Boston University School of Medicine, Boston, Mass. 02118.

Aqueous dispersions of N-stearoylsphingomyelin (SSPH) were examined by scanning calorimetry, fluorescence depolarization of diphenylhexatriene (DPH), and x-ray diffraction. Highly purified samples exhibited an endotherm at 57C (ΔH = 19 kcal/mol). SSPH containing 0.1 mol % DPH or 1.3 mol % cholesterol showed an endotherm at 43-45C (ΔH = 7 kcal/mol) when held at 20-25C for 2 hours after cooling from 60C. When impute SSPH was held at 20-25C overnight the 57C peak was seen. In some cases both endotherms were observed in the same sample, often with an intervening exotherm. X-ray diffraction at 20C of a SSPH sample showing only the 43-45C peak showed a diffraction pattern typical of gel phase phospholipids, while a sample giving the 57C endotherm was significantly more ordered. The data imply that upon cooling from high temperature SSPH assumes a metastable conformation which slowly converts into a highly ordered form.

T-AM-Po42 LIPID ANALOG LATERAL DIFFUSION IN PURE AND CHOLESTEROL-CONTAINING PHOSPHOLIPID MULTIBILAYERS. Zenon Derzko[a](*) and Ken Jacobson[b], [a]Biophysics Department,State University of New York at Buffalo,Buffalo NY 14263, [b]Dept of Experimental Pathology,Roswell Park Memorial Institute, Buffalo NY 14263.

The method of fluorescence recovery after photobleaching (FRAP) has been used to measure the lateral diffusion coefficient (D) of the following fluorescent lipid probes: 3,3'-dioctadecyloxocarbocyanine (di-O-C_{18}(3)), 3,3'-dihexadecylindotricarbocyanine (di-I-C_{16}(3)), N-4-nitrobenz-2-oxa-1,3-diazole phosphatidylethanolamine (NBD-PE) and N-4-nitrobenzo-2-oxa-1,3-diazolaurate (NBD-C_{12}) in phosphatidylserine (PS), dimyristoylphosphatidylcholine (DMPC), and egg phosphatidylcholine (EPC) multibilayers (MBLS). The values of D for di-I, di-O and NBD-PE all lie within the range: (7.0 ± 2.0) X $10^{-8}$$cm^2$/sec around 35°C. In contrast, the NBD-C_{12} fatty acid probe shows a measurably faster D with a lower limit of: 1.3 X $10^{-7}$$cm^2$/sec. In DMPC MBLS at 6°C (below T_m), NBD-C_{12} also displays a faster D of: 1.1 X $10^{-9}$$cm^2$/sec,whereas di-I, di-O and NBD-PE typically yield values of: 1.0 X $10^{-10}$$cm^2$/sec or less. Varying the length of the hydrocarbon chains in the probe di-I from six to eighteen, shows a slight decrease in D for temperatures around 35°C, but the differences are within experimental error. Examination of the temperature dependence of D for di-I and NBD-PE in DMPC MBLS as a function of the mole percent cholesterol, show that the gel-to-liquid crystalline phase transition occurring @ 23.9°C is abolished between 23.1 and 28.6 mole percent cholesterol. More detailed analysis of the FRAP data indicates the presence of two distinct diffusions in the cholesterol-containing MBLS, as opposed to single diffusions in pure MBLS. This work was supported by NIH Grant CA-16743. K.J. is an Established Investigator of the American Heart Association.

T-AM-Po43 MECHANISM OF SPONTANEOUS PHOSPHOLIPID EXCHANGE. M.A. Roseman,* and T.E. Thompson (Intr. by C.F. Schmidt), University of Virginia, Charlottesville, VA., 22908.

Although several laboratories have reported that phospholipids spontaneously exchange between phospholipid vesicles, it is not yet clear whether exchange proceeds via, (1) aqueous transfer of lipid monomers, or, (2) collision of vesicles. To determine the mechanism, we have studied the exchange kinetics of 1-palmitoyl-2-pyrene decanoyl phosphatidylcholine between sonicated vesicles of dimyristoylphosphatidylcholine. The half-time for exchange, as measured by the decrease in the eximer:monomer flourescence ratio, is about 26 hr at 36°. The important observation is that the half-time does not depend on the concentration of acceptor vesicles. This result is consistent only with mechanism (1). Light scattering studies strongly indicate that dilution of the label does not result from the fusion of entire vesicles. (This study was supported by PHS Grant GM 14628.)

T-AM-Po44 INVESTIGATION OF CHOLESTEROL-PHOSPHATIDYLCHOLINE DOMAINS IN LIPID BILAYERS. B. R. Lentz, D. A. Barrow*, and M. Hoechli* (Intr. by J. White), University of North Carolina, Chapel Hill, N.C. 27514.

Aqueous dispersions of mixtures of cholesterol with 1,2-dipalmitoyl phosphatidylcholine have been studied by fluorescence depolarization of 1,6-diphenyl-1,3,5-hexatriene as well as by freeze-fracture electron microscopy. The results have been used to construct a partial temperature-composition phase diagram for this system, with the freeze-fracture electron micrographs being used to check the assignments of one- and two-phase gel-like regions. A compilation of results from the literature has been used to corroborate this phase diagram. The proposed phase diagram suggests that most of the stoichiometric complexes proposed for phosphatidylcholine-cholesterol mixtures correspond to phase boundaries in the gel phase of the mixture studied here. Also, no indication of a two-phase region was found within the liquid-crystalline phase. In addition, similar studies have been performed on co-dispersions of egg phosphatidylcholine and cholesterol. Although a phase diagram for this complex system cannot be clearly defined, a crude temperature-composition diagram has been suggested by the data. Comparison of this diagram with that for 1,2-dipalmitoyl phosphatidyl-choline-cholesterol suggests that the interaction of cholesterol with saturated phosphatidyl-cholines should be distinguished from the interaction of cholesterol with unsaturated, natural phosphatidylcholines.

T-AM-Po45 QUANTITATIVE DETERMINATION OF GAUCHE CONFORMATION IN PHOSPHOLIPID BILAYERS - THEORY AND EXPERIMENT. R. Priest,* J. Sheridan,* (Intr. by A. DeRocco), Naval Research Laboratory, Washington, D. C. 20375.

The most convenient quantitative measure of organization in the interior of a phospho-lipid bilayer is the fraction of bonds in the alkyl chains which are gauche. We have developed a theoretical model for the lipid bilayer which gives quantitative predictions for this measure of order in both single component and binary mixture systems. The theory is in very good agreement with the traditional benchmark data such as the dependence of main transition temperature and latent heat on chain length in the phosphatidyl-choline series. The binary mixture phase diagrams predicted by the theory are also in good agreement with experiment. We have reinvestigated the problem of obtaining quantitative information from the analysis of Raman line intensities. Our approach has been to measure the temperature dependence of the ratio of the 1130 cm^{-1} and 720 cm^{-1} bands of phosphatidylcholines dissolved in chloroform and other solvents. These solvents provide an isotropic environment for the alkyl chains. The conformational structures can therefore be easily calculated by the methods discussed by Flory. This allows a calibration of the Raman intensity ratio as a function of conformational structure. The extrapolation of the calibration curve permits a quantitative measure of the fraction of gauche bonds in bilayer systems. A comparison of the theory and of data analyzed as described will be presented.

T-AM-Po46 ^{13}C-NMR OF PHOSPHOLIPID/GLYCOLIPID VESICLES. W. Curatolo, B. Sears, D. Small*, Boston Univ. Med. School, and L.J. Neuringer*, F. Bitter Natl. Magnet Lab, M.I.T., Cambridge, Mass. (Intr. by B. Wallace).

Unsonicated dispersions of di-(12-^{13}C-methyl-stearoyl)-phosphatidylcholine (^{13}C-PC) exhibit one broad asymmetric ^{13}C-NMR resonance with linewidth $\Delta\upsilon_{\frac{1}{2}}$= 119 Hz (at 68MHz, 25°C). Incorporation of 10 mole% N-palmitoyl lactosylceramide (LC) into ^{13}C-PC dispersions results in a 2-fold increase in ^{13}C linewidth to 231 Hz. The ^{13}C-NMR spectrum of sonicated ^{13}C-PC consists of one sharp resonance with $\Delta\upsilon_{\frac{1}{2}}$= 7 Hz. Incorporation of 10 mole% LC again results in a 2-fold increase in linewidth to 14 Hz. Addition of Ricinus communis agglutinin (RCA), a carbohydrate-binding protein, to sonicated ^{13}C-PC/LC vesicles results in agglutination into multi-vesicular aggregates (Curatolo, et al. (1977) JACS 99, 6771). Vesicular structure is not disrupted by this lectin-induced agglutination since addition of lactose completely reverses the agglutination as determined both by turbidity measurements and by electron microscopy. Upon RCA-induced agglutination of sonicated ^{13}C-PC vesicles containing 10 mole% LC, the ^{13}C-NMR linewidth increases to 21 Hz. The large linewidth differences usually observed between unsonicated dispersions and sonicated vesicles of phosphatidyl-choline have been attributed by various workers to either: (1) motional averaging due to an increased rate of tumbling for the vesicles, or (2) increased disorder in the vesicles (accompanied by an increased lateral diffusion rate). Our observation that large aggregates of lectin-agglutinated ^{13}C-PC vesicles exhibit a relatively sharp resonance (21 Hz) compared to an unsonicated dispersion (231 Hz) provides strong empirical evidence that the increased tumbling rate of sonicated vesicles cannot be the major mechanism for the NMR line-narrowing observed upon sonication of phospholipids.

T-AM-Po47 COMPLEX PHASE MIXING IN DIPALMITOYL PHOSPHATIDYLCHOLINE-BOVINE BRAIN PHOSPHATIDYLSERINE SYSTEM. T.P. Stewart+, S.W. Hui+, A. Portes*, and D. Papahadjopoulos*, +Department of Biophysics, Roswell Park Memorial Institute, Buffalo, New York 14263, and *Cancer Research Institute, University of California at San Francisco, School of Medicine, San Francisco, CA 94143.

The phase behavior of dipalmitoylphosphatidylcholine (DPPC) and bovine brain phosphatidylserine (PS) mixtures is studied by differential scanning calorimetry, freeze fracture electron microscopy and x-ray and electron diffractions. The pure DPPC has two well defined solidus phases, $P_{\beta}'$and L_{α}', and a liquidus phase, L_{α}, while the pure PS has a broad transition from L_{β} to L_{α}. The mixtures exhibit DPPC characteristics in compositions of up to 30% PS. At compositions of >30% PS the P_{β}' phase no longer exists. An addition of 3% PS is found to be sufficient to destroy the sharp L_{β}'-P_{β}' transition of pure DPPC. The transition from P_{β}' to L_{β}' of these mixtures is broadened as depicted by all three techniques, but freeze fracture gives more definite information of the continuous transition. Transition regions where two or more phases coexist are found in all mixtures. Upon addition of excess calcium to the mixtures of >30% PS, pure PS is separated from the mixture and forms cocleates (cylindrical rolls) while the remaining PC-enriched lipids are in the vesicular form. Phase diagrams of the binary mixtures have been derived from freeze-fracture, diffraction and calorimetric data, both in the presence and absence of the calcium ion.

T-AM-Po48 MEASUREMENT OF LATERAL PRESSURE WITHIN AND REPULSIVE FORCES BETWEEN PHOSPHOLIPID BILAYERS. V.A. Parsegian, N.I.H., Bethesda, MD 20014, and L.J. Lis, M.J. McAlister*, N.L. Fuller*, and R.P. Rand, Brock University, St. Catharines, Ontario, Canada.

Three kinds of pressure -- osmotic, mechanical and vapor -- have been used to measure the work of removing water from phospholipid multilayers; we have observed the structural result of water removal by x-ray diffraction. The rate of change of phospholipid free energy can be divided into a lateral pressure for moving together the polar groups of molecules in the same bilayer and a repulsive pressure between two adjacent bilayers. We have examined six phosphatidyl cholines -- egg, dilauroyl, dimyristoyl, dipalmitoyl, distearoyl and dioleyl -- as well as egg phosphatidylethanolamine. All substances show strong "hydration" forces (Biophys. J. (1977) 18:209, Biochem. (1978) 17:3163) whose exponential variation shows a 2 to 2.6Å decay length (except when 50% cholesterol is mixed with the phospholipid to give much softer 3.3Å decay). "Hydration" repulsion increases steadily even to bilayer contact and reaches thousands of atmospheres pressure for bilayer separations of a few Angstroms. The lateral pressure is of similar magnitude for phospholipids with liquid or frozen hydrocarbon chains. It is not related in any simple way to lateral pressures seen in monolayers. An immediate consequence of our measurements is to question those theories of bilayer stability whose principal verification has come from predicting monolayer π-A curves.

T-AM-Po49 DEFECT STRUCTURES IN MONODOMAIN LIPID LIQUID CRYSTALS, S.A. Asher and P.S. Pershan, Division of Applied Sciences, Harvard University, Cambridge, MA 02138.

A careful examination has been made of the defect textures observed in the lyotropic liquid crystals formed from various phosphatidylcholines. Both polarizing and dark field microscopy are used to characterize the defects and detailed structural models are proposed. Some of these defects occur during the alignment of the lipid into the monodomain form. One of these defects, which appears as birefringent threads under the polarizing microscope, has been observed to be the site for the localization of some impurities expelled from well-oriented domains. Other defects result from small elastic or thermal stresses on the sample. Due to the large negative thermal expansion coefficient of the lipids normal to their layers careful temperature control is required to maintain well-aligned defect-free samples. The evolution of all of the defects as samples are annealed at elevated temperatures into the monodomain form will be discussed. In addition, a new mechanical alignment technique which effects sample alignment at temperatures slightly above the gel transition will be discussed. For example, 80 μm thick samples of dilaurylphosphatidylcholine containing 20% water by weight can be aligned at room temperature. This new alignment technique is significant since it avoids any thermal decomposition which may occur during the high temperature annealing process and it permits the incorporation of thermally labile adducts.

This work was supported by NSF Grant DMR 76-22452.

T-AM-Po50 STATISTICAL MECHANICS OF LIPID BILAYERS. J. Day,* C. R. Willis,* R. Bansil (Intr. by R. L. Hall), Boston University, Boston, Massachusetts 02215.

We present a self-consistent statistical mechanical theory of interacting lipid molecules to explain the gel to liquid-crystal phase transition in bilayer systems. The partition function is a strong functional of the single chain density of states $\omega(\epsilon,a)$. Due to the anisotropy of this problem the a dependence is crucial. The latent heats of these transitions indicate that many internal degrees of freedom of the single chain are activated [J. F. Nagle, J. Chem. Phys., 58, 252 (1972)]. Using this fact we investigated $\omega(n_g,a)$ (n_g = number of gauche bonds) for a single chain and found surprizing results. We were able to determine $\omega(n_g,a)$, $\omega(n_g,z)$, and $\omega(n_g,\theta_i)$ (a = area, z = length of configuration, θ_i = orientation of the ith carbon) by generating random sequences on the computer and computing the distributions of these parameters relative to the symmetry axis of the configuration. Configurations that intersected themselves and entered the polar region were rejected. By sampling only 2% of the possible configurations we were able to characterize the entire population (total number = 3^{14}) due to the statistical equivalence of the sub-populations of our sampling (moments agreed to within a few percent). Some of the interesting results that will be discussed are (i) the number of configurations accepted was very close to 100% except for large n_g (ii) the average configuration was twice as long as wide (iii) $\langle a \rangle$ decreased with increasing n_g (iv) $\langle a/z \rangle$ increased with n_g and (v) $\langle \theta_i \rangle$ increased with increasing n_g and i. We will also discuss the application of $\omega(\epsilon,a)$ to the interacting theory and the calculated thermal averages (i) X-ray spacings (ii) N.M.R. quadrupolar splitting and (iii) average n_g.

T-AM-Po51 RAMAN SPECTROSCOPIC STUDIES OF SPECIFICALLY DEUTERATED PHOSPHOLIPID DISPERSIONS. J. Day* and R. Bansil, Boston University, Boston, MA 02215 and E. Oldfield*, University of Illinois, Urbana, Illinois 60618.

The CH_2 stretching vibrations in the Raman spectrum are known to be sensitive to the gel to liquid-crystal phase transition in membranes. In contrast to the average "fluidity" (or disorder) obtained from the dependence of the CH_2 spectra on temperature the substitution of single CH_2 groups by CD_2 allows one to probe the local fluidity at a specific level in the hydrocarbon interior of the bilayer. Using this technique we have studied the variation of fluidity with temperature in fully hydrated dispersions of DMPC (dimyristoyl phosphatidyl choline) that have been selectively dueterated at various positions on the 2 chain. Our results show that $\Delta\nu_s$ and $\Delta\nu_a$, the widths of the CD_2 symmetric and antisymmetric stretching vibrations, respectively, increase with increasing temperature. Using $\Delta\nu_s$ as an empirical parameter of the amount of disorder we find that $\Delta\nu_s$ shows a sharp increase at the melting temperature for DMPC labelled at positions 4 and beyond on the 2-chain. However, $\Delta\nu_s$ for DMPC labelled at position 3 remains essentially unaltered. The implication of this result in terms of the proposed crystalline structure of the 2-chain will be discussed. We also observe that the magnitude of the width change at melting increases as the distance of the labelled CD_2 group from the polar group increases, suggesting that the bilayer is progressively more disordered in the hydrocarbon interior. Furthermore, the frequency of the CD_2 vibrations at position 3 is significantly greater than at positions 4 and beyond (approx. 23 cm^{-1} for ν_s and 30 cm^{-1} for ν_a) suggesting that this technique can also be used to detect the influence of the polar group on the first few CH_2 groups.

T-AM-Po52 THE BILAYER STRUCTURES OF DIMYRISTOYLLECITHIN AND OF ITS MOLECULAR COMPLEX WITH CHOLESTEROL. M. Suwalsky* (Intr. by J.L. Oncley), Biophysics Research Division, The University of Michigan, Ann Arbor, MI 48109.

The structures of dimyristoyllecithin (DML) have been studied by X-ray diffraction. Different types of patterns, corresponding to various conformations and/or packing arrangements were found. All have the bilayer structure. These patterns were water-dependent and underwent reversible transitions on merely changing the degree of hydration of the specimens. At low hydration the phosphorylcholine groups are bent with respect to the fully extended and parallel hydrocarbon chains. Electrostatic interactions between the oppositely charged groups stabilize the formation of planar sheets. Higher hydrations straightened the molecules and they became more disordered. A highly crystalline and oriented DML:CHOL 1:1 complex was prepared. When photographed, containing about three molecules of water per DML:CHOL, about 200 reflections were observed. Model studies, which are consistent with the X-ray patterns, indicate that the molecules pack linearly with the sequence...DML - DML - CHOL - CHOL - DML... The neighboring parallel chains are shifted along the long axis in such a way that CHOL molecules are in contact with the hydrocarbon chains of neighboring DML molecules and vice versa. This arrangement forms 2-dimensional planar sheets. The 3-dimensional structure is formed by stacks of these planar sheets, in which CHOL molecules pack atop DML and vice versa. This paper is based in large part on work performed at Harvard Medical School, and supported by NIH grant AM07300, as well as NIH grant HL18737 at The University of Michigan.

T-AM-Po53 MODELS FOR THE INFLUENCE OF HEAD GROUP INTERACTIONS ON LIPID BILAYER PHASE TRANSITIONS. H. L. Scott, Jr., Oklahoma State University, Stillwater, Oklahoma 74074.

The chain melting phase transition has been well documented in many lipid bilayer systems. While the basic nature of the order-disorder process is common to all the systems, the actual transition parameters such as temperature and enthalpy change vary with head group composition acyl chain length, and the nature of the suspending medium. In an attempt to understand some of the underlying mechanisms for some of these effects, I have considered several different modifications of a theoretical model published earlier (BBA 406,329,1975). These changes are simple and are directly interpretable in terms of intermolecular interactions. In this paper I describe the modifications considered, give the rationale for each, and describe the results.

T-AM-Po54 ^{2}H NMR STUDIES OF THE INTERACTION OF CEREBROSIDES WITH DIPALMITOYLPHOSPHATIDYLCHOLINE(DPPC) IN BILAYERS. L.J. Neuringer* and B. Sears, F. Bitter National Magnet Lab.,† M.I.T. Cambridge, MA and F. Jungalwala*, E.K. Shriver Center for Mental Retardation, Waltham, MA.

Cerebrosides constitute the simplest glycosphingolipid since they consist of a single carbohydrate moiety (i.e. galactose) attached to a lipophilic component (i.e. ceramide). They are major components of the myelin membrane. We have begun the study of phospholipid-cerebroside bilayers as a first step in the investigation of glycolipid-phospholipid interactions in myelin and in other natural membranes. We have used high field deuterium nmr (41.4 MHz) to probe the interaction of non-hydroxy fatty acid (NFA) cerebroside and 2-hydroxy fatty acid (HFA) cerebroside with the polar head group and with the acyl chains of DPPC in unsonicated bilayers. For these experiments we synthesized $(CD_3)_3N$+-DPPC and DPPC labeled with deuterium at the C-10 position in the acyl chain. The deuterium quadrupolar splittings $\Delta\nu_Q$ of the head group and the C-10 position were measured at T=35, 45, 53 and 60°C and at concentrations of 0, 10, 20, 33 and 55 mole % cerebroside. The magnitude of $\Delta\nu_Q$ at the C-10 position increases uniformly with increasing concentrations of NFA cerebroside. At T=45°C the values of $\Delta\nu_Q$ observed for NFA and HFA cerebroside are the same within experimental error, but at higher temperatures $\Delta\nu_Q$ is different for each type of cerebroside. There are marked differences in the effects produced by each type at the head group, with NFA cerebroside causing a collapse of the quadrupole powder pattern at low concentration (10 mole %). Thus, the interior of the bilayer becomes more ordered as cerebroside content increases whereas the surface of the bilayer, as reflected by the head group motion, becomes disordered. The extent of the disorder at the surface depends on the type and concentration of cerebroside.

† Supported by the National Science Foundation.

T-AM-Po55 GLUCOCEREBROSIDE-DIPALMITOYL PHOSPHATIDYLCHOLINE INTERACTIONS. M.C. Correa-Freire,* E. Freire, Y. Barenholz,* R.L. Biltonen, and T.E. Thompson. Dept. of Biochem., Univ. of Virginia, Charlottesville, VA 22908.

The thermotropic behavior of multilamellar liposomes prepared from mixtures of glucocerebroside and dipalmitoyl phosphatidylcholine has been studied by high sensitivity scanning calorimetry. Glucocerebroside has a marked effect on the gel-liquid crystalline transition of Dipalmitoyl Phosphatidylcholine. The pretransition seen in pure samples of Dipalmitoyl Phosphatidylcholine is undetectable at mole fractions of glucocerebroside less than 10%. The main transition is shifted to higher temperatures and becomes broader and less cooperative as the mole fractions of glucocerebroside is increased. The enthalpy change of the main transition decreases in a non-linear fashion with increasing glucocerebroside mole fraction. Glucocerebroside itself does not show a separate transition in the temperature range of these studies (10-75°C). The origin of these effects and their dependance on the glucocerebroside content suggests that the in-plane distribution of glucocerebroside molecules is affected by the physical state of the lipid bilayer and by the glucocerebroside: phospholipid mole ratio.

This study was supported by P.H.S. grants GM-23573 and GM-20637.

T-AM-Po56 DENSITY STUDIES OF PHOSPHATIDYL CHOLINE MIXTURES. D.A. Wilkinson and J.F. Nagle, Carnegie-Mellon University, Pittsburgh, Pa. 15213.

We have used a highly sensitive, differential dilatometer in conjunction with a vibrating tube densimeter to study the temperature-volume relationship of mixtures of DMPC and DSPC. Mixing was performed by a method of cosonication and also by the conventional method using organic solvents. The cosonication method led to more consistent results with the mixtures showing better-defined transitions than they did when mixed in chloroform. Special care was also taken to come as close as possible to equilibrium conditions through the use of slow scan rates, long periods between successive heating runs, and efforts to anneal the mixtures. The phase diagram thus obtained did not show monotectic behavior even at very low (1.8 mole %) concentrations of DSPC although the system is very close to being monotectic. The volume changes, ΔV through the transition for X moles of DSPC and 1-X moles of DMPC equals $X\Delta V_{DSPC} + (1-X)\Delta V_{DMPC}$ where ΔV_{DMPC} and ΔV_{DSPC} are the volume changes for pure DMPC and DSPC respectively. Similarly, the density of the mixture is given by $Xd_{DSPC} + (1-X)d_{DMPC}$ where the d's are the densities of the pure components. These studies are being extended to binary mixtures of PC's where the alkyl chain length difference is more than four carbons.

T-AM-Po57 WATER PERMEABILITY OF SOLVENT-FREE AND DECANE-CONTAINING PLANAR LIPID BILAYER MEMBRANES. A. Walter and J. Gutknecht, Duke Univ. Marine Lab, Beaufort, N.C. 28516.

The osmotic water permeability of unmodified lipid bilayer membranes (BLM's) is similar to that of most "nonporous" biological membranes, which suggests that water traverses both types of membrane through the bilayer portion. However, the presence of substantial amounts of hydrocarbon solvents in planar lipid bilayers makes the comparison between model membranes and biological membranes ambiguous. It has been shown by others that the large hydrocarbon squalene is not incorporated into planar or vesicular bilayers. We formed large "solvent-free" planar bilayers and compared the osmotic permeability of these with that of decane-containing BLM's. BLM's were formed from either egg phosphatidylcholine (PC) in decane or egg PC in squalene on the end of a polyethylene tube. The net water flux created by an osmotic gradient was measured with a micrometer syringe. AT 30°C, the water permeability of PC-squalene membranes was $8.7\pm1.8 \times 10^{-3}$ cm sec^{-1} (mean±SD) which is significantly greater than the permeability of PC-decane membranes, $5.6\pm0.8 \times 10^{-3}$ cm sec^{-1}. The ratio between these permeabilities is 1.5 which is similar to the ratio of published values for the thickness of these two bilayers of 1.7. From these data, the rate limiting step for water transport appears to be the movement through the apolar region of the bilayer. (Supported in part by USPHS Grant HL 12157 and NRSA 5 T32-GM07046-03.)

T-AM-Po58 THE ANTAGONISTIC EFFECTS OF SODIUM AND CALCIUM ON THE SURFACE PRESSURE OF PHOSPHATIDIC ACID MONOLAYERS. J.A. DeSimone, G.L. Heck* and S.K. DeSimone*, Department of Physiology, Medical College of Virginia, Richmond, Virginia 23298.

We have constructed a surface film apparatus which permits us to transfer a phospholipid monolayer at constant area from the subphase upon which it is formed to an adjacent subphase of different composition. The time course of re-equilibration is followed continuously by monitoring changes in surface tension. Typically, the film and a 1 mm thickness of the original subphase are transferred. When a phosphatidic acid monlayer is transferred from water to solutions of NaCl at constant bulk pH, the surface tension initially declines (surface pressure increases). If the NaCl solution is less than about 0.2 M, the surface tension asymptotically approaches a limiting value. For NaCl solutions in excess of 0.2 M, a minimum appears in the time course. The higher the salt concentration used, the closer the minimum to the origin. The time course can be described by assuming the equilibrium structure of the double layer is diffusion-controlled and the surface charge density determined by the local pH. The sodium concentration is assumed to control the concentration of the surface hydrogen ions through its effect on the surface potential. The result is a non-monotonic time course in the surface pressure when the NaCl concentration exceeds 0.2 M. Transferring a film from a 0.1 M NaCl subphase to a similar subphase with added Ca^{++} ion always results in condensation. The result can only be explained by assuming that, like H^+ ion (but unlike Na^+ ion), Ca^{++} forms a direct linkage with the surface film. These observations correlate strongly with electrophysiological and psychophysical studies on salt, acid and "water" taste reception in mammals. The sour taste reported when a NaCl solution on the tongue is replaced by water can be explained by this model as can the non-monotonic character of the electrophysiological response in mammals.

T-AM-Po59 MOLECULAR DYNAMICS SIMULATION OF PHOSPHOLIPID MONOLAYERS. Terence R. Thompson and David A. Goldstein, Dept. of Radiation Biology & Biophysics, The University of Rochester, Rochester, New York 14642.

A dynamic, deterministic model of a phospholipid monolayer was constructed which moves phospholipid-like centers of force according to an integrated law of motion in finite-difference form. Forces on each phospholipid analogue were derived from the gradient of the local potential which is the sum of Coulombic and short-range terms. The Coulombic term was obtained by solving a finite-difference form of Poisson's equation in three dimensions, while the short-range term resulted from finite-radius, pairwise summation of one of several phenomenological potentials. Boundary potentials were treated in such a way that the model is effectively infinite in extent in the plane of the monolayer. The two-dimensional virial theorem was used to find the surface pressure (π) of the monolayer as a function of molecular area (A). π-versus-A curves, plotted for different values of model parameters such as structure and orientation of head groups and hydrocarbon tails, were compared to similar curves derived from experiment. Implications for the physical theory of the structure of phospholipid monolayers and bilayers were developed.

T-AM-Po60 LATERAL TRANSPORT OF AN AMPHIPATHIC APOLIPOPROTEIN BOUND TO PHOSPHATIDYLCHOLINE AND PHOSPHATIDYLCHOLINE/CHOLESTEROL BILAYERS. Winchil L. C. Vaz[a](*), En-Shin Wu[b], and Ken Jacobson[a], [a]Department of Experimental Pathology, Roswell Park Memorial Institute, Buffalo, N.Y. 14263, and [b]Department of Physics, University of Maryland-Baltimore County, Baltimore, Md. 21228.

Lateral diffusion of the amphipathic apolipoprotein, Apo C-III, labeled with fluorescein, has been studied using the method of fluorescence recovery after photobleaching in bilayers of dipalmitoyl phosphatidylcholine (DPPC), egg phosphatidylcholine (EPC), and a 1:1 molar ratio mixture of egg phosphatidylcholine and cholesterol (EPC/CHOL). In DPPC bilayers plots of the diffusion coefficient (D) versus temperature show different slopes below 30° and above 35°C. Comparison of cholate-dialysed DPPC liposomes prepared in the presence (lipid/protein molar ratio of 50) and absence of protein using 16-anthroyl palmitate as a fluorescence polarization probe of the lipid phase transition indicates that both preparations show a main transition at about 42°C but the protein-containing preparation does not show the pre-transition at about 35°C. Also, the protein-containing liposomes show a large turbidity change at about 35°C which is not seen in the absence of the protein. In DPPC bilayers D is about 2×10^{-9} cm^2 sec^{-1} at 20°C and about 9×10^{-8} cm^2 sec^{-1} at 45°C. Arrhenius activation energies for the diffusion process in DPPC bilayers are 28.5 and 7.0 kcal mole^{-1} between 15 and 30°C and between 35 and 45°C respectively. No breaks in the slopes of plots of D versus temperature are seen in EPC and EPC/CHOL bilayers between 10 and 40°C. In EPC and EPC/CHOL bilayers at 20°C D is about 3×10^{-8} cm^2 sec^{-1} and 1.4×10^{-9} cm^2 sec^{-1} respectively and the Arrhenius activation energies between 15 and 35°C are 8.1 and 15.1 kcal mole^{-1} respectively. This work was supported by NIH Grant CA-16743. K.J. is an Established Investigator of the American Heart Association.

T-AM-Po61 HALOTHANE EFFECTS ON PHOSPHOLIPID BILAYERS L. S. Koehler, M. K. Jain, E. T. Fossel, and K. A. Koehler, University of North Carolina, Chapel Hill, NC 27514

The responses of several nmr parameters indicative of dynamic properties of the head group of phospholipids indicate a linear concentration dependent response of the head group to halothane. Carbon-13 T_1 values and apparent linewidths, and deuterium quadrupolar splittings all report linear responses to halothane concentration in the membrane phase. Changes in phosphatidylcholine phosphorous-31 chemical shift tensors are also noted upon partitioning of anesthetic into the membrane. The effects of temperature and lipid composition on the shape of the halothane:membrane fluorine-19 nmr signal have also been examined. The relationship between hydrocarbon chain conformation and head group motion is discussed in the light of these results.

T-AM-Po62 DIVALENT CATION INTERACTIONS WITH PHOSPHATIDYLSERINE (PS) VESICLES: INHIBITION OF BOTH THE MARKED PREFERENCE OF PS FOR Ca^{2+} OVER Mg^{2+} IN COMPETITION EXPERIMENTS AND THE UNIQUE Ca-INDUCED CHAIN CRYSTALLIZATION BY THE PROTEIN SPECTRIN. C. Newton, Kalamazoo College, Kalamazoo, Mich. 49007.

Binding studies of Ca^{2+} and Mg^{2+} to phosphatidylserine (PS) vesicles after equilibrium dialysis indicate that both cations are able to form stochiometric (2:1) PS/metal complexes with the apparent binding constant for Ca^{2+} being about 2.5 times greater than for Mg^{2+}. Binding studies of Ca^{2+} in the presence of Mg^{2+} indicate that Ca^{2+} is highly effective in competing with and displacing Mg^{2+} to a degree much more pronounced than that expected from the apparent binding constants of each ion alone. Differential scanning calorimetry reveals definite differences in the thermal properties of the PS/Ca and PS/Mg complexes. The large protein spectrin binds to PS vesicles in the presence of Ca^{2+} or Mg^{2+} without markedly affecting the binding of either divalent cation. However, the presence of spectrin drastically affects the competition between the two divalent metal ions so that it now approximates that expected from the apparent binding constants. Spectrin is also effective in short-term inhibition of the unique PS/Ca crystalline complex. Thus in the presence of spectrin, the effects of Ca^{2+} and Mg^{2+} are similar. One interpretation of these results is that the unique effects of Ca^{2+} involve close apposition of vesicle membranes with the strong possibility of an intermembrane trans-complex between Ca^{2+} and PS headgroups on both membranes. Binding of metal ions to PS headgroups on only one bilayer (cis-complex) would occur with Mg^{2+} alone or with Ca^{2+} when spectrin sterically hinders close vesicle-vesicle contact. The significance of this proposal for mechanisms of membrane fusion will be discussed.

T-AM-Po63 DIVALENT CATION-INDUCED INTERACTION OF PHOSPHOLIPID VESICLES WITH MONOLAYER MEMBRANES S. Ohki and N. Düzgüneş. Dept. of Biophysical Sciences, SUNY at Buffalo, N.Y. 14214.

The effects of phospholipid vesicles and divalent cations in the subphase solution on the surface tension (γ) of phospholipid monolayer membranes were studied in order to elucidate the nature of the divalent cation-induced vesicle-membrane interaction. Various concentrations of unilamellar phospholipid (phosphatidylserine (PS), phosphatidylcholine (PC), and their mixtures) vesicles and divalent cations were introduced into the subphase solution of the monolayers. The changes in γ of monolayers, with respect to divalent ion concentrations and time, were measured with a teflon Wilhelmy plate. When a PS monolayer and vesicles of PS:PC (1:1) were used, the critical, or threshold concentrations of divalent cations, which produced large reductions in γ of the monolayer were: 16mM for Mg^{2+}, 7mM for Sr^{2+}, 6mM for Ca^{2+}, 3.5mM for Ba^{2+} and 1.8mM for Mn^{2+}. With a PC monolayer and PC vesicles, up to 25mM of any divalent ion used produced no change in γ. For a PS monolayer and PC vesicles, the order of divalent ion concentrations needed to effect the large reduction in γ was $Mg^{2+} > Ca^{2+} > Mn^{2+}$ and their critical concentrations were in between the former two cases. The threshold concentrations also depended upon vesicle concentrations as well as the area per molecule of monolayers. For PS monolayers and PS/PC (1:1) vesicles, above the critical concentrations of Mn^{2+} and Ca^{2+}, γ decreased to a value close to the equilibrium pressure of the monolayers within one-half hour. This decrease in γ of the monolayers, which was not reversible upon the addition of EDTA, is interpreted partly as the consequence of fusion of the vesicles with the monolayer membranes. The order and magnitude of divalent cation concentrations at which PS/PC (1:1) and PS vesicle suspensions showed a large increase in turbidity were similar to those obtained in the above mentioned experiments. This work was partly supported by a grant from U.S. National Institutes of Health. (GM28840).

T-AM-Po64 THE INTERACTION OF PHOSPHOLIPID VESICLES WITH PLANAR PHOSPHOLIPID BILAYERS: THE EFFECT OF CALCIUM AND OTHER DIVALENT IONS. N. Düzgüneş and S. Ohki, Dept. of Biophysical Sciences, State University of New York at Buffalo, Buffalo, NY 14214

The interaction of unilamellar phosphatidylserine(PS)/phosphatidylcholine(PC)(1:1) vesicles with planar PS bilayers was followed by measuring the conductance of the latter. When the $[Ca^{2+}]$ in the aqueous solution was raised to a threshold value of 3-5 mM the conductance began to fluctuate and sharply increase, possibly because of the incorporation of domains of PC into the bilayer or due to individual fusion events. This concentration range was not sufficient to induce the aggregation of the vesicles, which preferentially interacted with the PS membrane. If vesicles were added to the solution already containing 5 mM Ca^{2+} the conductance was unaffected, but specks developed on the planar membrane, most likely indicating adhesion of the vesicles. Further increasing the Ca^{2+} initiated the fluctuations of conductance. Thus, the introduction of Ca^{2+} and not merely its presence seemed to be essential for "fusion". Multilamellar vesicles did not affect the conductance appreciably when the $[Ca^{2+}]$ was increased up to 10 mM. The threshold concentrations at which Ba^{2+}, Sr^{2+} and Mg^{2+} mediated the interaction of unilamellar vesicles with bilayers were, respectively, about 1 mM, 2 mM and 3 mM. The interaction of PS bilayers with PS vesicles containing gramicidin A as a probe was enhanced upon raising the $[Ca^{2+}]$ from 0.9 to 1.2 mM, as detected by an abrupt increase in the ionophore-induced conductance, interpreted to be due to the close contact or fusion of the vesicles with the planar membrane. The effect of Ca^{2+} could be correlated with fusion phenomena in vesicle-vesicle and vesicle-monolayer interactions.

The first author acknowledges the support of a SUNY/B Biomembranes Graduate Group fellowship and a NATO fellowship awarded by the Scientific and Technical Research Council of Turkey.

T-AM-Po65 EFFECT OF NEUTRAL ANESTHETICS ON BILAYERS MADE FROM MONOLAYERS. J. Reyes* and R. Latorre, Dept. of Physiology, Harvard Medical School, Boston, Mass. 02115.

The neutral anesthetics chloroform and benzyl alcohol, at concentrations that block the nerve impulse, greatly modify the transport parameters of the lipophilic ions tetraphenylarsonium and tetraphenylborate in lipid bilayers made from monolayers. Both chloroform and benzyl alcohol increase the membrane permeability to these ions and increase the translocation rate for tetraphenylborate. It was also found that the membrane capacitance increases linearly with the concentration of benzyl alcohol. At 51 mM benzyl alcohol the increase in capacitance is about 6%. Chloroform also increases the membrane capacitance; this increase in capacitance was found to be 6% at 18 mM chloroform. An analysis of the changes in the transport parameters of the lipophilic ions together with the changes in membrane capacitance suggests that benzyl alcohol and chloroform mainly modify the dipole potential and the dielectric constant of the membrane.

T-AM-Po66 MEASUREMENT OF LATERAL DIFFUSION COEFFICIENT OF ION CARRIERS IN LIPID BILAYERS USING CONDUCTANCE MEASUREMENTS. R. Laprade, F. Grenier*, and S. Asselin*. Département de Physique, Université de Montréal, Montréal, Canada, H3C 3J7.

The low voltage carrier-mediated ion conductance of monoolein-decane membranes has been studied as a function of the time after addition of carrier in the aqueous phases and as a function of membrane radius (R). The carriers used were nonactin and its homologues. To minimize loss of carrier on the chamber walls, the membranes were formed on small teflon discs separating two 20 ml glass compartments. The radius of the membrane was varied from 0.025 to 0.25 cm by using discs of increasing hole aperture. Aqueous solutions of NaCl 1M or NH_4Cl of various concentrations at 1M constant ionic strength (with LiCl) were used. The rate of stirring was controlled and monitored. Upon addition of the carrier, the conductance increases exponentially by several orders of magnitude to its final steady-state value. The time constant (τ) and the steady-state conductance per unit area (G_o) were found to increase and reach a plateau as R increases. At a given R, τ decreased with increasing rate of stirring. The value of G_o for 0.25 cm membranes is typically 20 times larger than that of 0.025 cm membranes. The above findings indicate that the rate of entry of the carrier in the membrane is limited by diffusion in the unstirred layer and suggest that lateral diffusion towards the torus of the membrane is responsible for the decrease of G_o with decreasing R. A model taking into account these considerations has been worked out and allows the evaluation of the carrier lateral diffusion coefficient (D_s*) from the knowledge of τ and the dependence of G_o vs R. D_s* for the various carriers has been found to vary around 5 x $10^{-6} cm^2 - s^{-1}$.

Supported by N.R.C. (Canada) and F.C.A.C. (Quebec).

T-AM-Po67 MODIFICATION OF ION TRANSPORT IN LIPID BILAYER MEMBRANES IN THE PRESENCE OF HERBICIDES, 2,4-DICHLOROPHENOXYACETIC ACID. P. Smejtek, M. Paulis-Illangasekare*, and K. Hsu, Department of Physics, Environmental Science Program, Portland State University, Portland, Oregon 97207.

We have found that 2,4-Dichlorophenoxyacetic acid (2,4-D) has the ability to increase the rate of transport of positive ions, such as nonactin-K^+ complex (NON-K^+) and tetraphenylarsonium ($TPhAs^+$), and inhibit transport of negatively charged tetraphenylborate ions ($TPhB^-$). Only the neutral form of 2,4-D is transport active, the ionized molecules are ineffective and do not permeate through the membrane. The effect of 2,4-D on nonactin mediated transport of K^+ can be explained in terms of a simple carrier model. At 2,4-D concentration about 3 x 10^{-4} M the K^+ transport in lecithin-cholesterol and glycerolmonooleate membranes is enhanced to such a degree that, depending upon the K^+ concentration, it becomes limited by the NON-K^+ recombination rate and/or by back diffusion of the unloaded nonactin. The blocking of $TPhB^-$ transport by 2,4-D is dominated by the suppression of $TPhB^-$ diffusion across the membrane rather than by the decrease of adsorption of $TPhB^-$ at the membrane surface. From the changes of kinetic parameters of NON-K^+ transport, $TPhAs^+$ membrane conductance, the membrane current relaxation time constant and the amount of translocated $TPhB^-$ during the relaxation process, we conclude that the electric potential of membrane interior decreases in the presence of 2,4-D. Results of membrane conduction studies are supported by the observed changes of electric potential difference across air/water, and air/lipid monolayer/water interfaces in the presence of 2,4-D. The effect of 2,4-D on ion transport in lipid bilayers can be attributed to a layer of oriented 2,4-D molecules located on the hydrocarbon side of the membrane/water interfaces.

This work is supported by NIH Grant R01 ES 00937-03 and 2R01 ES 00937-04.

T-AM-Po68 CHANNELS FORMED IN PLANAR BILAYER MEMBRANES BY MUTANT DIPHTHERIA TOXIN MOLECULE. Bruce L. Kagan and Alan Finkelstein,* Departments of Physiology, Neuroscience and Biophysics, Albert Einstein College of Medicine, Bronx, NY 10461.

Diphtheria toxin (MW 62,000) is believed to kill cells by inactivating (via ADP-ribosylation) elongation factor - 2 and thus shutting off protein synthesis. However, the mechanism by which the enzymatic "A" fragment (MW 22,000) of the molecule enters the target cell to carry out its evil deed remains a mystery. The "B" fragment, which is required for toxicity, is thought to be involved in transport of the A fragment across the plasma membrane. We report here that CRM 45 (MW 45,000), a mutant diphtheria toxin, can form ion-permeable channels when added to one side (the cis side) of planar phospholipid bilayer membranes. Entry of the channels into the membrane is asymmetric and irreversible. The conductance of a single channel is about 10 pmho in 0.1 M KCl. The channels also exhibit voltage sensitivity, being opened by cis (+) voltages and closed by cis (-) voltages. Pronase digestion from the trans side shows that the CRM 45 channel spans the membrane. This channel-forming activity may be involved in the transport of the A fragment across the plasma membrane of the target cells. We thank Dr. A. M. Pappenheimer, Jr. for providing us with CRM 45 and valuable advice. Supported by NIH grants NS 14246-01 and 5T32 GM 7288.

T-AM-Po69 MODEL MEMBRANE STUDIES USING PHOTOCHEMICAL CROSSLINKING REAGENTS. W. Curatolo, C.M. Gupta,* and H.G. Khorana,* Massachusetts Institute of Technology, Cambridge, MA 02139.

A series of phospholipids which carry carbene-generating photosensitive groups have been synthesized which are capable of covalently crosslinking to lipids and proteins in model membrane systems upon irradiation (Gupta, Radhakrishnan, and Khorana (1977) Proc. Natl. Acad. Sci. 74, 4315). The behavior of one of these phospholipids, 1-C_{16}-2-ω-trifluorodiazopropionyl-C_{11}-phosphatidylcholine (PC*), has now been characterized under a variety of conditions of lipid composition and physical state. After photolysis of sonicated vesicles composed of PC* and various amounts of dipalmitoyl lecithin (DPL) at 47°C (above T_m for DPL), the observed crosslinked product distribution indicates an approximately equal probability of forming PC*-PC* and PC*-DPL dimers. This result is consistent with complete miscibility of PC* and DPL above T_m, and indicates that the active carbene intermediate reacts indiscriminately with both DPL and PC*. Scanning calorimetry (DSC) of unsonicated dispersions of PC* and DPL (1:1, m/m) indicates that the two components undergo a phase separation at temperatures below ∿35°C. Photolysis experiments at various temperatures indicate that, as the temperature is decreased through the phase separation temperature determined by DSC, PC*-PC* dimer production increases and PC*-DPL dimer production decreases. Thus the crosslinking method can detect phase separations and has the capability of indicating which particular molecular species is undergoing phase separation. Experiments in which DPL and dioleyllecithin compete for crosslinking with PC* indicate no clear preference of the carbene intermediate for either the saturated or the unsaturated lipid. Thus photolabeled phospholipids appear to be well suited for studies of lateral organization of lipids in biological membranes. Work supported by NSF and NIH.

T-AM-Po70 IONIC SELECTIVITY OF LOBSTER NERVE SODIUM CHANNELS INCORPORATED INTO SOYBEAN LIPOSOMES. Madalina Condrescu-Guidi* and Raimundo Villegas, Centro de Biofísica y Bioquímica, Instituto Venezolano de Investigaciones Científicas, (IVIC), Apartado 1827, Caracas 101, Venezuela.

Na^+ channels from lobster nerve membranes stored frozen in sucrose were incorporated into soybean liposomes by the freeze-thaw-sonication procedure (Biochim.Biophys.Res.Comm., 79: 210, 1977). In order to estimate the permeability ratios directly from measurements of the ion fluxes, a sulfate solution (pH 7.5) containing equal concentrations (75 mEq/l) of Na^+, K^+, Rb^+ and Cs^+ was used for reconstitution. In some experiments Na^+ (150 mEq/l) and only one of the other cations (also at 250 mEq/l) were present. ^{22}Na, ^{42}K, ^{86}Rb and ^{137}Cs, were employed to follow the fluxes. The control fluxes, i.e., in the absence of drugs, were approximately the same. Veratridine (0.5 mM) or grayanotoxin I (150 μM) increased the fluxes and tetrodotoxin (100 nM) specifically abolished the increments (K_i=5 nM measured with ^{22}Na). The permeability ratios of the veratridine- and tetrodotoxin-sensitive fluxes, were 0.44 ± 0.14 (n=6) for K^+/Na^+, 0.22 ± 0.09 (n=8) for Rb^+/Na^+, and 0.05 ± 0.13 (n=4) for Cs^+/Na^+. For the grayanotoxin I- and tetrodotoxin-sensitive fluxes, equivalent ratios were 0.46 ± 0.17 (n=6) for K^+/Na^+, 0.25 ± 0.08 (n=8) for Rb^+/Na^+ and 0.07 ± 0.10 (n=3) for Cs^+/Na^+. The fluxes of $^{35}SO_4$, $^{32}PO_4$ and ^{36}Cl were found insensitive to veratridine and tetrodotoxin. These results reveal that the Na^+ channels incorporated into the liposomes, do exhibit ionic selectivity. Partially supported by Grant 31.26.S1-0702 of CONICIT, Venezuela.

T-AM-Po71 KINETICS OF Ca^{2+}-INDUCED AGGREGATION OF CHROMAFFIN GRANULE MEMBRANES.
Stephen J. Morris and Duncan H. Haynes, Max Planck Institute for Biophysical Chemistry, D-3400 Goettingen, FRG, and U. of Miami Medical School, Miami, Fla., 33152, USA.

Chromaffin granules (CG) isolated from bovine adrenal medulla will aggregate and fuse in the presence of millimolar concentrations of Ca^{2+}. We can model these processes as "recognition" (encounter complex formation), contact (stable complex) and subsequent membrane fusion. Since molecular details of these processes may elucidate mechanisms involved in exocytosis, we have studied these reactions by electronmicroscopy and stopped flow mixing experiments. Light scattering (turbidity) changes were used to follow the aggregation reaction of CG ghosts, which could be induced by Ca^{2+} or Mg^{2+} with a k_m of 4.5 mM. Monovalent cation k_m's were 10^2 higher. The rate constant (k_{app}) and activation energy for Ca^{2+}-induced dimerization approached that predicted for diffusion control. Vesicles prepared by sonicating CG lipids could be aggregated by cations but the values for k_{app} were 100-fold lower than for native membranes and the amplitude k_m was 5-fold smaller for Ca^{2+} than for Mg^{2+}. We propose the following mechanism:(a) Membranes are held apart be electrostatic repulsion of their negatively-charged surfaces. (b) Divalent and monovalent cations shield these charges allowing closer approach of the membrane surfaces. (c) Aggregation rates of CG membranes are determined by proteins which protrude 10-15 Å from the (phospholipid) surface of the membrane and serve as primary contact points. Contact does not require full neutralization of surface charge and potential arising from the negatively charged phospholipids. (d) After contact between proteins is established, the interaction between membranes is strengthened through transmembrane hydrogen bonding of phosphatidyl ethanolamine polar head groups, divalent cation-mediated salt bridging between negatively charged phospholipids and by segregation of phosphatidyl choline out of the region of contact.